DM

Dendrimers
The fluorination approach

MASTER DISSERTATION

Lydia Nadège Abreu dos Orfãos
MASTER IN NANOCHEMISTRY AND NANOMATERIALS

UNIVERSIDADE da MADEIRA
A Nossa Universidade
www.uma.pt

February | 2020

Dendrimers
The fluorination approach

MASTER DISSERTATION

Lydia Nadège Abreu dos Orfãos
MASTER IN NANOCHEMISTRY AND NANOMATERIALS

SUPERVISION
João Manuel Cunha Rodrigues

CO-SUPERVISION
Helena Maria Pires Gaspar Tomás

Dendrimers: The fluorination approach

Dissertation submitted to the University of Madeira for the fulfilment of the requirements for the degree of Master in Nanochemistry and Nanomaterials

By Lydia dos Orfãos

Work developed under the supervision of Professor João Manuel Cunha Rodrigues
and co-supervised by Professor Helena Maria Pires Gaspar Tomás

Faculdade de Ciências Exatas e da Engenharia

Centro de Química da Madeira

Campus Universitário da Penteada

Funchal – Portugal

February 2020

Declaration

I hereby declare that this thesis is the result of my own work, is original and was written by me. I also declare that its reproduction and publication by Madeira University will not break any third-party rights and that I have not previously (in its entirety or in part) submitted it elsewhere for obtaining any qualification or degree. Furthermore, I certify that all the sources of information used in this thesis were properly cited.

Funchal, February 13th 2020

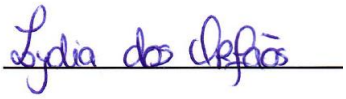

(Lydia dos Orfãos)

Conference Contributions

Oral communication:

- Lydia dos Orfãos, João Rodrigues, Helena Tomás. Fluorescent dendrimers - The fluorination approach. 6th CQM Annual Meeting held in Porto Moniz (Portugal), O-27, page 45, 26th - 27th April 2019.

Poster communication:

- Lydia dos Orfãos, Cláudia Camacho, Helena Tomás, João Rodrigues. Functionalization of generation four PAMAM dendrimer - the fluorination effect. XXVI Encontro Nacional da Sociedade Portuguesa de Química held in Oporto (Portugal), CPM13, page 273, 24th - 26th July 2019.

- Lydia dos Orfãos, Cláudia Camacho, Helena Tomás, João Rodrigues. Fluorinated and Nonfluorinated Generation Four (G4) PAMAM Dendrimers. 11th International Dendrimer Symposium (IDS11) held in Funchal (Portugal), PC34, page 134, 14th - 18th July 2019.

Acknowledgements

The conclusion of this Master Thesis was only possible thanks to all the people and institutions involved to which I would like to acknowledge and show my deepest gratitude.

To my supervisors Prof. João Rodrigues and Prof. Helena Tomás for the guidance, the remarks, and the opportunities to expand my knowledge and view in the field with the many conferences, workshops and seminars promoted.

To Cláudia Camacho and Duarte Fernandes for their help, patience, knowledge, for the tips, advice, discussions, and most of all for the friendship and companionship. You were tireless and I am thankful for that.

To all my colleagues, friends, and family that in one way or another walked this path alongside me. Mostly to Nilsa Abreu and Beatriz Andrade for their always contagious good mood, friendship, and sharing. To Yu Zou and Sabriie Vatansever, my master's colleagues, that were there through the classes and with whom I shared thoughts, experiences and know-how.

To the CQM – Centro de Química da Madeira and all its members for providing the installations, materials, chemical reagents, and qualified personnel for the realization of the experiments. With additional care to the LQCMM staff of CQM, Dina Maciel, Nilsa Oliveira, and those whom, passing by, shared a kind and enthusiastic word and bite of knowledge, Carla S. Alves, Rita Castro, Nádia Nunes, Ana Olival, Mara Gonçalves and Marijana Petkovic. To the LBCC staff of CQM also, Filipe Olim for guiding me through the biological studies, along with Ana Neves and Mariana Vieira. To the Chemistry Department laboratory technicians, Paula Andrade and Paula Vieira, as well as Engineer Teresa Abreu from CQM, for the laboratory support.

This work could not be developed without the support of FCT - *Fundação para a Ciência e a Tecnologia* (CQM PEst-OE/QUI/UI674/2019, Portuguese Government funds), Madeira 14-20 Program through the project PROEQUIPRAM – *Reforço do investimento em Equipamentos e Infraestruturas Científicas na RAM* (M1420-01-0145-FEDER-000008), and the project M1420-01-0145-FEDER-000005 – Centro de Química da Madeira – CQM^{+} (ARDITI - *Agência Regional para o Desenvolvimento da Investigação Tecnologia e Inovação*, Madeira 14-20 Program).

As the tiles are settled together, the journey comes to its end. The people, however, will always remain and be remembered. For that, I thank you all for being who you are and for making this an unforgettable voyage.

Abstract

The developments in materials science have provided new approaches for the detection, diagnosis and treatment of several diseases. Dendrimers have been intensively studied for their unique properties as probes and drug/gene delivery vehicles, mainly due to their multivalency and possibility of surface functionalization with a wide variety of compounds.

This thesis aimed at the functionalization of generation four amine-terminated poly(amidoamine) ($PAMAMG_4$-NH_2) dendrimers with the compound 2,3,5,6-tetrafluoro-4-hydroxybenzoic acid (TFHBA) for the obtention of new gene delivery vectors having increased transfection efficiency and high cytocompatibility, taking advantage of the "fluorine effect". The traceability potential of this system using ^{19}F-TFHBA in nuclear magnetic resonance, although not studied in the present thesis, was also a significant reason for the developed work. The functionalization of the $PAMAMG_4$-NH_2 dendrimer was performed with two functionalization degrees using TFHBA/dendrimer ratios of 32.5 and 64.5. A control using 4-hydroxybenzoic acid (HBA), the non-fluorinated counterpart of TFHBA, was also used at the same functionalization degrees. Several techniques were applied for the characterization of the synthesized materials, such as Nuclear Magnetic Resonance (NMR), Fourier Transform Infrared (FTIR), Ultraviolet/Visible (UV/Vis), and fluorescence spectroscopies, as well as Dynamic Light Scattering (DLS) and Electrophoretic Light Scattering (ELS), to confirm the success of the conjugation. Biological studies of the prepared compounds were performed, too, namely cytotoxicity, pDNA condensation and charge neutralization capability, and transfection efficiency.

The functionalization of $PAMAMG_4$-NH_2 dendrimers with TFHBA and HBA at both functionalization degrees was achieved successfully. Compared to pristine $PAMAMG_4$-NH_2, the functionalized dendrimers presented lower cytotoxicity, similar pDNA condensation ability, and better transfection efficiency in HEK293T cells. Based on the obtained data, no significant differences were observed between the TFHBA and HBA functionalized dendrimers as transfection agents.

Resumo

O desenvolvimento da ciência dos materiais providenciou novas técnicas para a deteção, diagnóstico e tratamento de várias doenças. Os dendrímeros têm sido amplamente estudados pelas suas propriedades de sensor únicas e de veículos de entrega de drogas/genes, devido sobretudo a sua multivalência e possibilitarem a funcionalização da sua superfície com uma variedade de compostos.

O objetivo principal desta tese é a funcionalização de dendrímeros de poli(amidoamina) de quarta geração (PAMAMG_4-NH_2) com o ácido 2,3,5,6-tetrafluoro-4-hidroxilbenzóico (TFHBA) para a obtenção de novos vetores para a entrega de genes que possuam uma elevada eficiência de transfecção e citocompatibilidade, tirando vantagens do "efeito do flúor". A possibilidade de utilizar ressonância magnética nuclear ^{19}F-TFHBA nestes sistemas, dotando-os de um potencial de rastreabilidade, embora não estudada na corrente tese, foi, também, uma razão importante para o desenvolvimento deste trabalho. A funcionalização do dendrímero PAMAMG_4-NH_2 foi realizada com dois graus de funcionalização distintos usando rácios de TFHBA/dendrímero de 32.5 e 64.5. Foi, também, utilizado um controlo com o ácido 4-hidroxibenzóico (HBA), o homólogo não fluorado do TFHBA. Várias técnicas de caracterização foram usadas para a caracterização dos materiais sintetizados, tais como, espectroscopias de RMN, FTIR, UV/Visível e fluorescência, bem como DLS/ELS, para a confirmação do sucesso da conjugação. Estudos biológicos foram também efetuados, nomeadamente citotoxicidade, capacidade condensação e neutralização de carga do pDNA, e eficiência de transfecção.

A funcionalização do dendrímero PAMAMG_4-NH_2 com o TFHBA e o HBA em ambos graus de funcionalização foi bem-sucedida. Comparado com o dendrímero de PAMAMG_4-NH_2 nativo o dendrímero funcionalizado apresenta menor citotoxicidade, condensação e neutralização de carga do pDNA similar, e revela uma melhor eficiência de transfecção em células HEK293T. Até ao momento, e baseado nos resultados obtidos, não se denota quaisquer diferenças significativas entre o dendrímero funcionalizado com TFHBA e HBA como veículos de transfecção.

Table of Contents

List of Figures

List of Tables

List of Equations

List of Abbreviations

Abbreviation	Definition
ACQ	Aggregation-caused quenching
AIE	Aggregation-induced emission
COSY	Correlation spectroscopy
DA	Diamine
DAB	Diaminobutane
DLS	Dynamic light scattering
dsDNA	Double-stranded DNA
EDA	Ethylenediamine
EDL	Electric double-layer
EDTA	Ethylenediaminetetraacetic acid
ELS	Electrophoretic light scattering
FTIR	Fourier transform infrared spectroscopy
GFP	Green fluorescence protein
G_x	Generation x (being x the number of the generation)
HBA	4-hydroxybenzoic acid
HSQC	Heteronuclear single-quantum correlation spectroscopy
IC	Internal conversion
IR	Infrared
ISC	Intersystem crossing
LB	Luria-Bertani
MALDI-TOF	Matrix-assisted laser desorption ionization mass spectroscopy
MWCNTs	Multiwalled carbon nanotubes
NADPH	Nicotinamide adenine phosphate dinucleotide
NMR	Nuclear magnetic resonance
NTIL	Non-traditional intrinsic luminescence
PAMAM	PolyAmidoAmine
$PAMAMG_4$-NH_2	Generation four amine-terminated PAMAM dendrimer
P-MWNT/PANI	PAMAM-multiwalled nanotube/polyaniline
PPI	Poly(propylene Imine)
rISC	Reverse intersystem crossing
TADF	Thermally-activated delayed fluorescence

TE	Tris-EDTA
TFHBA	2,3,5,6-tetrafluoro-4-hydroxybenzoic acid
TNBSA	Trinitrobenzenesulfonic acid
UV	Ultraviolet
UV/Vis	Ultra-violet/Visible spectroscopy

Chapter I: Introduction

1.1. Dendrimers

The word *dendrimer* comes from the Greek where *dendron* means "tree" and *meros* means "part" - this designation appeared for the first time in the work of Tomalia published in 1985[1] and was later widely spread among the scientific community[2]. Indeed, although dendrimers were first synthesized in 1978 by Fritz Vögtle, they became better known after the works of George R. Newkome and Donald Tomalia in the 1980s[3,4]. Dendrimers are thus a particular type of hyperbranched synthetic polymer having a 3D tree-like structure and characterized by being monodispersed when compared with the classical hyperbranched polymers. While the latter are usually produced in a single step and using relatively simplified reactions, dendrimers are prepared in a thoroughly and iteratively controlled manner that will result in well-defined structures and molecular weights[5]. Dendrimers are thus composed of a multifunctional core, different layers (generations) and an exterior surface consisting of many terminal groups (the number of these groups is dependent on the dendrimer generation (G_x)) (**Figure 1**)[1,2,6].

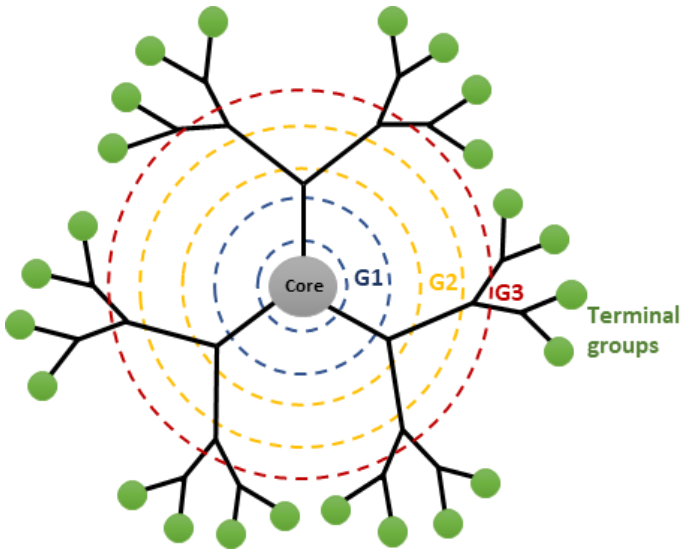

Figure 1: Scheme of a dendrimer architecture. G1: Generation 1; G2: Generation 2, G3: Generation 3.

Dendrimers are extremely versatile molecules, and their properties can be finely tuned, either by changing the generation/molecular weight or by playing with their chemical composition. The functionalization of the terminal molecules with distinct functional groups can also be done and this may affect their solubility, photophysical properties and chemical reactivity[5,7]. The "dendritic effect", or "dendrimer effect", shown by these systems is one of their most interesting properties. This term is commonly used to describe the unusual physicochemical trends or property patterns observed in both

dendrimers and dendrons. The dendritic effect may be a generation effect where, upon the increase of the generation, there is a variation on the properties; or a multivalency effect related to the presence of multiple surface groups close to each other[8,9].

It is not by chance that the name dendrimer became the most widely used to characterize this type of polymers. The dendritic architecture can be found in countless examples in nature, such as snow crystals, lightning patterns, vascular systems of animal and plants, tree roots and branching[10], and neurons[11,12]. Dendrimers can also be found in many applications, such as catalysts[13], sensors[14], bioimaging[15], and dyes[16]. They are particularly interesting for biomedical applications since their terminal groups enable multivalent binding to biological receptors and since they can carry drugs[5] or proteins[17] by encapsulation inside their internal void spaces or by chemical conjugation to the chemical groups at their surface. As nanocarriers, dendrimers may show a high drug loading capacity, help in the reduction of the required drug dose, increase the drug delivery to the target, allow multiple administration routes, control the biodistribution of the drug, and reduce mortality and morbidity since they contribute to a decrease in the adverse effects of the drug[18–20]. Nevertheless, little is known concerning their exposure pathways and effects on processes and biochemical pathways in mammalian systems, and their implementation and development costs can also constitute problematic issues[20].

1.1.1. Types of Dendrimers

Since their discovery and until nowadays, a wide range of dendrimers has been synthesized in the search for the best performing ones, or the ones presenting the most interesting features.

Depending on the application or wanted properties, several types of dendrimers can be used, such as PolyAmidoAmine (PAMAM) dendrimers[21,7], Poly(Propylene Imine) (PPI) dendrimers[22,23], metallodendrimers[24,25], Poly(aryl ether) dendrimers[26,27,28,], polyester dendrimers[29], Polylysine dendrimers[30,31], carbosilane dendrimers[32], triazine-based dendrimers[33], among many others.

PAMAM dendrimers (**Figure 2**) can be prepared with high yields and at molecular weights ranging from several hundred to over one million Daltons, depending on their generation[11]. These dendrimers usually contain a diamine (DA) core, methyl acrylate repeating units[34] and different terminal groups such as NH_2[35,36].

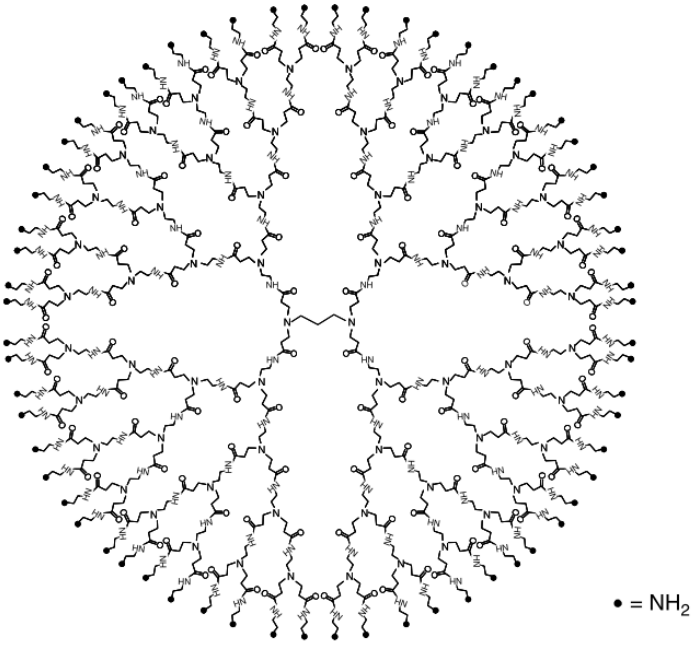

Figure 2: PAMAM dendrimer of generation four. Adapted from reference[5].

PPI dendrimers or POMAM (another designation for these dendrimers that stands for Poly (Propylene Amine)) (**Figure 3**) are usually synthesized by a divergent method and using dioaminobutane (DAB) or EDA as the core. They have primary amines as terminal groups, and the interior comprises numerous tertiary *tris*-propylene amines. These dendrimers are extensively explored for drug delivery applications and are commercially available until generation five (G_5)[23,37]. However, as the generation increases, the number of cationic groups at the surface increases and can induce cytotoxic effects. As such, the outermost part of the dendrimer needs to be modified or functionalized to reduce the cytotoxicity before its use *in vivo*[18,23,38].

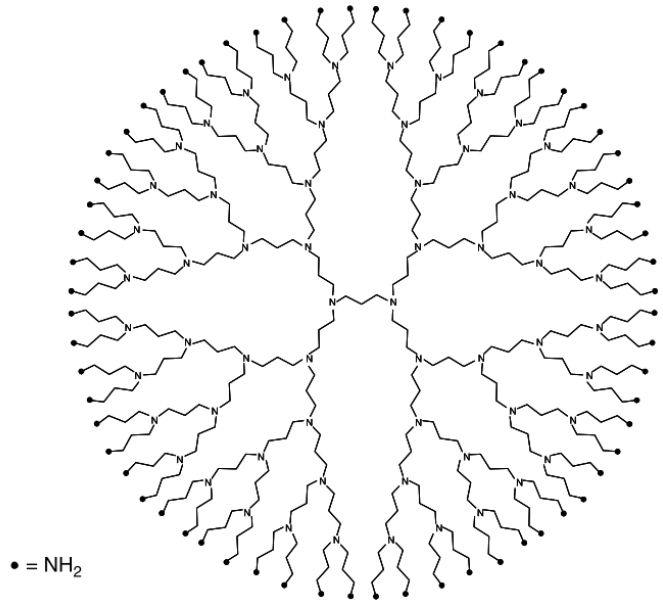

Figure 3: PPI dendrimer of generation four. Adapted from reference[5].

Metallodendrimers (**Figure 4**), another type of dendrimer, that combine the properties of these hyperbranched molecules with those of metals/metal complexes, are very interesting since they may be used as catalysts, being regenerable and ecologically viable. Their efficiency can even equalize that of the homogenous mononuclear catalysts and they can be straightforwardly recovered and re-used[25]. They may also be applied in other fields such as photo-physics, molecular light-harvesting, drug delivery, and redox anion recognition[24,39]. In a metallodendrimer, the active centre can be situated in different locations: on the outer edge, within the branches, or at the centre. In the area of catalysis, the most common metals and oxidation state used in the preparation of metallodendrimers are Co (III), Rh (III), Pd (II), Cu (II), Ru (II), and Fe (I). They can be prepared by thiolene reactions, click chemistry, azide-alkyne reactions, and also Diels-Alder reactions[39] among others.

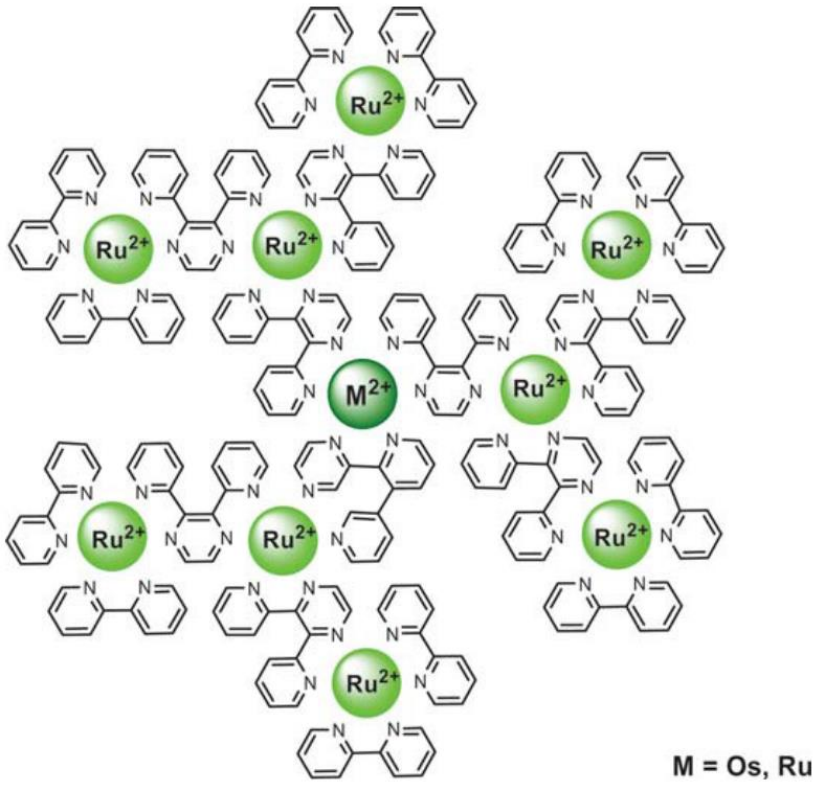

Figure 4: Metallodendrimer. Adapted from reference[2].

Poly(aryl ether) dendrimers (**Figure 5**) are, as their name indicates, dendrimers constituted of aryl ethers. These dendrimers have been shown to have haemolytic activity against blood cells of rat[37]. The convergent synthesis of these polyether dendrimers was developed by Hawker and Fréchet who were successful in obtaining monodispersed macromolecules[40] that were later analysed by Matrix-Assisted Laser Desorption Ionization Mass Spectrometry (MALDI-TOF)[41]. They were mainly studied as drug carriers since they allow the encapsulation of a drug inside their cavities acting as a shield against the unfavourable environment of the body[28,42,43]

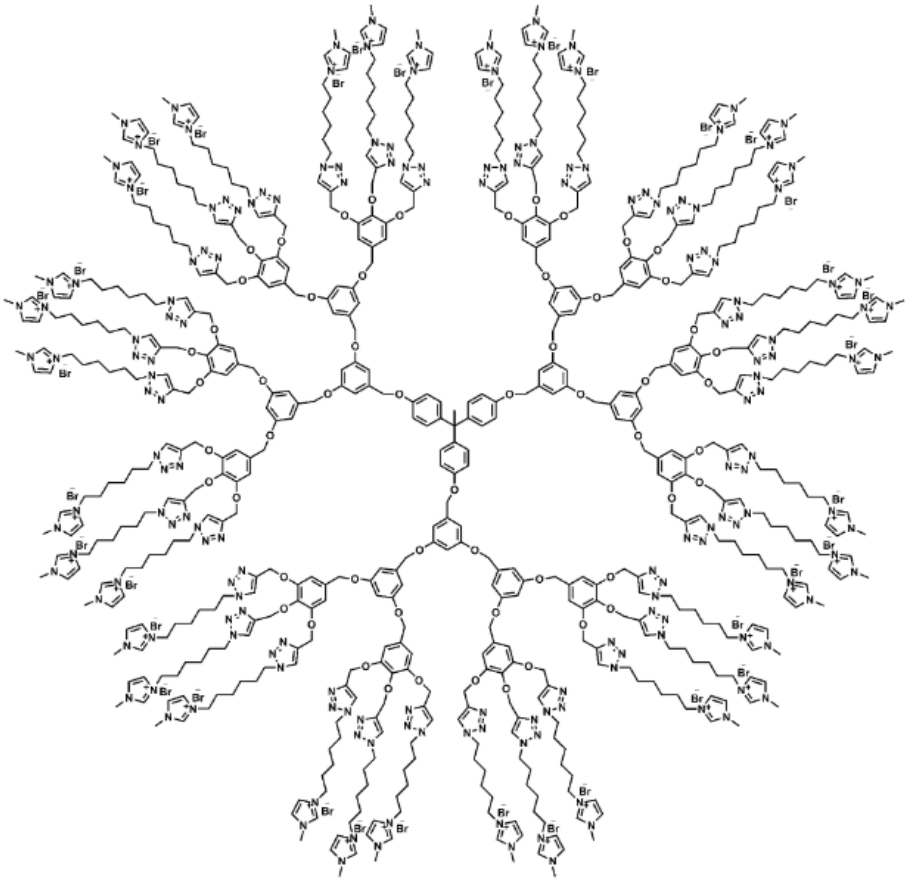

Figure 5: Poly (aryl ether) dendrimer with imidazolium end groups. Adapted from reference[26]**.**

Polyester dendrimers (**Figure 6**) are very similar to the polyether ones, with the only difference being that instead of ether they have ester linkages in their structure. The ester bond is quite advantageous since it is a hydrolysable linkage and, as such, allows the biodegradability of the dendrimer[43]. This property, along with the non-toxicity of this type of dendrimer, has made them the object of interest for many applications. Mostly in the biomedical field and, the development of aromatic polyester dendrimers has been growing ever since[29].

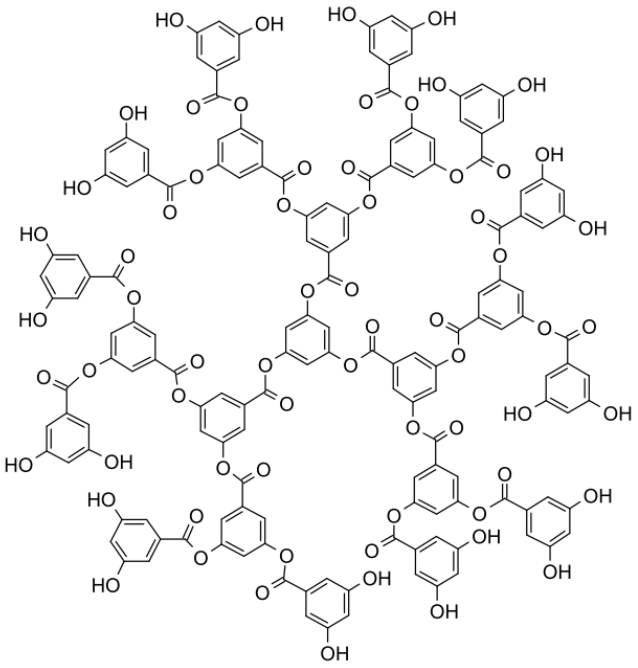

Figure 6: Polyester dendrimer. Adapted from reference[29].

Polylysine dendrimers (**Figure 7**) are the most commonly used peptide-based dendrimers that contain L-lysine in their branching parts. Since they contain amino acids in their structure, they may present protein functionalities[31,44]. Apart from being employed in drug delivery, such as the previous dendrimers, these molecules have been studied for their ability to show antiangiogenic activity in solid tumours after intravenous administration[30], as well as their capability to be quickly removed from plasma after systemic administration, even though they are metabolized, and the released L-lysine enters in endogenous synthetic processes[31]

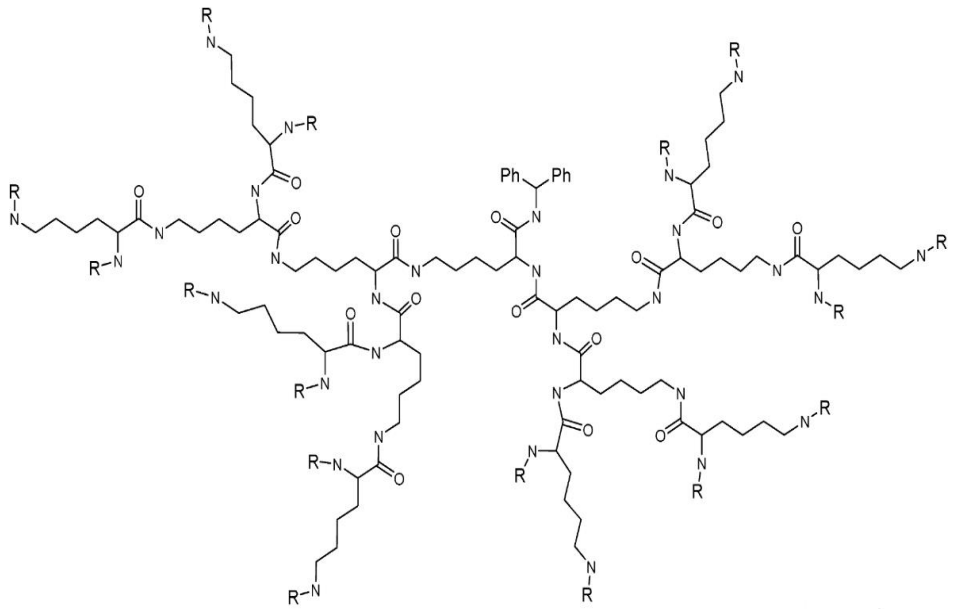

Figure 7: Poly-L-Lysine dendrimer. Adapted from reference[45].

Carbosilane dendrimers (**Figure 8**) have silicon and carbon atoms in their skeleton and differ from the other dendrimers by the high mobility of their peripheral branches and the core apolarity. They have been studied for their antiviral (e.g. anti-HIV), and viscoelastic properties[32,46–48] among others.

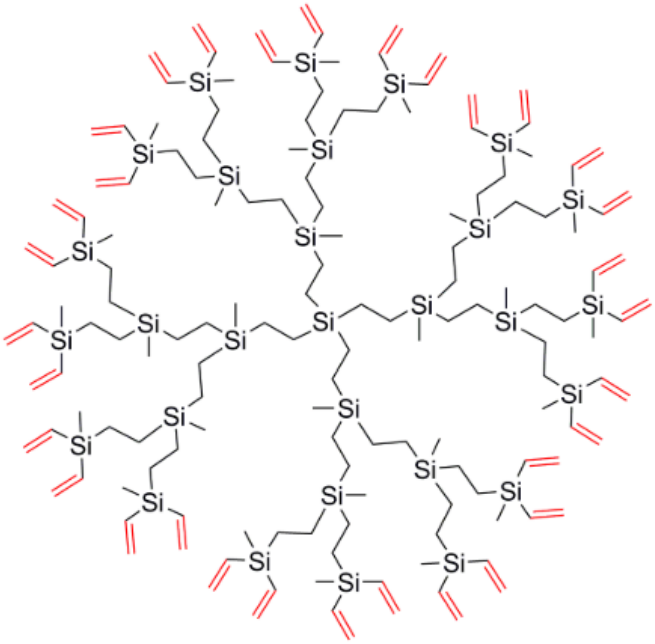

Figure 8: Carbosilane dendrimer. Adapted from reference[7].

Triazine-based dendrimers (**Figure 9**) have, as a core or in the branching units, the 1,3,5-triazine ring, and can be synthesized in various manners, such as, by a cycloaddition reaction, for the formation of the triazine ring, by a cyanuric chloride ($C_3N_3Cl_3$) nucleophilic aromatic substitution, or by the cyclotrimerization of organic cyanates, more commonly used for the preparation of hyperbranched polymers[33,49]. Triazine, particularly melamines, are interesting due to their capacity of molecule recognition by the acceptance and donation of hydrogen bonds, π-π interaction, and metal chelation. These abilities, associated with their electromechanical and electroluminescence properties[50], ease of synthesis and control of their composition, make them very attractive for molecular recognition, gene and RNA oligonucleotide delivery vehicles, and the preparation of metal complexes and dendritic ligands[33,49,51,52].

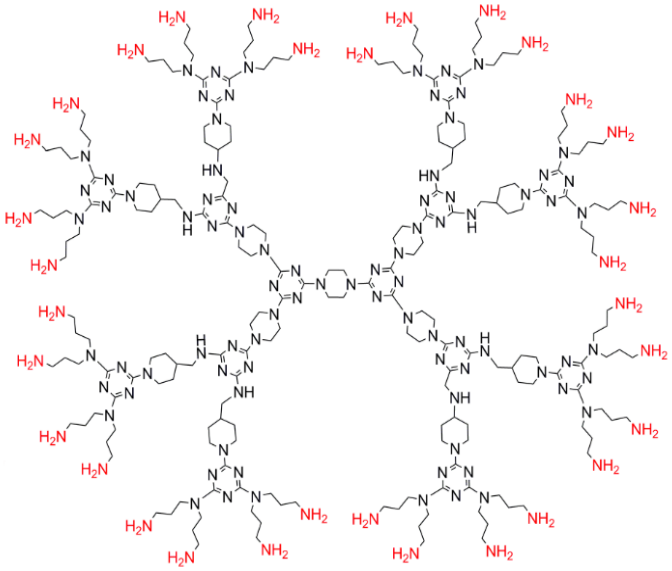

Figure 9: Triazine-based dendrimer. Adapted from reference[7].

Phosphorus-based dendrimers (**Figure 10**) are dendrimers that possess at each branching point, at specific places, phosphorus atoms. Their synthesis, quite straightforward and straightforward, is commonly owed to the existence of very reactive groups, either aldehydes or $P(S)Cl_2$ groups[53]. These polymers hold fascinating properties and are being studied for several applications in the field of biology, materials science, and catalysis. The latter has been the most commonly investigated since the existence of atoms of tricoordinate phosphorus, typically at the end groups, enable the complexation of a multitude of organometallic derivatives with catalytic properties[54,55].

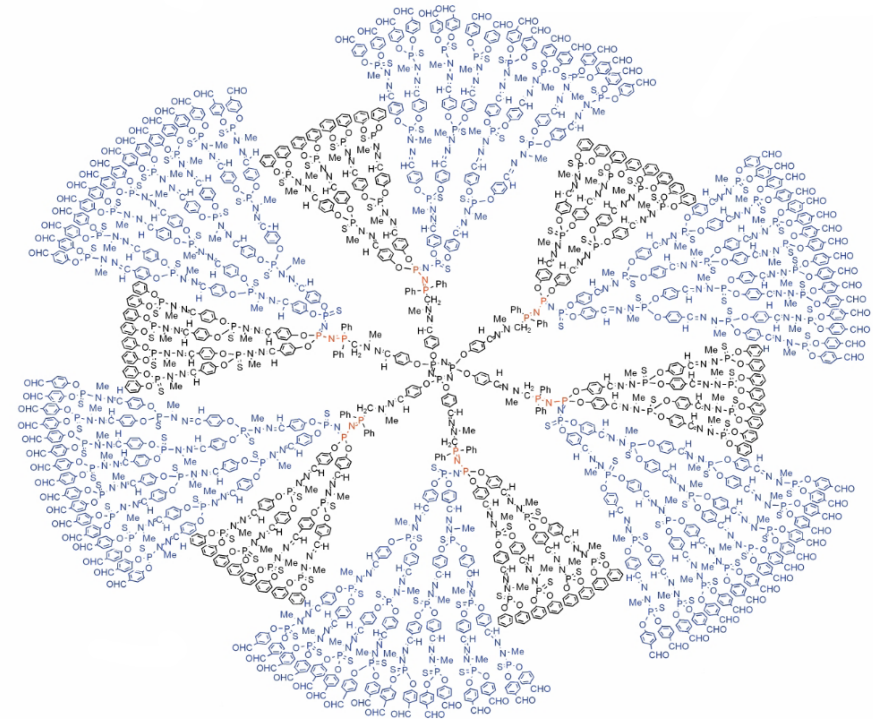

Figure 10: Phosphorus-based dendrimers. Adapted from reference[55].

1.1.2. PAMAM dendrimers

PAMAM dendrimers were successfully synthesized by Tomalia in 1985, using a modified synthetic methodology employed by Vögtle and co-workers[2,11]. The synthesis of such dendrimers involves a two-step process, namely a Michael addition of an initiator core of amine with methyl acrylate, and extensive amidation with an excess of ethylenediamine (EDA) of the resulting esters, where the iteration process leads to the next generation[1,34]. The first generations that arose from such polymers were from generation 1 (G_1) to generation 7 (G_7). Then, after some time, a group of researchers synthesized PAMAM dendrimers up to generation 11 (G_{11})[56]. However, an important strain occurs throughout the structure of the G_{10} PAMAM dendrimer and intensely increases for the next generation, which can be explained by the availability of the surface area per monomer, causing a significant stretching of the dendrimer interior [1,56,57]. The steric interactions of the surface groups prevent the growth of complete generations beyond G_{10}, being this the limiting generation for this kind of dendrimer[56]. Other difficulties concerning dendrimer growth, already discovered in Tomalia's synthesis include terminal functionality solvolysis, intramolecular cyclization, fragmentation due to retro-Michael addition, and incomplete Michael addition[1].

Considering that the growth of dendrimers is done by increasing the generation number, the terminal groups, molecular weight, and the number of atoms all increase exponentially throughout the generations, although the radius only increases by 10 Å per generation. PAMAMG_4-NH_2, for instance, has 64 primary amine terminal groups, a molecular weight of 14215 Da, and, in solution, have a spherical conformation with a diameter of approximately 4.5 nm[5,29,46]. An important point needs to be considered regarding the dendrimer terminal groups since, when the dendrimers are growing, a considerable folding back of these groups is observed which influences the surface group availability and the dendrimer conformation[56].

When using this type of dendrimer, safety and toxicity are relevant concerns. The toxicity of PAMAM dendrimers is dependent on their generation, concentration, and charge. That said, the cationic derivatives will present significant toxicity compared to their negatively charged or neutral counterparts, and their cytotoxicity will increase with an increase in concentration and generation[57,58].

The amino groups of PAMAM dendrimers are the ones accountable for the positive charge of the dendrimer. Cationic molecules, in this case, the PAMAM dendrimers, may cause cell lysis since they destabilize cell membranes[59]. However, the amine groups within the PAMAM dendrimer are very sensitive to the pH of a solution. In fact, at a very high pH, the tertiary amines at each branching point in the dendrimer are not protonated, the primary amines start to protonate at a pH of approximately 9, and all the tertiary amines are protonated at a pH of 4[59–64].

Nevertheless, the positive charge of these amine terminated PAMAM dendrimers also has some advantages since it allows for the condensation of DNA (negatively charged due to the phosphate groups in the DNA backbone) into a nanometric globular size and, subsequently, facilitates transfection and favours the interaction with the negatively charged membrane of cells. The high amount of tertiary amine groups present inside the PAMAM results in a "proton sponge" effect during the escape of the polyplex from the endolysosome[59,61,63,65].

The surface modification or functionalization of dendrimers is widely used to decrease their cytotoxicity. One of the most commonly used molecules for this purpose is polyethylene glycol (PEG), since it presents hydrophilicity, shields the positively charged terminal groups of the dendrimer, and may increase tumour accumulation due to the Enhanced Permeability Retention (EPR) effect and plasma circulation[66–69]. Other molecules have also been used for a variety of applications. A study from 2008[66] used PAMAM dendrimers functionalized with $[Ru^{III}(EDTA)(H_2O)]^-$ to deliver, in a controllable manner, Nitric Oxide (NO) into a specific location. In another study from 2014[70], the surface of PAMAM dendrimers was modified with lipids to deliver drugs/genes into the central nervous system; the system was then compared with the pristine PAMAM-NH_2, showing that the lipid-PAMAM dendrimers were less toxic than the ones containing amines. Also, in a study from 2018[71], amine-terminated PAMAM dendrimers were functionalized with multiwalled carbon nanotubes (MWCNTs) to afford P-MWNT/PANI (PAMAM-multiwalled nanotube/polyaniline) electrodes with supercapacitor properties.

1.1.3. Fluorescent dendrimers

1.1.3.1. Fluorescence

Fluorescence is a physical phenomenon that requires energy absorption (**Figure 11**). The absorbed energy will take the molecule from the ground state to an excited electronic state that is not stable. There are different pathways for the electrons to return to the ground state, namely radiationless transitions (without photon emission) and radiational transitions (relaxation of the molecule from the excited state to the ground state with the emission of photons)[72,73].

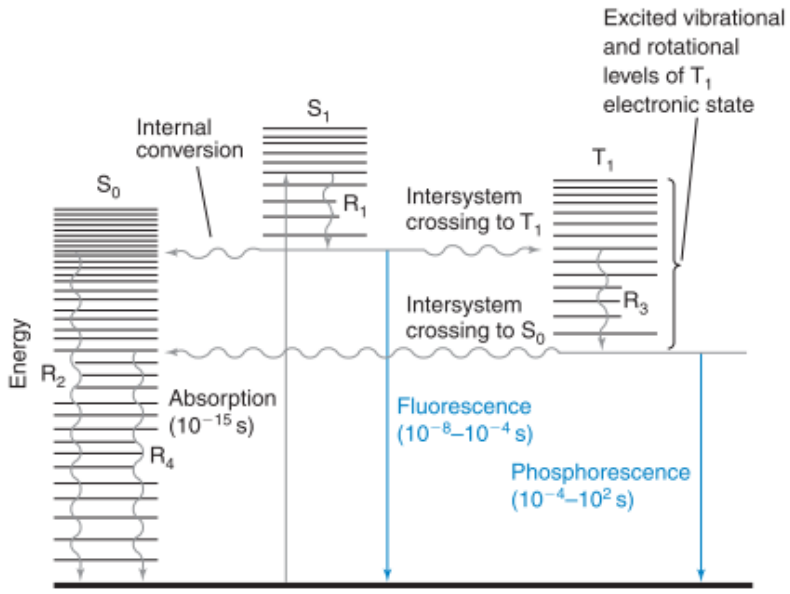

Figure 11: Scheme of the physical processes that can arise after the absorption of an ultraviolet or visible photon. S0: ground electronic state; S1: lowest excited singlet state; T1: lowest triplet electronic state; R: vibrational relaxation; Wavy arrows: radiationless transitions; Straight arrows: processes involving photons. Adapted from reference[72].

Vibrational relaxation is, generally, the first process that occurs after the absorption of an ultraviolet or visible photon. In this transition, the vibrational energy is transferred, through collisions, to other molecules, usually the solvent. Part of the energy of the absorbed photon is converted into heat that spreads throughout the entire medium[72].

Two categories are present in the radiationless transitions: intersystem crossing (ISC) and internal conversion (IC). In the first case, the transition occurs between states that have different spin quantum numbers while, in the latter one, the transition takes place between states with equal spin quantum number[72,74].

The emission of a photon (radiation transition) can be done in two different ways - by fluorescence or by phosphorescence. Probably, the most important difference between these two types of luminescence is their kinetics, that is, while fluorescence has an emission lifetime of 1 ns to 1 µs, phosphorescence has an emission lifetime that goes from 1 ms to seconds or even minutes. This effect is due to the spin quantum number change between the final and the initial states. If the spin quantum number is different, the transition is spin forbidden and it is called phosphorescence. If, on the other hand, these quantum numbers are equal, the transition is spin-allowed and it is a fluorescence phenomenon[72,75,76].

Fluorescence is a relevant, exciting and convenient property of certain materials that allow for the development of probes and markers that are widely used in the medical and biological sciences. It may provide knowledge of the surrounding local environment of the fluorescent molecule, the molecular composition of the sample, and the location of the probe. Endogenous fluorophores commonly used

for tissue characterization in biological studies include structural proteins, like collagen, collagen cross-links, elastin, aromatic amino acids (e.g. phenylalanine, tyrosine and tryptophan), porphyrins, flavin adenine dinucleotide (FAD), and enzyme metabolic co-factors, like Nicotinamide Adenine Phosphate Dinucleotide (NADPH)[77–80].

1.1.3.2. Dendrimers as fluorophores

The developments in material science have contributed to a rise in nanomaterials with quite attractive luminescence properties, combined with high sensitivity and biocompatibility, which allows for their use in biological imaging[80]. A fluorescent probe should, ideally, follow some requirements, such as being non-toxic, not affect the cell metabolism, and specifically and efficiently be internalized by cells[81]. Among the fluorescent probes, dendrimers are considered interesting objects of study due to their already discussed properties. Concerning the fluorescence of such molecules, it has been found that dendrimers with tertiary amines at their branching points emit fluorescence with a signal that varies upon the adjustment of the pH value. PAMAMG_4 dendrimers show an increase in fluorescence intensity with a decrease of pH from 6 to 2.5, being this last value the maximum fluorescence intensity reached by this dendrimer generation[82–85].

The incorporation of luminescent units into the dendritic structure is a common procedure to ensure the fluorescence properties of such molecules and, especially, to give a signal intensity adequate for the intended application. This incorporation can be done non-covalently by surface adsorption or encapsulation of the luminescent units inside the dendrimer's cavities; or covalently by binding the unit to the surface terminal groups of the dendritic structure[86]. Various studies proposed different kinds of fluorescent dendrimers, such as the use of a copolymer-based dendrimer-PEG for fluorescence sensing[87], PAMAM dendrimers with sulforhodamine B covalently attached to the core as a potential diagnostic tool for biomedical tracing[88], a water-soluble dendrimer with a carboxylated perylene bisimides dye as core and PAMAM dendron arms for long-term imaging of live cells[89], fluorescent carbazole dendrimer as an accelerant and nitroaliphatic taggants detector[90], among many others.

1.1.3.3. Non-traditional intrinsic fluorescence of dendrimers.

The traditional luminescence paradigm involves the excitation of electrons (from the ground state to an excited one) due to the absorption of high energy radiation, and the emission of a particular lower energy radiation when the excited electrons relax back to the ground state. This emission of

luminescence is recognised to be generally quenched by aggregation (or at a high concentration) and to be concentration dependent[91,92].

PPI and PAMAM dendrimers were initially designed to be soluble in aqueous media, where their nitrogen atoms, under acidic conditions, are protonated. However, blue background fluorescence was observed in these molecules which was, at first, considered as owed to contaminations, since there was not any building block in the dendrimer structure that could be considered as a traditional fluorophore[93–95]. This weak blue fluorescence assigned to the PAMAM dendrimers, especially when excited at near or in the ultraviolet (UV) region, was later attributed to their intrinsic fluorescence[94,96].

The background blue fluorescence that appeared in the PAMAM dendrimers was further investigated. Since the traditional luminescence paradigm did not fit with some of the phenomena observed with this fluorescence, a new concept emerged that was recently named "non-traditional intrinsic luminescence" (NTIL)[91,97].

NTIL differs from traditional luminescence since it involves hetero-atomic sub-luminophores (HASLs), such as oxazolines, esters, amines, amides, imines, hydroxyls, carboxylic acids, and the emission is enhanced by the confinement, rigidifications and/or aggregation of the assemblies that contain these HASLs. It comprises the physicochemical confinement and/or the clustering/aggregation of electron-rich, hetero-atomic, usually non-emissive, functional moieties, and happens in the absence of traditional luminophores. The NTIL systems can present aggregation-enhanced emission or aggregation-induced emission (AIE) and when in aggregated states and concentrated solutions, are highly emissive[91,92,98].

Unlike aggregation-caused quenching (ACQ), in AIE the aggregation induces the emission of fluorescence. That is, when in discrete form, the chromogens are poorly luminescent, but when they aggregate, they become more luminescent. Since its emergence, this phenomenon has appeared in the literature to explain the NTIL of several compounds[99–105].

Larson and his co-worker Tucker, in their study on the intrinsic fluorescence of PAMAM-carboxylate-terminated dendrimers[96], proposed that this emission of fluorescence might be due to a $n \rightarrow \pi^*$ transition from various amino groups[93,94]. Another study from 2004[106], working with OH-terminated PAMAM dendrimers, suggested that the blue luminescence was not due to the backbone of these dendrimers but to their terminal groups; however, when adjusting the pH value, the dendrimers with tertiary amines in their branching points emitted a strong fluorescence, which indicated that the backbone of the dendrimer would contribute to the fluorescence[83,84,105,107,108]. Other studies associated the fluorescence emission of the PAMAM dendrimers to the tertiary ammonium and the imidic acid amide resonance found in their structure[94,95,109,110]. Not only PAMAM dendrimers

but also PPI and polylysine ones with NH_2 terminal groups were found to have this type of fluorescence[83,93,111].

1.1.4. Fluorinated dendrimers

Fluorine (F), with an atomic weight of roughly 19 Da and electronegativity of 3.98 is not readily available for biological systems since the insoluble form of terrestrial F prevents its uptake by bioorganisms[112–114]. However, fluoride is common on the earth´s crust and can be found in air, soil, and water. Fluoride plays an important role in dental health especially on the calcification of the enamel of children of age below eight years, and as an agent in the prevention of dental caries. The fluoride ion decreases the solubility of the hydroxyapatite mineral phase in mineralized tissues and biomaterials, increasing their stability, and it also disturbs bacterial cells through cellular enzyme inhibition, such as glycolytic enzymes and H^+-ATPases. The cytoplasmic pH and the permeability of the membrane are also affected by this ion, decreasing the acid production of glycolysis[115–119].

The incorporation of fluorine in molecules is a strategy used in the development of several drugs, such as Atorvastatin (Lipitor), Capecitabine (Xeloda), Moxifloxacin (Avelox), Fluoxetine (Prozac®), among many others[120–122]. This incorporation of fluorine into the molecule moieties, or "fluorination", increases the pharmacokinetic behavior of the drugs and improves protein stability without biological alteration. Fluorine reduces the basicity and enhances the acidity of a basic group or an adjacent acid, correspondingly[113,123,124].

Fluorinated compounds display a huge phase separation tendency in both non-polar and polar environments and exhibit lipophobic and hydrophobic characteristics. Fluorinated polymers will preferably associate, at low concentrations, with each other since they have low surface energy. The unusual chemical, biological, and/or physical behavior and properties of fluorinated compounds are sometimes referred to as the "fluorine effect"[113,125,126].

Fluorination of cationic polymers will reduce their cytotoxicity, increasing their capacity for gene delivery[127]. Therefore, the fluorination of PAMAM-NH_2 dendrimers has been shown to improve their transfection efficiency, due to a significant protection and DNA condensation ability, serum stability, cellular uptake, endosomal escape, and easier intracellular release of the carried DNA (**Figure 12**)[113,124,127–133].

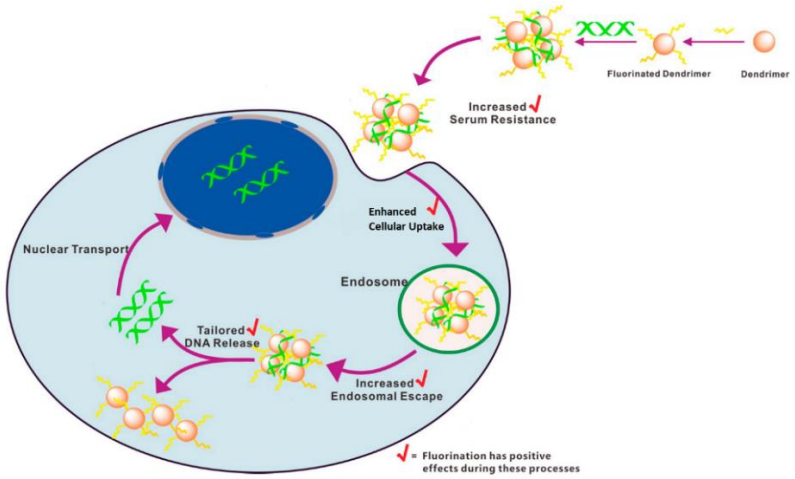

Figure 12: Transfection mechanism highlighting the effect of fluorination. Adapted from reference[124].

Since ^{19}F Nuclear Magnetic Resonance (NMR) is a very sensitive probe, similar to ^{1}H NMR, the incorporation of fluorine in dendrimers may make them suitable for ^{19}F NMR enabling the use of these systems as contrast agents in bioimaging and guided drug therapy. In addition, the absence in natural systems of organofluorine compounds giving no background spectra makes it appropriate for probing biological systems. It is also, due to its highly sensitive chemical shifts of local conformation and environment, suitable for the characterization of unfolded structures[132,134,135].

1.1.5. Dendrimers as transfection agents

Transfection is a process whereby foreign nucleic acids (DNA or RNA) are introduced in cells, generating genetically modified cells. Transfection aims to inhibit (gene silencing) or enhance (gene delivery) protein expression[85,136].

DNA by itself is unstable in biological environments and, as countermeasures, living bodies developed strategies such as the nucleus and the cell membrane to prevent changes in their genome by endogenous or exogenous species that may leak from the immune system. Therefore, for successful transfection, the vector that will deliver the nucleic acid needs to protect the compacted gene from the immune system and needs to assist in crossing biological membranes. Vectors that are capable of this task are divided into two main categories: viral and non-viral. Other strategies are also used for gene delivery that do not require vectors, being them physical methods[85,137,138].

Physical methods, as mentioned before, do not need the use of vectors. Instead they use various physical tools for the delivery of the nucleic acid. These methods force the entry of the nucleic acid into the cell. Several tools are used for the accomplishment of transfection, such as microinjection[139] where the genetic material is injected with a syringe into the desired location; electroporation, where pores are formed in the cell membrane by applying an electric field greater than the cell membrane capacitance[140]; sonoporation, where the cell membrane is permeabilized with the use of ultrasounds;

photoporation, that creates pores in the cell membrane with a single laser pulse to enable the entrance of the nucleic acid; among others. Nevertheless, these methods are rough, demand specialised equipment, skillful users, and are often harmful to cells[85,136,137,141].

Viral vectors are those in which viruses, like lentivirus, adenovirus or retrovirus are used to deliver the nucleic acid into the desired cells. Due to their natural ability of transfection, these vectors are very efficient in transfection and usually lead to high gene expression levels. However, safety concerns such as inflammatory effects, immunogenicity, cytotoxicity, and the possibility of an interruption in the activation of vital genes or oncogenes are major drawbacks in the use of these delivery methods[136,142–144].

Nonviral vectors, as the name indicates, are vehicles that do not make use of viruses to deliver nucleic acids to cells. Chemical entities such as cationic lipids, cationic polymers, and calcium phosphate may be used as non-viral vectors. Although these vectors are less efficient than the viral ones in terms of the transfection process, they usually have lower toxicity and immunogenicity and do not carry extra DNA nor lead to mutagenesis. Their efficiency often depends on the pH of the solution, molar charge ratio, and cell membrane conditions. The positive charge of these chemicals will compact the negatively charged nucleic acid forming vector/nucleic acid complexes. The negatively charged cell membrane will be then attracted by these complexes[136,138,143,144].

Cationic polymers are interesting for gene delivery since they are capable of nucleic acid charge neutralization and condensation, thus helping DNA to be effectively internalized by cells. However, due to their excessive positive charge, they can show severe toxicity, and most of them are non-biodegradable[142,143,145]. The most studied cationic polymer, polyethylenimine (PEI), even though it has excellent properties as a vector (*e.g.* condensation of DNA and transfection efficiency both *in vivo* and *in vitro*, as well as effective endolysosomal escape and cell uptake of the formed complexes), it aggregates and establishes non-specific interactions with the blood, and is cytotoxic[143,146].

Polycationic dendrimers, such as PAMAM dendrimers, have been studied as gene carriers since they exhibit a rather high gene transfection efficiency, a well-defined structure, and the possibility of surface functionalization. The amino groups of the PAMAM-NH_2 dendrimers are responsible for the positive charge of the dendrimers, which contributes to the condensation of the nucleic acid and their inherent cytotoxicity. Nevertheless, the functionalization of dendrimers can result in the shielding of the positively charged groups, decreasing the dendrimer cytotoxicity and improving its transfection efficiency[61,137,142,147].

The endolysosomal escape of dendrimers complexed with nucleic acids is thought to be due to the proton sponge effect. This phenomenon happens because, inside the acidic environment of the endolysosomes, the dendrimer tends to absorb protons which will result in an increase of the influx of

H^+ (in fact H_3O^+) into that vesicle. This influx of protons will cause an influx of Cl^-, thus increasing the osmotic pressure in the endolysosomal interior and, ultimately, its bursting to release its content to the cell cytosol[85,148–150].

1.1.6. Main chemical reactions used in dendrimer chemistry

The synthesis of dendrimers is done by an iterative process that can begin inside and move outwards (divergent synthesis) or that begins from the outside and moves in (convergent synthesis)[3,23]. The divergent approach entails a stepwise process of activation and coupling of monomers. The inner core of the molecule will react with the monomer that will have a reactive site and two protected groups. Then the protected groups are activated for the coupling of more monomers giving the next generation. These steps are repeated until the desired generation is reached[21,37,62,85].

The synthesis of PAMAM dendrimers (**Figure 13**), developed by Tomalia and coworkers in 1985[1], is an example of the divergent method. Synthesis involves the Michael addition of methyl acrylate to ammonia and the conversion of the resulting ester into primary triamine with a reaction involving an ethylenediamine excess. The repetition of these reaction steps leads to the different generations of PAMAM dendrimers. As previously reported, it is possible to synthesize these dendrimers up to generation eleven[2,62,148].

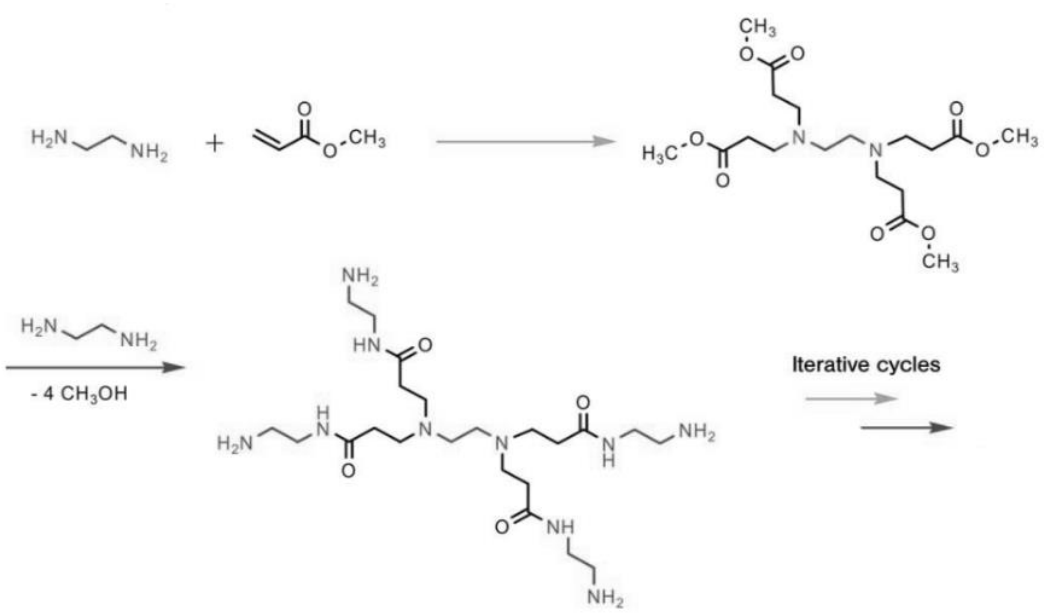

Figure 13: Tomalia's synthesis approach for PAMAM dendrimers. Adapted from reference[2].

The increase in the dendrimer generation decreases its perfection and purity. Most of these imperfections and impurities are due to Retro-Michael addition, missing repeat units, or inter/intramolecular cyclization. This leads to a point where beyond a certain generation, a limiting

generation, a perfect structure is impossible to be prepared[34,91,160]. The increase of generation by the divergent approach exponentially increases the space needed for the terminal groups, resulting in the crowding of the outer shell of the dendrimer. This dense packing of terminal groups will limit further reaction, leading to growth defects[2].

The convergent synthesis approach is also performed by an iterative process of coupling and activation. However, since the number of simultaneous reactions for each growth step is small, the control of the dendrimer structure as well as its purity is higher than with the divergent approach. This improves yield and increases the rate of reaction[21,62,151]. Beginning with the terminal groups, the branches or dendrons are grown inwards by an iteration process of protection/deprotection of the monomer sites, until the desired size. The dendrons are then connected to a central core, leaving the end groups unmodified throughout the dendrimer synthesis[37,85].

The convergent method of dendrimer construction is, however, limited to lower generations due to steric issues at the nanoscale upon the linking of the dendrons to the core, and the modification of the surface group is hampered. Nevertheless, this approach has several advantages such as good symmetry and monodispersity, low level of impurities (since the purification of the dendrons before their connection to the core is better) and the possibility of production of dendrimers with diverse core functions [62,85,151]. An example of this method is the synthesis of polyether dendrimers that was used by Fréchet and coworkers (**Figure 14**)[152]. For this, a two-step synthesis was needed. First a 3,5-dihidroxybenzyl alcohol with benzyl bromide reaction was performed, and then a transformation of the benzyl alcohol into the benzyl bromide allows the coupling of more monomers, repeating the reactions steps[2].

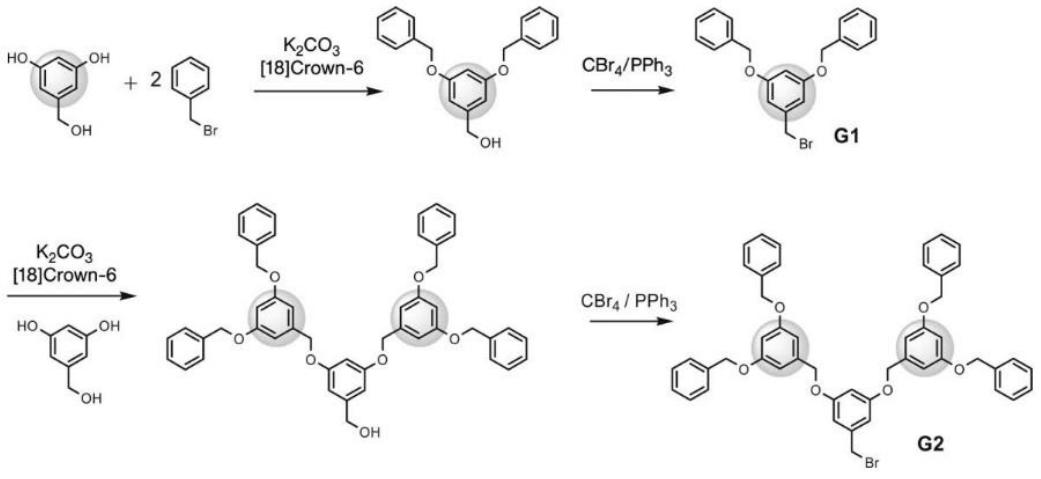

Figure 14: Fréchet´s convergent synthesis approach of polyether dendrimer. Adapted from reference[2].

1.2. Objectives

The main objective of this thesis was to develop PAMAM dendrimers functionalized with the compound 2,3,5,6-tetrafluoro-4-hydroxybenzoic acid (TFHBA, **Figure 15 a**) for the obtention of new gene delivery vectors, presenting high cytocompatibility and increased transfection efficiency by taking advantage of the "fluorine effect". A schematic representation of the work is presented in **Figure 16.** Although not tested herein, the future possibility of using ^{19}F-TFHBA in these systems endowing them traceability potential by magnetic resonance bioimaging techniques is also an important reason underlying the developed work.

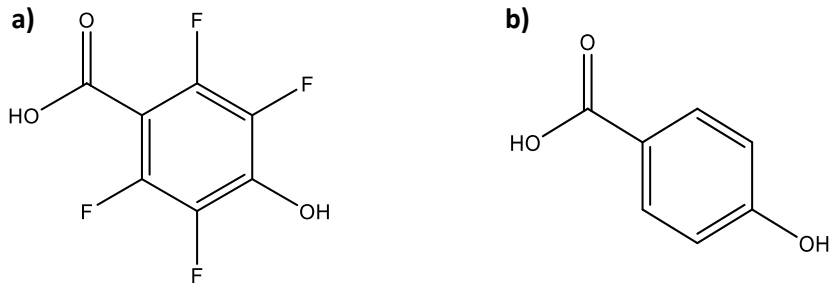

Figure 15: The chemical structures of a) TFHBA and b) HBA.

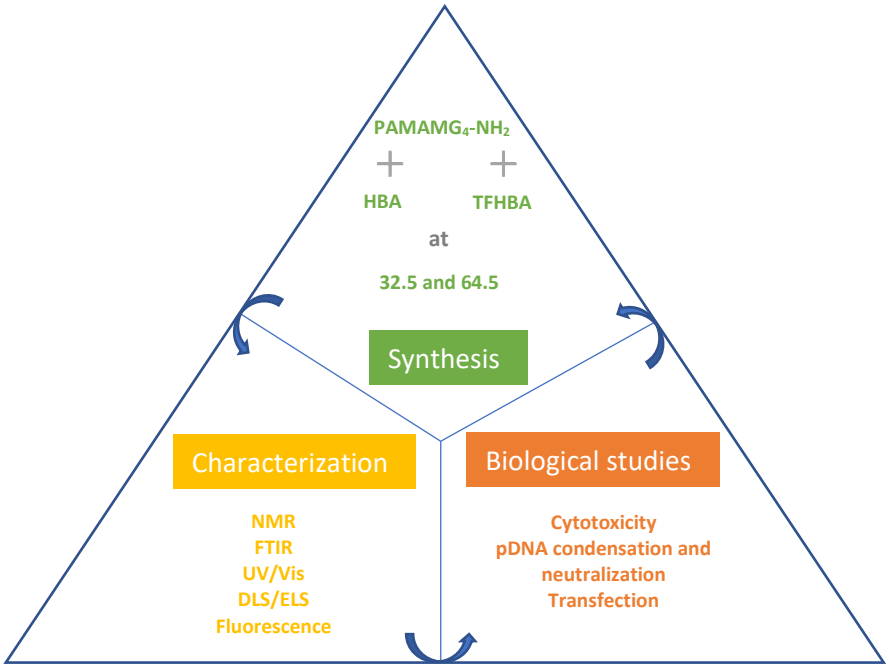

Figure 16: Schematic representation of the developed work.

In more detail, this thesis aimed at:

a) The preparation of PAMAMG_4-NH_2 functionalized with TFHBA to study the effect of fluorination. The dendrimers were also functionalized with the compound 4-hydroxybenzoic acid (HBA, the non-fluorinated counterpart of TFHBA, **Figure 15 b**) which was used as a control. Both were surface modified at two different degrees through stoichiometric control (ratios of compound/dendrimer of 32.5 and 62.5 were used);
b) The characterization of the prepared dendrimers by suitable physicochemical techniques, namely by NMR, Ultraviolet/Visible spectroscopy (UV/vis), Fourier Transformed Infrared spectroscopy (FTIR), Fluorescence spectroscopy, Dynamic Light Scattering (DLS) and Electrophoretic Light Scattering (ELS);
c) The study of the stability of the dendrimers along time;
d) The evaluation of the *in vitro* cytotoxicity of the fluorinated and non-fluorinated dendrimers using a metabolic activity assay (resazurin reduction assay);
e) The study of the capacity of the fluorinated dendrimers to condense pDNA and neutralize its charge (that is, the study of dendriplexes);
f) The evaluation of the *in vitro* transfection efficiency achieved by the fluorinated dendrimers *vs* the non-fluorinated ones; additionally, the evaluation of the effect of the degree of functionalization over transfection efficiency.

The TFHBA molecule (**Figure 15 a**) has a molecular weight of 210 Da and was chosen as the source of fluorine since there is not much done with this molecule in terms of conjugation with PAMAM dendrimers. Besides, the combination of fluorination and dendrimers may reveal properties that might be interesting for future applications (such as in the field of ^{19}F NMR imaging, drug/gene delivery). TFHBA has been used in the synthesis of polymeric activated resins for the production of pure compound libraries[153], in the development of activity-based probes for non-invasive optical imaging of cancer[154], and in the construction of tetrafluorophenol acrylamide 3D gels for the synthesis of small molecules and the generation of an amides' library using the catch-and-release chemistry[155].

The HBA molecule (**Figure 15 b**), used for preparing the control dendrimer conjugates due to its resemblance to TFHBA, is small with a molecular weight of 138 Da and has a high affinity for sigma and dopamine receptors. Sigma receptors have a substantial predominance at the mitochondria-associated endoplasmic reticulum membrane, and both of them (sigma and dopamine receptors) are abundant in the central nervous system [156–160]. This molecule also has antimicrobial activity against a vast number of either Gram-positive or Gram-negative bacteria [161–163]. It also has potential properties for biomedical applications, such as targeted therapy and diagnosis[156].

Chapter II: Materials and Methods

2.1. Materials

The reagents HBA (99+%), potassium bromide (KBr, spectroscopy grade), and Petri dishes for cell culture (10 cm^2) were bought from Thermo Fisher Scientific (MA, USA); TFHBA (>98.0%) was from TCI Chemicals (Japan); the ultrapure water used throughout the work was obtained using a Millipore Water Purification System (≥ 18.2 MΩ/cm); PAMAMG_4-NH_2 dendrimers, 19.06% (w/w) in methanol, were purchased from Dendritech®, Inc. (MI, USA); dialysis membranes were acquired from Spectrum™ (Spectra/Por™).

Dulbecco's phosphorus buffer saline powder (PBS, without calcium), deuterium oxide (D_2O, 99.99%), Dulbecco's Modified Eagle's Medium (DMEM), bichinchoninic acid (BCA), copper(II) sulfate (4% w/v), Luria-Bertani (LB) medium and resazurin were obtained from Merck (Germany); trypsin-ethylenediaminetetraacetic acid (trypsin-EDTA, 0.25%), Tris-EDTA at 0.25% (TE 20x), fetal bovine serum (FBS), antibiotic/antimycotic solution (100X), and collagen (collagen I rat protein, tail) were from Gibco™. The 1x RLB lysis buffer and Luciferase Assay System kit were from Promega (USA). The Quant-iT™ PicoGreen® double-stranded DNA (dsDNA) Assay Kit was from Invitrogen (USA).

2.2. Synthesis of the conjugates

The conjugation of the PAMAM dendrimer with the compounds (either HBA or TFHBA) was done at room temperature.

To accomplish this, PAMAMG_4-NH_2 was dialysed with a 6-8 kDa dialysis membrane against two litres of distilled water for 24h and changing water seven times. After the dialysis, the PAMAMG_4-NH_2 was freeze dried (Labconco FreeZone® 4.5 Liter Freeze Dry Systems) and stored in the freezer at a temperature of -20^oC.

The conjugation of PAMAMG_4-NH_2 with the compounds was done at different functionalization degrees of HBA and TFHBA, namely using 32.5 and 64.5 compound/dendrimer ratios. The amount of compound needed was weighed out, dissolved in ultrapure water and the pH was read with a VWR® benchtop pH meter (SB21 sympHony™). The amount of PAMAMG_4-NH_2 required, which was set to 50 mg at a concentration of 20 $mgmL^{-1}$, was also dissolved in ultrapure water and the pH assessed.

Having the two solutions ready, the PAMAMG_4-NH_2 solution was put in a round bottom flask under magnetic stirring and then the solution containing either compound (i.e. HBA or TFHBA at 32.5 or 64.5 ratios, respectively) was added dropwise into the stirring PAMAMG_4-NH_2 solution. The mixture

was left to react for 48h (the final volume of the solutions were of 13.0 mL, 20.7 mL, 17.0 mL, and of 27.8 mL for G4_HBA 32.5, G4_HBA 64.5, G4_TFHBA 32.5, and G4_TFHBA 64.5, respectively).

After the reaction time ended, the pH of each reaction mixture was read and a purification step was performed. For this, a 3.5 kDa dialysis membrane (standard RC tubing) was used and the dialysis was done for 24h against 2 L of distilled water, changing the water 5 times (at 30 min, 1h, 2h, 3h and overnight). The product(s) was then lyophilized and characterized. **Table 1** shows all the compounds involved in the synthesis, the final products and their designations.

Table 1: Compounds used and their designations.

Compounds	Designation	Molecular Weight ($gmol^{-1}$)
Generation four amine terminated PAMAM dendrimer	$PAMAMG_4\text{-}NH_2$	14215
4-hydroxybenzoic acid	HBA	138.12
2,3,5,6-tetrafluoro-4-hydroxybenzoic acid	TFHBA	210.08
$PAMAMG_4\text{-}NH_2$ conjugated with 4-hydroxybenzoic acid at 32.5 molar equivalent	G4_HBA 32.5	18058
$PAMAMG_4\text{-}NH_2$ conjugated with 4-hydroxybenzoic acid at 64.5 molar equivalent	G4_HBA 64.5	21902
$PAMAMG_4\text{-}NH_2$ conjugated with 2,3,5,6-tetrafluoro-4-hydroxybenzoic acid at 32.5 molar equivalent	G4_TFHBA 32.5	20361
$PAMAMG_4\text{-}NH_2$ conjugated with 2,3,5,6-tetrafluoro-4-hydroxybenzoic acid at 64.5 molar equivalent	G4_TFHBA 64.5	26507

2.3. Characterization of the conjugates

2.3.1. NMR Spectroscopy

The ^{1}H, ^{13}C, ^{19}F NMR, correlation spectroscopy (COSY) and heteronuclear single-quantum correlation spectroscopy (HSQC) characterizations were performed on a Bruker NMR Spectrometer, UltraShield™ 400mHz Plus Ultra Long Hold, Avance II+. For the stability assessment of the conjugates, the probe was set at a temperature of either 25°C or 37°C. The samples employed were the lyophilized ones (approximately 10 mg) and were dissolved in D_2O. The data treatment and acquisition were made

with the TOPSPIN Software (version 4.0.6). All the ^{1}H NMR spectra were calibrated using the residual solvent peak for the chemical shifts.

The magnetic properties of the atomic nuclei are the physical foundation of NMR. A magnetic nucleus under a magnetic field will assume one of the allowed different energy orientations. The magnetic moment can point in the opposite direction of the field or in the same direction. An energy (ΔE) that depends on the magnetic field strength and on the nuclear magnetic moment size, that is, the interaction strength between the field and the nucleus, separates these two states. Applying a radiofrequency radiation, the ΔE can be measured since this radiation will induce the flip from a lower to an upper energy level, assuring the resonance condition ΔE= hv (where h is Planck's constant and v the frequency)[164–166].

2.3.2. FTIR Spectroscopy

FTIR analysis was performed with the use of KBr pellets on a Perkin Elmer Spectrum Two Spectrometer and the data was obtained with the Spectrum Software with a range of 4000 – 400 cm^{-1}, a resolution of 4 cm^{-1}, and 36 scans. The samples used for this analysis were the freeze-dried ones, except for the pure compounds that were directly removed from the flask.

In FTIR spectroscopy, an infrared (IR) radiation is used to irradiate the sample. When the molecule is exposed to IR energy, it will absorb only frequencies that correspond to the molecular modes of vibrations in the electromagnetic spectrum region between microwaves (short waves) and red (visible). The bands that emerge in the vibrational spectrum, characterized by their amplitude and frequency, will arise from changes in vibrational motion[72,167].

2.3.3. UV/Vis Spectroscopy

UV/Vis spectra were acquired using a Perkin Elmer Lambda 25 spectrometer, employing a quartz cuvette, and the data was assessed with the Perkin Elmer UV WinLab software (version 5.2.0.0646). The samples used for this analysis were weighed out, dissolved to a concentration of 1 $mgmL^{-1}$ and diluted at a ratio of 1:480 with ultrapure water.

UV/Vis spectroscopy is based on the light that a sample absorbs upon emission of a light source. In other words, the UV/Vis spectrophotometer will scan a range of wavelengths and compare the intensity of the light before and after passing through the sample, giving an absorption spectrum. The light source of the near-UV radiation is usually a deuterium lamp while the visible radiation is produced by a tungsten filament[168,169]

2.3.4. Fluorescence spectroscopy

The fluorescence data acquisition was made using a Perkin Elmer LS 55 Fluorescence Spectrometer with a quartz cuvette and the Perkin Elmer FL WinLab Software (version 4.00.03). The samples for the acquisition of the spectra were weighed out and diluted with ultrapure water to a concentration of 50 µM. The excitation and emission wavelengths used were 335 nm and 430 nm, respectively, with an excitation slit at 10.0 nm and emission slit at 13.0 nm.

This type of spectroscopy is based on the emission of light of the sample upon excitation by a laser beam. The result is a wavelength distribution of the emission measured at a fixed excitation wavelength, that is, an emission spectrum. An excitation spectrum is also possible to be acquired upon the scanning of the excitation wavelength and measurement of the emitted light at a fixed emission wavelength.[170,171]

2.3.5. DLS and ELS

For these analyses a Zetasizer Nano ZS (Malvern Instruments Ltd.) equipment was employed. For the DLS, polystyrene latex disposable cuvettes DTS0012 were used and measurements were acquired at a temperature of 25^{o}C, with 11 runs done in triplicate. For the ELS, polystyrene latex disposable folded capillary cells DTS1070 were used and measurements were acquired at a temperature of 25^{o}C, with 15 runs in triplicate. Several dilutions of the conjugates and the dendriplexes were made to obtain final concentrations of 0.1; 0.25; 0.5; 0.75; 1.0; 1.5; and 2.0 mgmL^{-1}, and of 0; 0.1; 0.2; 0.3; 0.5; and 1.0 µM, respectively, using ultrapure water as the solvent. The data processing was done using the Zetasizer Software (version 7.12).

The DLS of both the conjugates and the dendriplexes and the ELS of the conjugates at a concentration of 1 mgmL^{-1} (the concentration that gave the most coherent results) can be found in sections 6.2 and 6.3 of the annex. Since the results obtained from this technique was not coherent, mostly due to the small size of the produced nanomaterial and the high polydispersive index (PDI), the data was not discussed.

ELS and DLS employ the potential difference of electrophoretically mobile particles at the characteristic slipping plane and the properties of colloid dispersion to assess the hydrodynamic radius (see **Figure 17**). In DLS the Doppler shift and the Brownian motion induced by the laser beam provides information about the size distribution and the size of the particles in suspension. The small frequency change in the scattered light, compared with the non-scattered one, the Doppler shift, after the irradiation of the suspension of particles in Brownian motion by a monochromatic laser beam is what provides the information about the size of the particles[172,173].

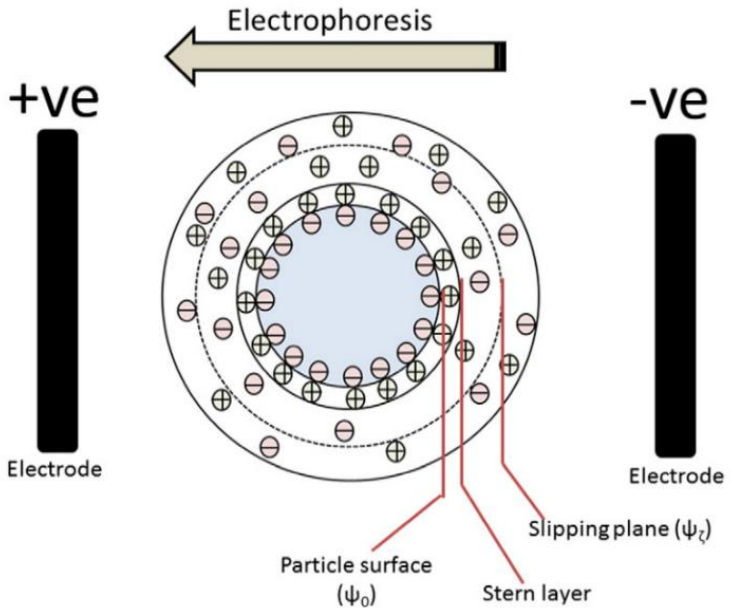

Figure 17: Schematic representation of the electric double layer on a negatively charged particle. Adapted from reference[173].

The ELS measures the zeta potential, which is the potential difference between the electric potential at the slipping plane in the electric double layer (EDL) and the potential in the bulk of the solvent. In an aqueous media, a colloidal dispersion develops an electric charge at its surface that will affect the ion distribution of the surrounding interfacial region. The increase in the concentration of counter ions close to the surface results in the formation of the EDL. This EDL comprises an outer layer, the diffuse layer, where the ions are not strongly associated, and an inner region, the Stern layer, where they are firmly bound. Inside the diffuse layer, a plane or boundary can be noted in which the particles and the ions form a stable entity. Upon the movement of the particles due to electrophoresis, the ions that are found inside the plane move with it while the ones beyond the plane will stay with the bulk dispersant. It is the potential at this plane, the slipping plane that gives the zeta potential[173,174].

2.4. Stability studies of the conjugates

Stability studies at 25°C and 37°C of the conjugates were performed with times t of 0; 30 min; 1h; 2h, 5h; 7h, 24h, 48h, 1 month, and 2 months. These stability studies were done by ^{1}H NMR for the G4_HBA 32.5 and G4_HBA 64.5 conjugates and ^{19}F NMR for the G4_TFHBA 32.5 and G4_TFHBA 64.5 conjugates.

2.5. Biological studies

2.5.1. Cytotoxicity of the conjugates

The cytotoxicity of the conjugates was done with a resazurin assay using the human embryonic kidney cell line (HEK 293T; ATCC® CRL-3216™). The cells were thawed and allowed to grow in DMEM media containing 1% of antimycotic and antibiotic and 10% of FBS (complete medium), on a Petri dish, in an incubator (37°C with 5.0% CO_2) until the desired number of cells was attained and the confluence did not reach 100%.

A 96-well plate was treated with collagen at 50 $\mu g mL^{-1}$, left for 20 min to 1h, and washed with PBS. After that, the Petri dish containing the cells was washed with 3 mL of PBS, 1 mL of trypsin was added, and the dish was incubated for 7 min to detach the cells from the bottom. After that time, the cells were resuspended in 2 mL of complete medium to stop the action of trypsin and the cells were counted. Then, each well of the 96-well plate was seeded with 5000 cells per well and the cells were incubated for 24h.

For the preparation of the conjugate solutions, ultrapure water was filtered with a cellulose-acetate filter of 0.22 µm and a syringe, and then the different samples were prepared to get a final concentration of 0.1; 0.5; 1.0; 2.0; and 5.0 µM in the wells (8 replicas were done for each sample). The medium in each well of the 96-well plate was removed and was replaced with 180 µL of complete medium plus 20 µL of sample to a final volume of 200 µL in each well. The plate was then incubated for more 48h.

Past incubation time, the medium in each well of the 96-well plate was removed, and the wells were washed with PBS (± 50 µL) to remove any residual sample. Then, a solution of resazurin (containing complete medium and 10% of resazurin (1 $mg mL^{-1}$)) was added into the wells (200 µL) and the plate incubated for 2h. After this period, 100 µL of each well was transferred to a white 96-well plate and the fluorescence was read in a microplate reader, Perkin Elmer VICTOR^{3TM} 1420 equipment, with an excitation wavelength of 530 nm and an emission wavelength of 590 nm.

The resazurin assay is a method where the blue resazurin dye is internalized and metabolically reduced in the cells to resorufin, a fluorescent pink compound that is released from the cells. This reduction of resazurin into resorufin is thought to be mediated by mitochondrial enzymes. As such, the quantity of resorufin generated is proportional to the number of viable cells[175–177].

2.5.2. Plasmid DNA (pDNA) extraction

Plasmid DNA encoding enhanced Green Fluorescent Protein and Firefly Luciferase (pEGFPLuc, 6.4 kb) was used after amplification using the DH5α *Escherichia coli* (*E. coli)* strain and after purification.

To extract the pDNA, it was first needed to pre-inoculate the bacteria containing the desired plasmid in LB medium. For this, 2 mL of kanamycin at a concentration of 25 $mgmL^{-1}$ was added into 1L of LB medium, 4 mL of this medium was then transferred to a 50 mL falcon and 10 µL of an *E. coli* glycerol stock was lastly added. This was done for two falcons. The tubes were placed on a shaker at 37°C for 6h. The content of both falcons was, afterwards, moved to the LB medium, gently shaken, distributed into sterile 500 mL Erlenmeyers, and placed on the shaker at 37°C overnight. The extraction itself was performed using an extraction kit (GenElute™ Endotoxin-free Plasmid Maxiprep kit) from Merck following the manufacturer's instructions.

For the quantitative analysis of the pDNA, 10 µL of the pDNA solution was mixed with distilled water to a final volume of 1 mL. The absorbance was read at 260 nm, and 280 nm, and the purity and quantity of the pDNA were calculated according to **Equation 1** and **Equation 2**. A solution containing 1.64 $\mu g\mu L^{-1}$ of pDNA was obtained with an acceptable purity degree for the realization of the studies.

Equation 1: Calculation of the purity of the extracted pDNA.

$$\frac{\text{OD at 260 nm}}{\text{OD at 280 nm}} > 1.6 \rightarrow \text{for the pDNA to be reasonably pure}$$

Equation 2: Calculation of the pDNA quantity.

$$\text{OD at 260 nm} \times 50\ \mu g mL^{-1} \times \text{dilution factor}$$

2.5.3. pDNA condensation and neutralization studies

The PicoGreen® assay was performed to evaluate the DNA condensation capability of the synthesized conjugates. Therefore, a Tris-EDTA 1x (TE 1x) solution was prepared from a TE 20x solution to dilute the pDNA to a concentration of 0.1 $\mu g\mu L^{-1}$ and to prepare the conjugate solutions for the analysis. The dendriplex solutions were prepared with the conjugates at concentrations of 0.1, 0.2, 0.3, 0.5 and 1.0 µM, and a fixed volume of pDNA solution (10 µL) in a final total volume of 1 mL. The samples were then incubated at 37°C for 15-20 min to allow the conjugates to condense the pDNA (that is, to form the dendriplexes).

The PicoGreen® solution was prepared in the meantime by diluting the stock solution 200 times. After the incubation time, a 100 µL volume of the dendriplexes was transferred to a white 96 well plate

and 100 µL of the PicoGreen® solution was added to each well. This was done in triplicate and a blank containing 100 µL of TE 1x and 100 µL of PicoGreen® solution was also done. The plate was incubated for 5 min at 37°C and, afterwards, the fluorescence was read in the microplate reader with an excitation wavelength of 485 nm and emission of 535 nm.

PicoGreen® is a fluorescent probe that selectively binds dsDNA and forms a bright fluorescent complex. When in solution with relaxed dsDNA, that is, DNA that is free in solution, the fluorescence is at its maximum. If the dsDNA is compacted, the PicoGreen® will be unable to bind with the dsDNA and the fluorescence will decrease[178,179].

2.5.4. Cytotoxicity of the complexes

The resazurin assay was also used to assess the metabolic activity of the HEK 293T cells in the presence of the dendriplexes. The methodology used was the same as for the cytotoxicity of the conjugates. The dendriplex solutions were prepared as previously described for the PicoGreen® assay at conjugate final concentrations of 0, 0.1, and 0.5 µM, and adding 10 µL of pDNA at 0.1 $\mu g \mu L^{-1}$ to each sample. The assay was performed after 2h of incubation.

The BCA assay for protein quantitation was also performed using a kit (Sigma) and was used to compare and verify the cytotoxicity of the complexes (this assay is explained in the next section).

2.5.5. Transfection studies.

On a collagen treated 48 well plate, an amount of 10 000 HEK 293T cells per well were allowed to grow for 24h. On the next day, the cells were exposed to the complexes at concentrations of 0, 0.1 and 0.5 µM, and incubated at 37°C, with 5% CO_2, for 48h. Afterwards, the medium of the wells was completely removed, the wells were washed with PBS and the plate was observed by fluorescence microscopy (Nikon TE2000-E). A digital image recording and image analysis were performed with the NIS Elements Advanced Research (version 2.31) software. Lysis buffer was then added to each well and the plate was put under ultrasounds for 5 min, and then frozen for a later assessment of the total protein and Luciferase activity.

After thawing the plate, the total protein assay was done using the BCA protein assay kit following the supplier's information (can be found in the annex in section 6.5). The luciferase activity assay was performed with Promega's luciferase kit following the supplier's instructions too (can be found in the annex in section 6.6). The plates were then read in the microplate reader.

The luciferase assay is based on the transformation of the luciferin substrate, through the luciferase enzyme, to produce the non-reactive bioluminescent oxyluciferin which can be measured[180,181].

The BCA assay requires the conversion of Cu^{2+} to Cu^{+} under alkaline conditions, which is then detected by the reaction with BCA resulting in an intense purple colour with an absorption maximum at 562 nm. The Cu^{+} production is a function of incubation time and protein concentration and as such, for the assessment of the protein content of the samples, a spectrophotometric comparison with a known protein standard is required[182]. In this study, the standard used was bovine serum albumin.

2.6. Treatment of the results

The data handling was done by using different equipment software or handled with the Microsoft Office 365 suite (version 16.0.11929.20.300) by the Microsoft Corporation and the Spectragryph software[183] (version 1.2.9) by Friedrich Menges.

Chapter III: Results and Discussion

3.1. Synthesis and characterization of the conjugates

The synthesis of the conjugates, as exemplified in **Figure 18**, was performed using HBA and TFHBA at compound/dendrimer molar ratios of 64.5 and 32.5 in order to obtain 100% and 50% functionalization degrees, respectively. The reagent solutions were prepared in ultrapure water, with PAMAMG$_4$-NH$_2$ at a concentration of 20 mgmL^{-1} (1.41 mM) and the compounds at a concentration of 4 mgmL^{-1} (28.96 mM for HBA and 19.04 mM for TFHBA). For the synthesis, the compound solution (HBA or TFHBA) was added dropwise into a stirred PAMAMG$_4$-NH$_2$ solution and the reaction mixture was left under stirring at room temperature for 48h. The solutions maintained their transparency throughout the reaction, with no change in color nor precipitate formation occurring. After dialysis against distilled water and freeze drying, the compounds were characterized by different techniques. The compounds obtained after lyophilization were a yellowish sticky material for the PAMAMG$_4$-NH$_2$ functionalized with HBA and a puffy, shining white material for the PAMAMG$_4$-NH$_2$ functionalized with TFHBA.

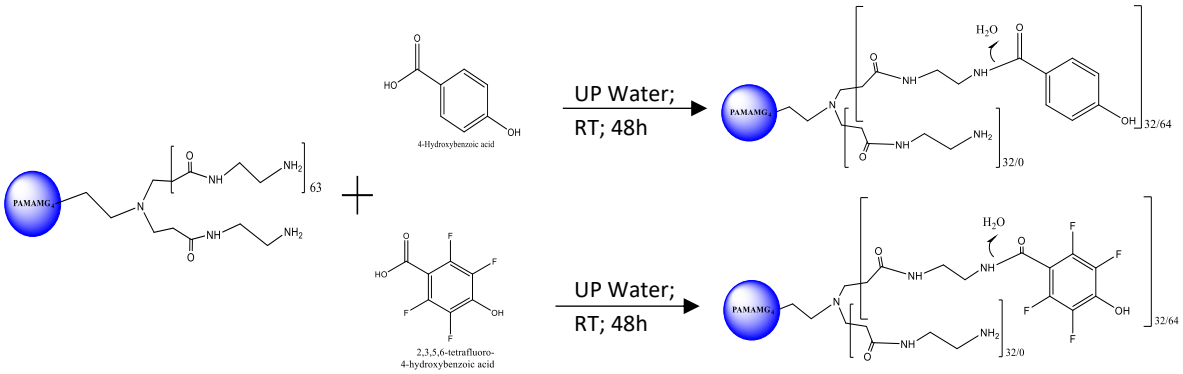

Figure 18: Schematic of the synthesis performed for the construction of the conjugates.

3.1.1. pH assessment before and after the synthesis reaction

At the beginning of the synthesis process, the pH of the reagent solutions was measured as shown in **Table 2**. As expected, the dendrimer solution was basic due to the presence of 64 amine groups in the molecule (pH=10). At a pH of 10, the PAMAMG$_4$-NH$_2$ is not protonated, only starting to protonate at a pH of nearly 9, beginning with the primary amines; the tertiary amines are protonated in a two-step manner at pH 6.4 and pH 3.5[63,64,110]. On the contrary, the HBA and TFHBA solutions were acid at the starting conditions (pH=3 and 2, respectively) due to the presence of the carboxylic group in their molecular structure. Owing to the presence of fluorides in its structure, TFHBA is a stronger acid than

HBA. At the end of the reaction, the addition of either HBA or TFHBA to the dendrimer solutions resulted in a decrease in pH of the overall solution as the reaction involved the amino groups in the dendrimer with the carboxylic groups in the added compounds. At the end of the reaction, as can be seen in **Table 2**, the pH was dependent on the functionalization degree of the dendrimer, decreasing when the molar ratio of HBA/dendrimer or TFHBA/dendrimer used in the synthesis increased from 32.5 to 64.5. In the case of HBA, the reduction in pH was from 8.0 to 6.0, while TFHBA was from 7.0 to 5.0. These changes in pH indicate that a reaction has occurred between the reagents.

Table 2: pH measurements of the synthesis products.

Starting reagents	pH	pH at the end of the reaction	Final product
PAMAMG$_4$-NH$_2$	10.0	8.0	G4_HBA 32.5
HBA	3.0		
PAMAMG$_4$-NH$_2$	10.0	6.0	G4_HBA 64.5
HBA	3.0		
PAMAMG$_4$-NH$_2$	10.0	7.0	G4_TFHBA 32.5
TFHBA	2.0		
PAMAMG$_4$-NH$_2$	10.0	5.0	G4_TFHBA 64.5
TFHBA	2.0		

3.1.2. NMR characterization of the conjugates

The successful conjugation of the compounds with the dendrimers was evaluated using NMR spectroscopy using D_2O as the deutereated solvent. This data was later complemented with the data obtained with other techniques (such as UV/Visible, fluorescence, and FTIR spectroscopies). In **Figure 19**, the ^{1}H NMR of the dendrimer functionalized with HBA is depicted. As can be seen, the signals of the PAMAMG$_4$-NH$_2$ change position after functionalization with HBA, namely the ones corresponding to the proton that may be found at the end of the branches of the dendrimer[184–186]. This switch in position and the appearance at 7.83 ppm and 6.91 ppm of the doublets characteristic of HBA with a small shift to the upperfield confirms the conjugation of HBA with the dendrimer. Interestingly, the doublet corresponding to the protons near the carboxylic group has a more significant shift than the one corresponding to the protons near the hydroxylic group. This tell us that something happened at the end of the carboxylic group of HBA and provides support that this group is involved in the conjugation of PAMAMG$_4$-NH$_2$ with HBA. The ^{13}C NMR (**Figure 20**) shows the same tendency seen in the ^{1}H NMR, with the shift of the signals corresponding to the carbons near the carboxylic group of HBA, thus confirming that this group is involved in conjugation with PAMAMG$_4$-NH$_2$. COSY and HSQC analysis were performed in order to determine which signals in the ^{1}H NMR as well as in the ^{13}C NMR

belong to which part of the molecules. In **Figure 21** and **Figure 22,** COSY and HSQC analysis of the sample G4_HBA 32.5 is shown. With the use of **Equation 3** the number of HBA molecules linked to the dendrimer could be determined[187]. In the synthesis with 32.5 molar equivalents of HBA, the achieved functionalization was 32 in 64 (50%), whereas the synthesis with 64.5 molar equivalents of HBA resulted in 54 of 64 (84%). Probably, the full functionalization of the dendrimer was impaired by steric hindrance[188].

Equation 3: Calculation of the number of HBA attached to the PAMAMG$_4$-NH$_2$[187].

$$N^{er}\text{ of functionalization} = \frac{\text{Experimental } n^{er}\text{ of aromatic H}}{4}$$

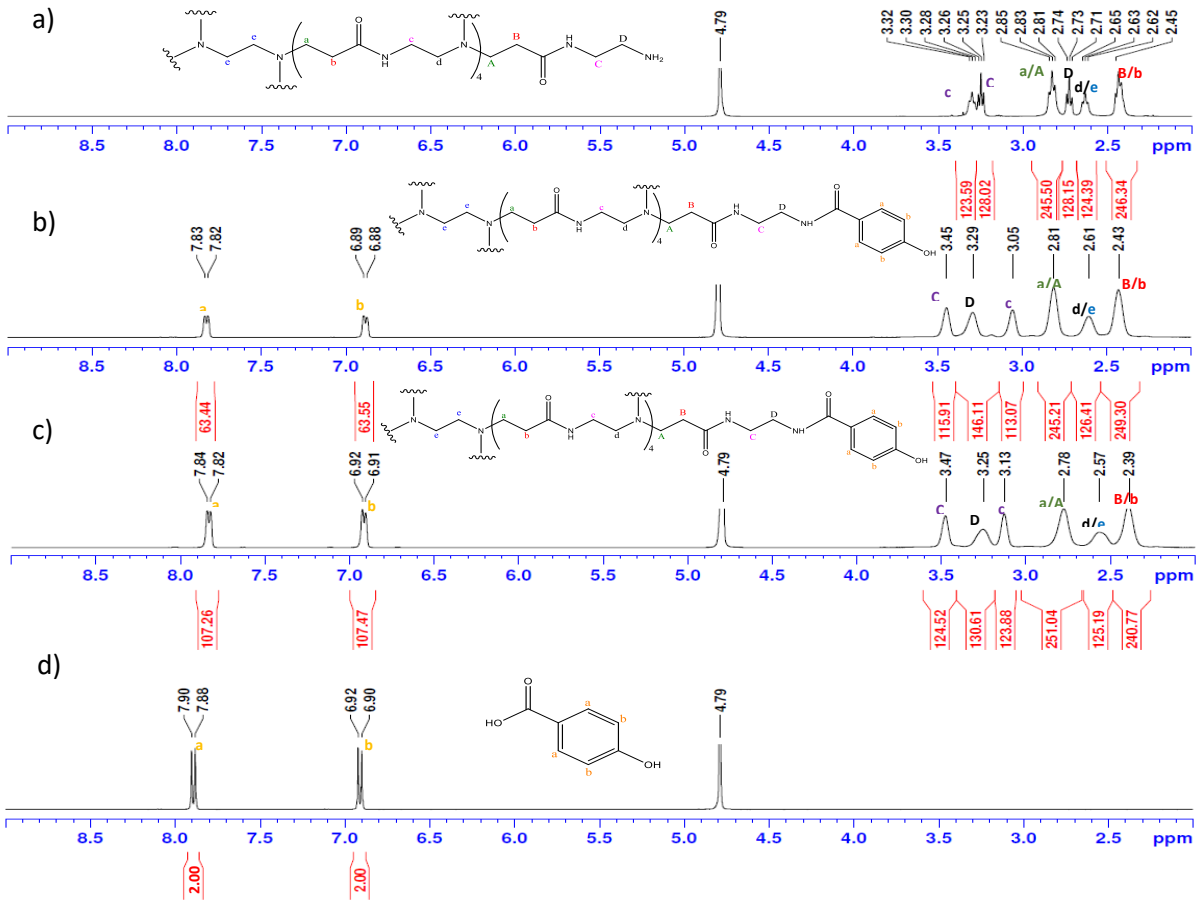

Figure 19: ^{1}H NMR in D_2O of a) PAMAMG$_4$-NH$_2$, b) G4_HBA 32.5, c) G4_HBA 64.5, and d) HBA.

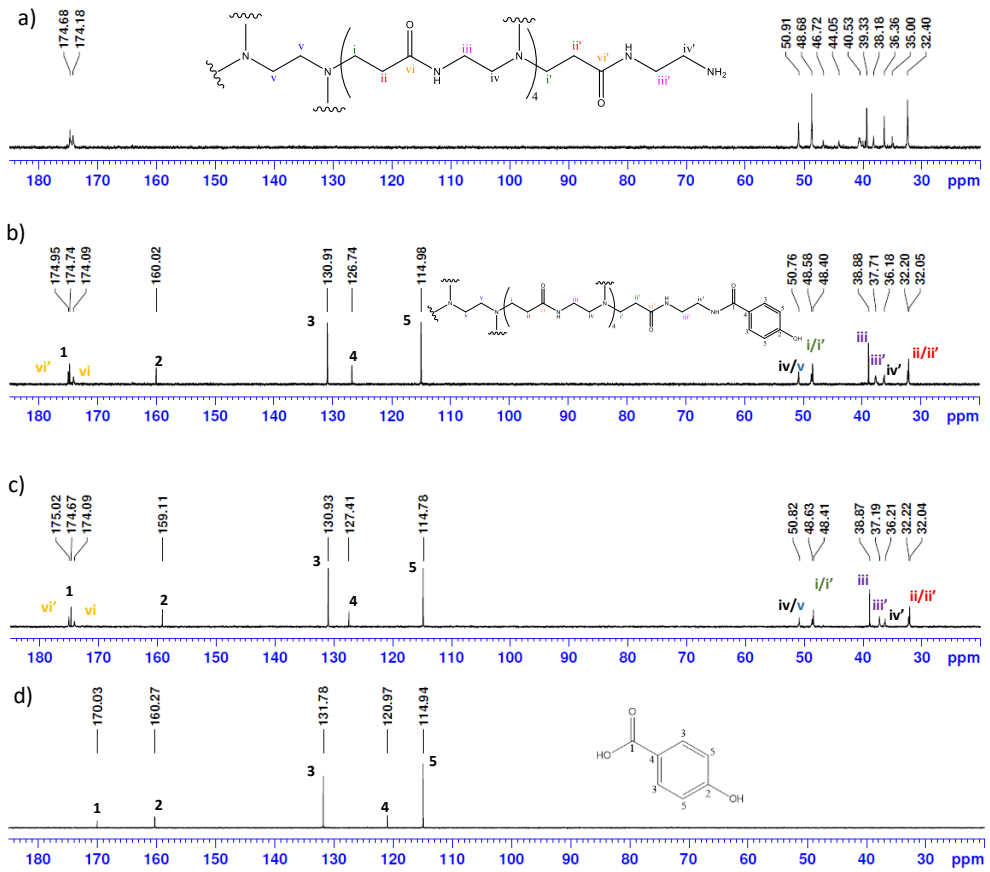

Figure 20: ^{13}C NMR of a) PAMAMG$_4$-NH$_2$; b) G4_HBA 32.5; c) G4_HBA 64.5; and d) HBA.

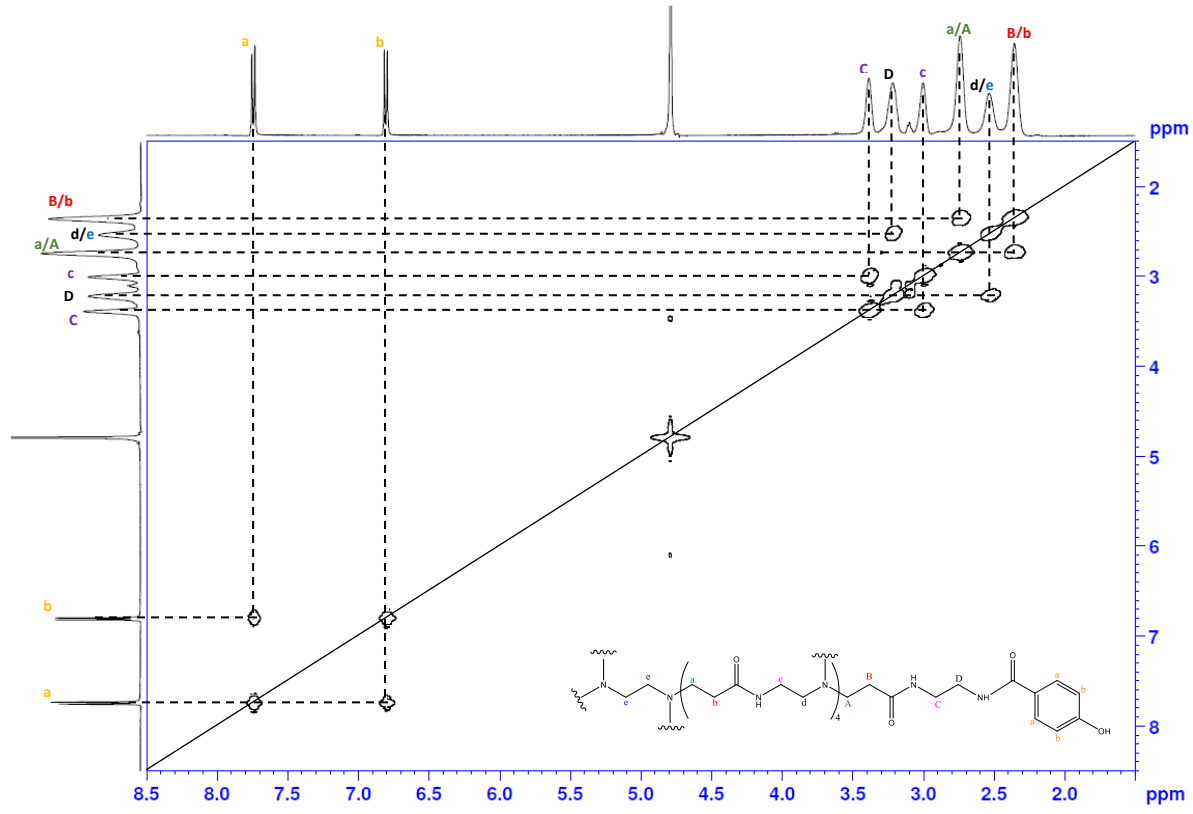

Figure 21: COSY of G4_HBA 32.5.

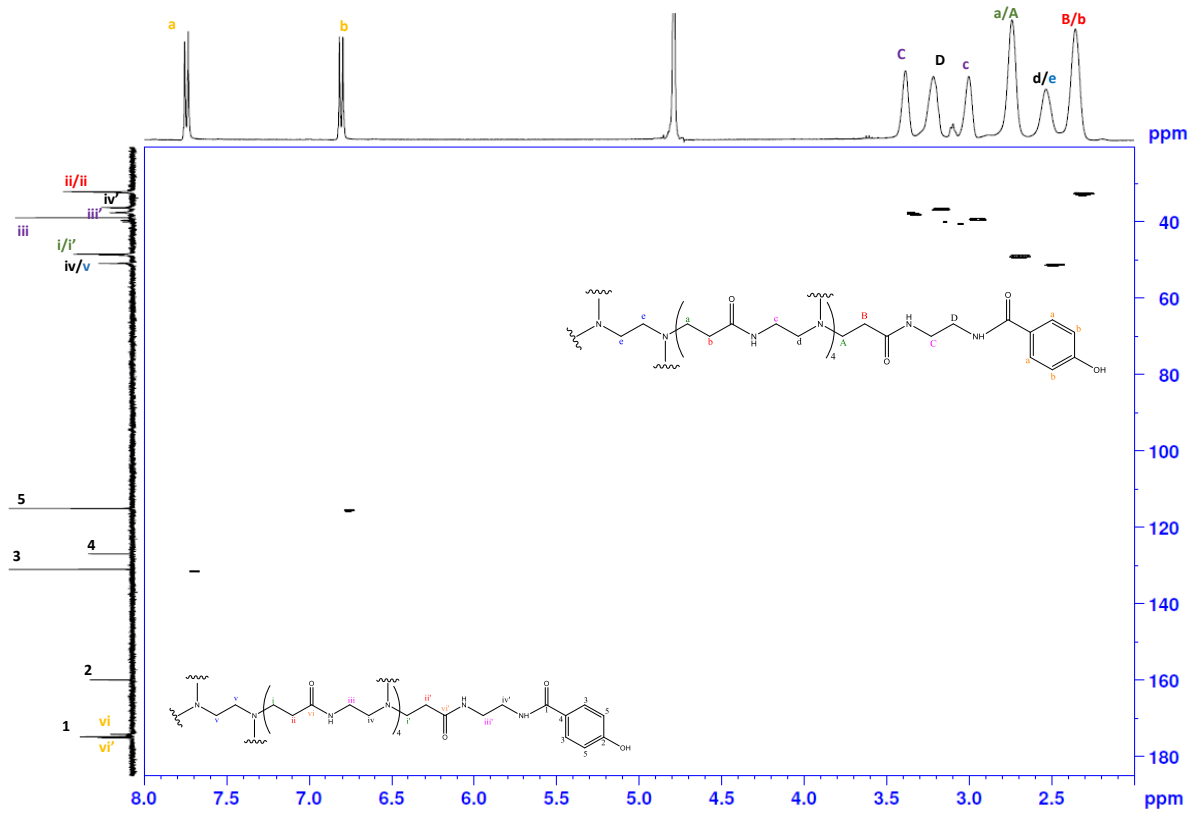

Figure 22: HSQC of G4_HBA 32.5.

The ^{1}H NMR of the G4_TFHBA conjugate functionalized with 32.5 and 64.5 molar equivalents can be found in **Figure 23.** Similar to the case of HBA, the functionalization of the PAMAMG$_4$-NH$_2$ with TFHBA led to a shift in the same signals of the dendrimer. Since the aromatic ring would not present any signals on the ^{1}H NMR, since instead of hydrogen atoms, it contains fluorine in the same positions, a ^{19}F NMR analysis was performed, and the results are presented in **Figure 24**. The characteristic signals of TFHBA are depicted in **Figure 24 (a)** at 142.45 ppm and 162.28 ppm and, when bonded to the dendrimer, there is an upperfield shift of approximately 6.0 ppm for the signal corresponding to the F near the carboxylic group (for both compound/dendrimer ratios) and of 4.5 and 4.1 ppm for the signal of F near the hydroxyl group (for the synthesis with 32.5 and 64.5 molar equivalents, correspondingly)[189]. Similarly to what happens with HBA, the shift of the doublet corresponding to the fluorines near the carboxylic group has a bigger shift than the one corresponding to the doublet corresponding to the fluorines near the hydroxylic group. From this the same conclusion can be taken: the carboxylic group of TFHBA is involved in the conjugation of PAMAMG$_4$-NH$_2$ with TFHBA. These shifts, as well as the change of position of the dendrimer signals, confirmed the conjugation of TFHBA with PAMAMG$_4$-NH$_2$.

Considering that there are no signals of the aromatic ring in the ^{1}H NMR, the equation used for HBA cannot be considered here to determine the functionalization degree achieved in the synthesis. Nevertheless, for further calculations, the degree of functionalization was assumed to be the same as HBA, when either TFHBA or HBA were used.

Complementing data such as ^{13}C NMR, HSQC, and COSY can be found in section 6.1 of the annex. These data were acquired to confirm the signal position of the prepared compounds in the NMR spectra.

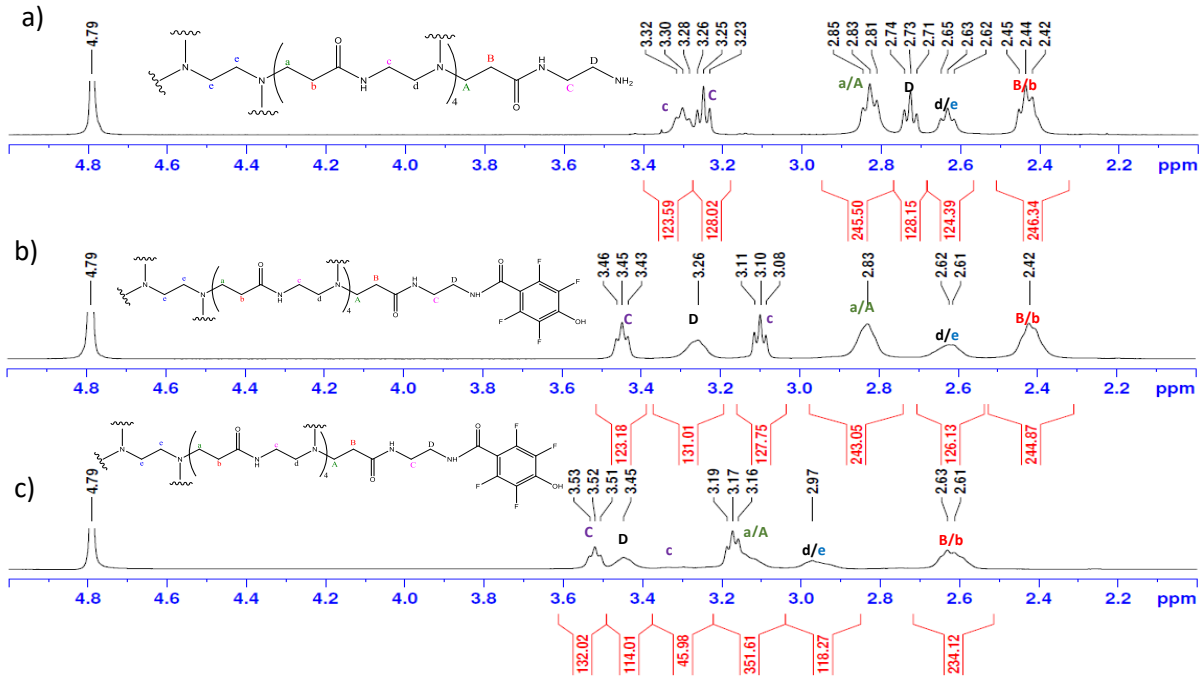

Figure 23: ^{1}H NMR in D_2O of a) $PAMAMG_4\text{-}NH_2$, b) G4_TFHBA 32.5, and c) G4_TFHBA 64.5.

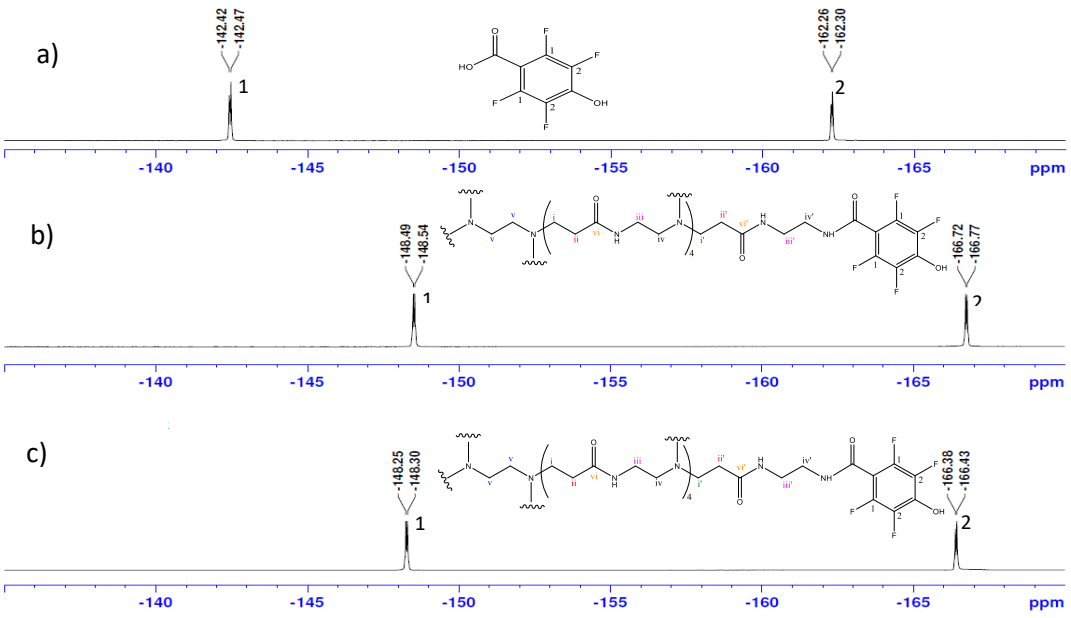

Figure 24: ^{19}F NMR in D_2O of a) TFHBA, b) G4_TFHBA 32.5, and c) G4_TFHBA 64.5.

3.1.3. FTIR characterization of the conjugates

FTIR analysis of the compounds did not provide enough evidence to confirm the conjugation of the dendrimer with HBA (**Figure 25**) or TFHBA (**Figure 26**). Nevertheless, the shift of the peaks of Amide I and II of PAMAMG$_4$-NH$_2$ to the right for HBA and to the left for TFHBA might be a result of the conjugation involving the -COOH of HBA or TFHBA with the NH$_2$ of PAMAMG$_4$-NH$_2$[156,190,191].

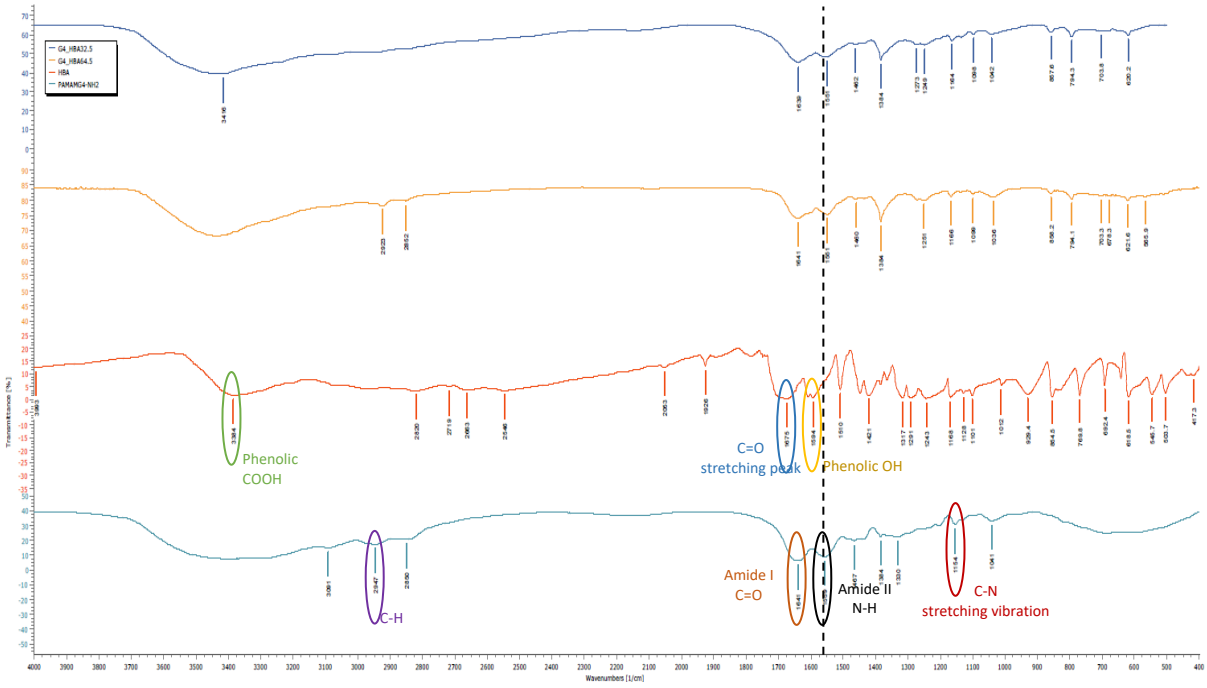

Figure 25: FTIR analysis with a KBr pellet of the dendrimer functionalized with HBA.

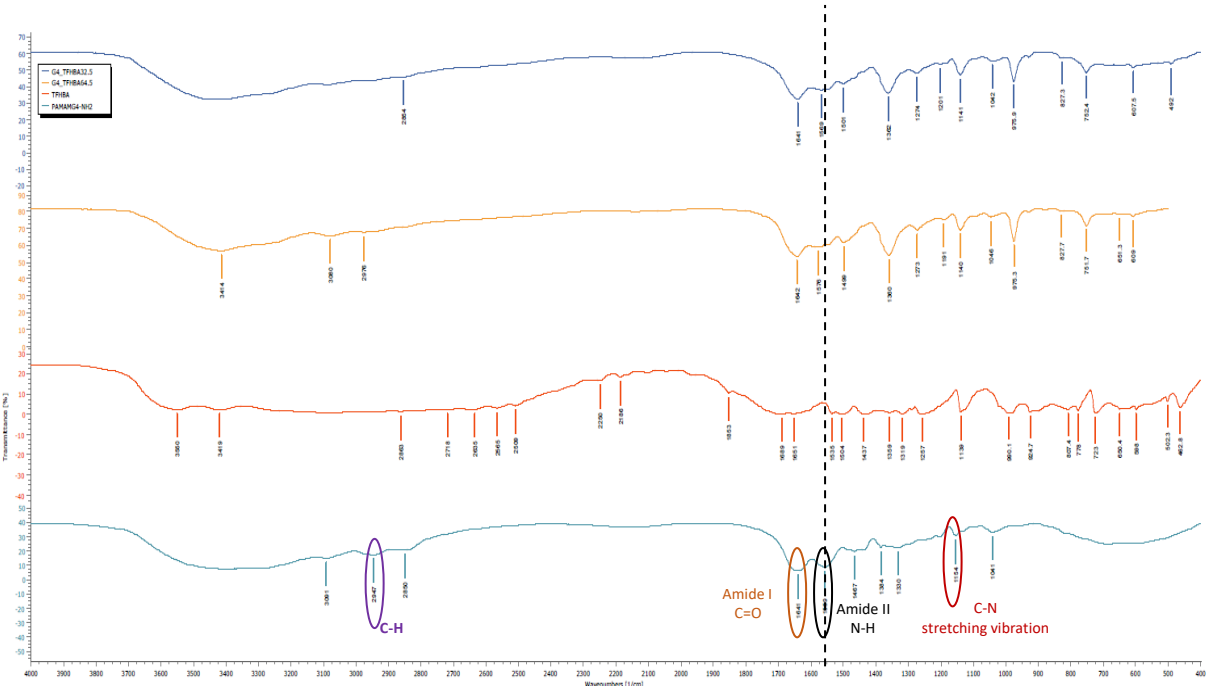

Figure 26: FTIR analysis with a KBr pellet of the dendrimer functionalized with TFHBA.

3.1.4. UV/Visible characterization of the conjugates

Figure 27 shows the UV/Vis spectra for the free HBA, the free TFHBA, the pristine PAMAMG$_4$-NH$_2$ dendrimers, and the functionalized PAMAM dendrimers. In the 225-300 nm wavelength range, the pristine PAMAMG$_4$-NH$_2$ dendrimers have a very low absorption, but when conjugated with the absorbing compounds HBA or TFHBA, the absorption is enhanced which is an evidence of the success of conjugation. This conclusion is also supported by the observed shifts in the wavelength of maximum absorption when comparing the results obtained with the conjugated HBA/TFHBA molecules and the free ones.

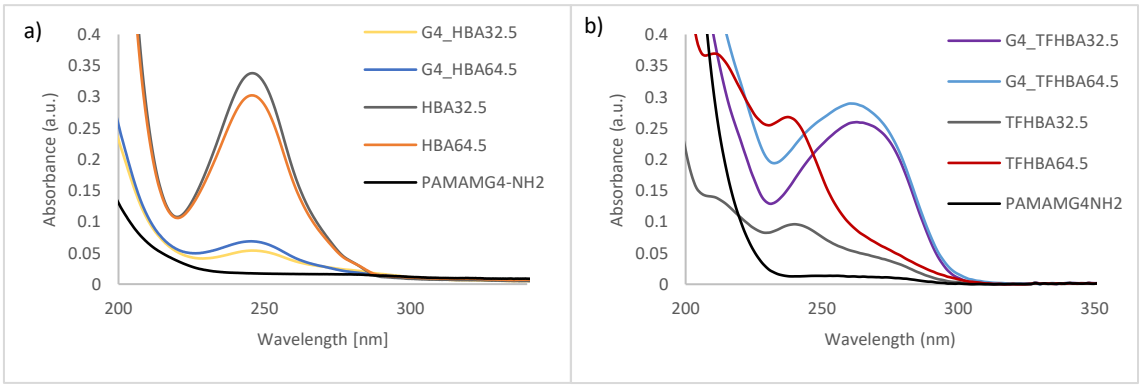

Figure 27: UV/Visible spectra of the conjugation of the dendrimers with the compounds (concentration of 1 mgmL^{-1} and diluted at a ratio of 1:480 with ultrapure water. a) Conjugation of the PAMAMG$_4$-NH$_2$ dendrimer with HBA at dendrimer/compound ratios of 32.5 and 64.5; b) Conjugation of the PAMAMG$_4$-NH$_2$ dendrimer with TFHBA at dendrimer/compound ratios of 32.5 and 64.5.

In the case of G4_HBA (**Figure 27 a**), the conjugation resulted in a slight hypsochromic shift of the maximum absorption wavelength to a higher energy (i.e. blue shift) from 251 nm to 247 nm. Also, the absorbance increased with the degree of functionalization, which was expected as a higher number of HBA molecules were conjugated to the dendrimer. Comparing the absorbance values measured for the conjugated compounds and the pure ones, the UV/Vis studies seem to support the idea that the attained dendrimer functionalization was effectively stoichiometric. Interestingly, when TFHBA was used (**Figure 27 b**), the conjugation resulted in a bathochromic shift of the maximum absorption wavelength to a lower energy (i.e. red shift) from 236 nm to 263 nm corresponding to a shoulder in the spectrum[192–194]. While it is clear that HBA presents much higher absorbance than TFHBA, the uncertainty in the molar concentration of the TFHBA-conjugated dendrimers does not allow to make conclusions from the correspondent absorption intensities depicted in the graph.

3.1.5. Fluorescence characterization of the conjugates

When excited with light at 335 nm, PAMAMG$_4$-NH$_2$ shows an emission peak of around 430 nm. The effect of the conjugation of HBA and TFHBA on the fluorescence behaviour of PAMAMG$_4$-NH$_2$ was

evaluated by fluorescence spectroscopy and is shown in **Figure 28**. Since there is uncertainty regarding the degree of dendrimer functionalization when TFHBA is used and taking into account that fluorescence spectroscopy is a very sensitive technique (fluorescence intensity can vary significantly upon small changes in concentration), one will not discuss these results regarding the fluorescence intensity. However, after functionalization, it is possible to observe a slight shift in the maximum emission wavelength for the peak that corresponds to the intrinsic fluorescence of dendrimers (around 430 nm)[82–85]. Thus, the fluorescence spectra indicate that the PAMAM dendrimer conjugation to HBA and TFHBA was effective.

The small bump between 360 nm and 400 nm in all the spectra are due to the solvent used, ultrapure water, and correspond to the Raman scattering band of water[195,196].

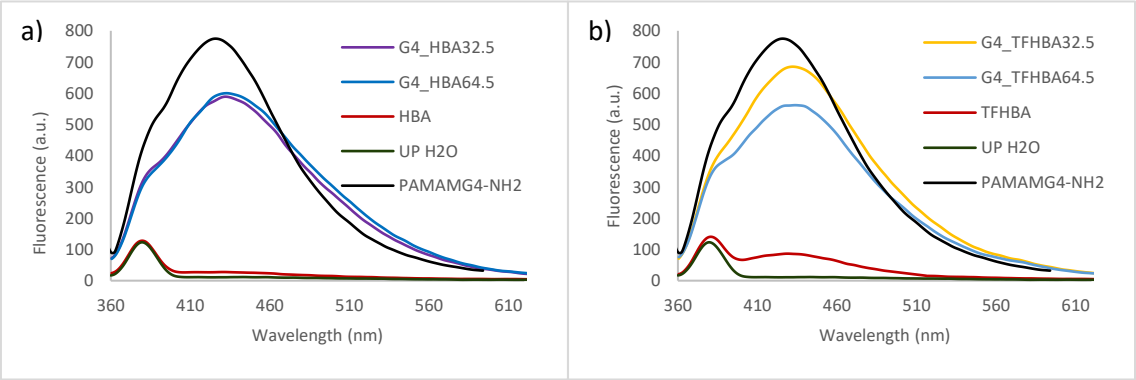

Figure 28: Emission spectra ($\lambda_{ex.}$= 335 nm) for the pristine and functionalized dendrimers in UP H_2O. a) G4_HBA 32.5, G4_HBA 64.5, and PAMAMG_4-NH_2; b) G4_TFHBA 32.5, G4_TFHBA 64.5, and PAMAMG_4-NH_2. The concentration of the samples was of 50 µM.

3.2. Stability Studies of the conjugates

Stability studies of the different conjugates made can be found in section 6.4 of the annex. From **Figure 29** to **Figure 32** the stability of G4_HBA and G4_TFHBA at the 64.5 compound/dendrimer ratio for the stability done at 25ºC and 37ºC are shown. Both functionalizations of the PAMAMG_4-NH_2 dendrimer, that is, the grafting of either TFHBA or HBA onto PAMAMG_4-NH_2, led to stable systems at 25ºC and 37ºC for more than one month.

In the ^{1}H NMR spectra for the conjugates with HBA, only after 1 month at 37ºC a change in the signals between 3.5 and 2.0 ppm corresponding to the PAMAMG_4-NH_2 can be seen. At 25ºC this change is not so visible. Moving to the ^{19}F NMR spectra done for the conjugate with TFHBA, after 2 months at 25ºC and 1 month at 37ºC, a small doublet at 145 ppm and another at 166 ppm appears and grows in prominence with time (from 1 month to 2 months at 37ºC). These changes indicate that the system started to break.

A more thorough analysis of the spectra revealed that the breaking of the system does not occur in the linkage of the aromatic ring with the dendrimer. If it was so, then the signals appearing in the ^{19}F NMR would be in the same region as the signals of the pure compound and that does not happen. This may indicate that the PAMAMG$_4$-NH$_2$ dendrimer is breaking inside-outward.

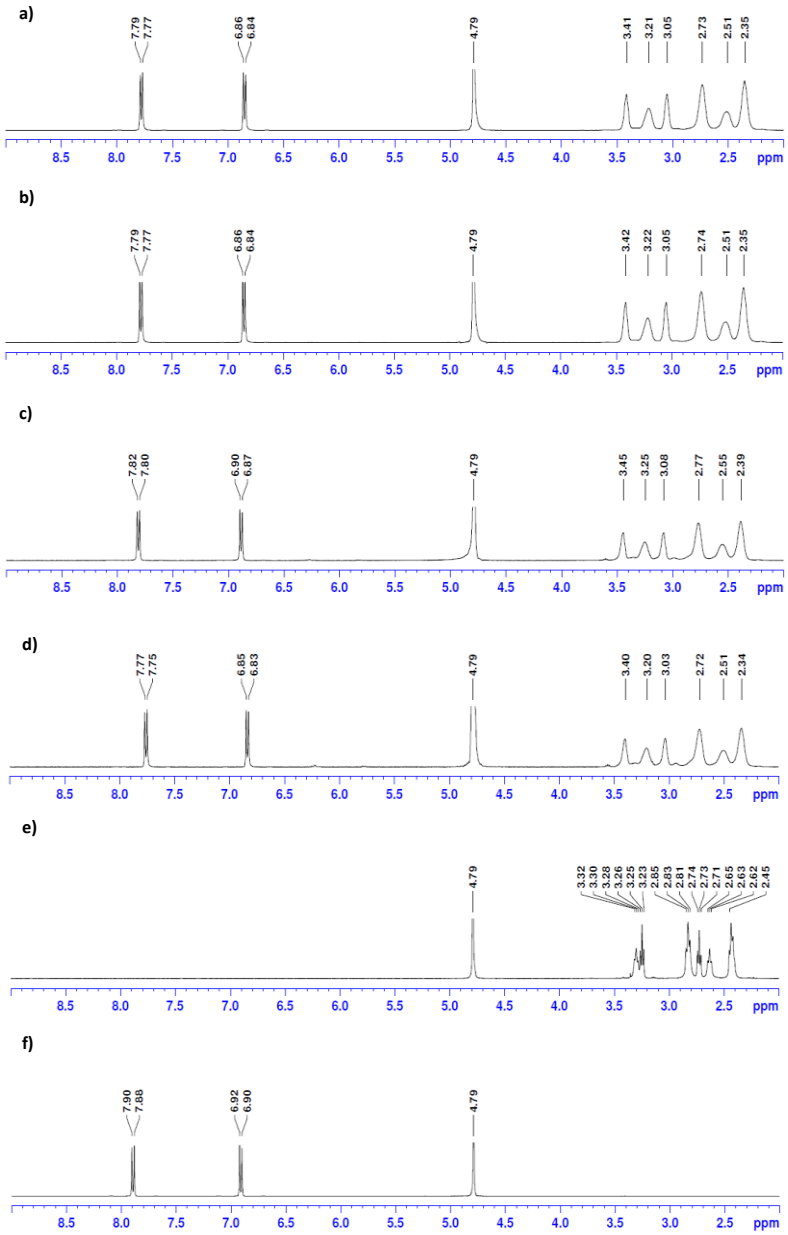

Figure 29: ^1H NMR stability studies of G4_HBA 64.5 at 25^oC in D_2O. . a) t = 24h; b) t = 48h; c) t = 1 month d) t = 2 months; e) PAMAMG$_4$-NH$_2$; and f) HBA.

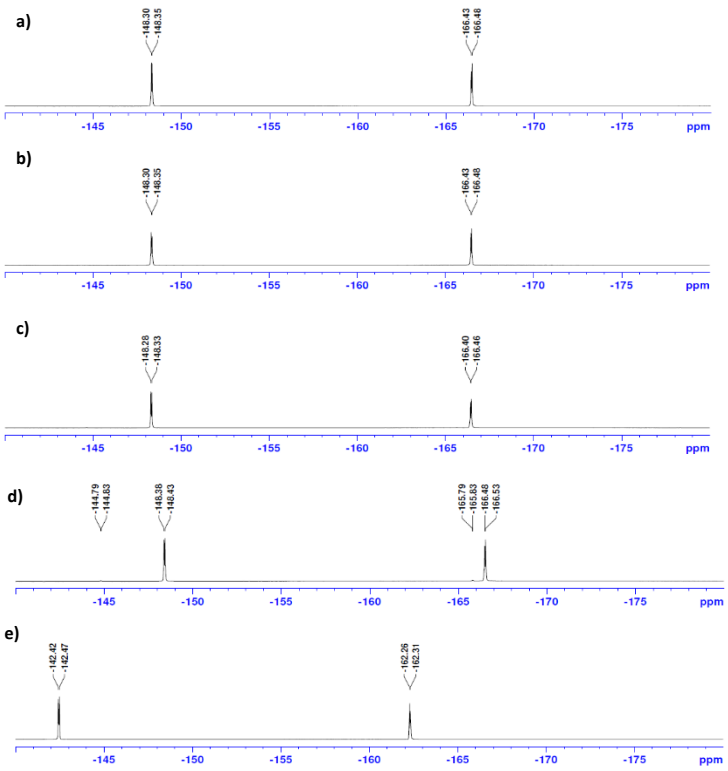

Figure 30: ^{19}F NMR stability studies of G4_TFHBA 64.5 at 25°C in D_2O. a) t = 24h; b) t = 48h; c) t = 1 month; d) t = 2 months; and e) TFHBA.

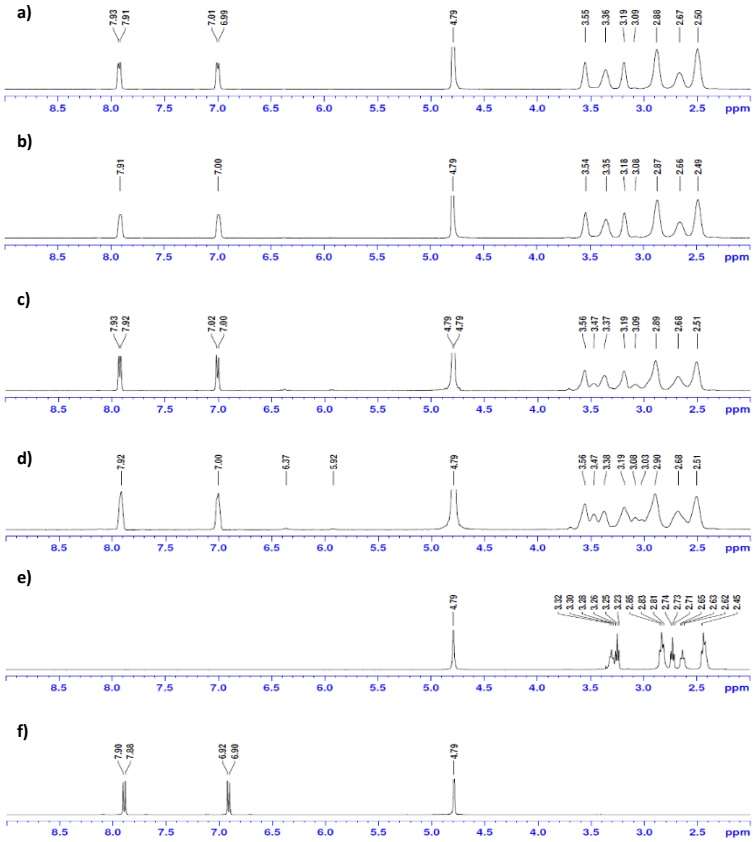

Figure 31: ^{1}H NMR stability studies of G4_HBA 64.5 at 37°C in D_2O. a) t = 24h; b) t = 48h; c) t = 1 month; d) t = 2 months; e) PAMAMG$_4$-NH_2; and f) HBA.

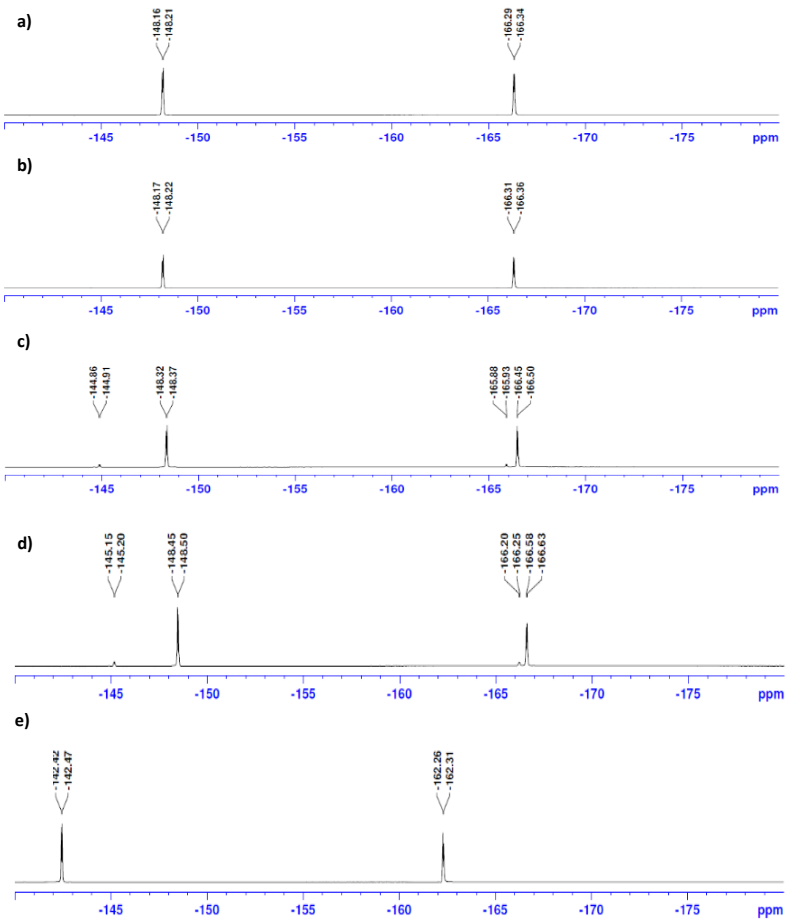

Figure 32: ^{19}F NMR stability studies of G4_TFHBA 64.5 at 37°C in D_2O. a) t = 24h; b) t = 48h; c) t = 1 month; d) t = 2 months; e) TFHBA.

3.3. Biological studies of the conjugates

After the synthesis and characterization of the conjugates, their biological behaviour was evaluated, namely by studying their cytotoxicity and transfection efficiency. HEK 293T cells were used in all assays.

3.3.1. Cytotoxicity of the conjugates

A metabolic activity assay, the resazurin reduction assay, was used as an indirect measurement of cell viability. That is, only viable cells are metabolically active. As shown in **Figure 33**, the study was done with compound concentrations ranging from 0.1 to 5 µM and the metabolic activity values were expressed as a percentage of the control (cells cultured only in the presence of culture medium). From the results it is clear that the metabolic activity of the cells decreased with an increase in the dendrimer concentration and that, in all cases under analysis, significant toxicity is only observed at

concentrations above 2.0 µM. At low concentrations (0.1 and 0.5 µM), the functionalization of the PAMAMG$_4$-NH$_2$ dendrimer with either HBA or TFHBA seems to improve cell viability. Moreover, cell viability increases with the degree of functionalization of the dendrimer. The same happens at higher concentrations (1.0 µM and higher), except for the G4_HBA 64.5 conjugate that seems to be the most cytotoxic. Overall, the dendrimers functionalized with TFHBA show the best cytocompatibility behaviour, particularly G4_TFHBA 64.5, which possesses a higher fluoride content. This decrease in cytotoxicity upon fluorination is in accordance with what is reported in the literature for other fluorinated dendrimers[124,127–130].

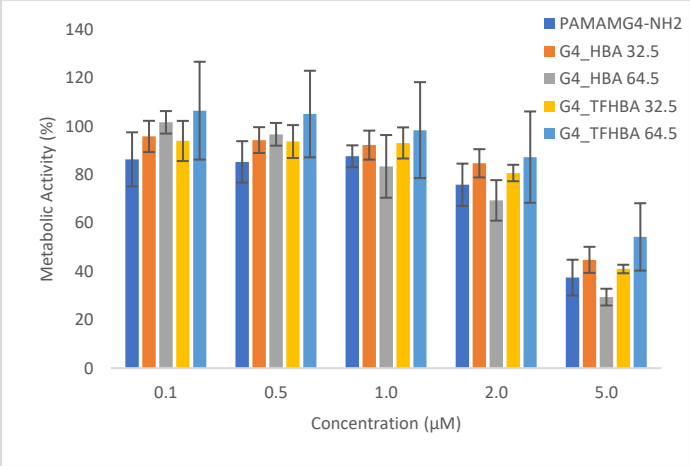

Figure 33: Cytotoxicity evaluation by the resazurin metabolic activity assay of the conjugates at different concentrations after 48h incubation at 37°C. Results are expressed as a percentage of the control ± standard deviation.

3.3.2. pDNA condensation and neutralization studies

In order to be good transfection agents, dendrimers should be able to neutralize the charge of pDNA and lead to its compaction. One possible method that can be used to assess pDNA compaction is the PicoGreen® assay. PicoGreen® shows a high fluorescence intensity when intercalated with pDNA, which happens when the nucleic acid is in an extended conformation. When pDNA is compacted, the dye cannot intercalate with pDNA and the fluorescence intensity is low[178,179]. **Figure 34** shows the PicoGreen® assay results obtained after the addition of the dye to the dendriplexes (complexes of dendrimers and pDNA) prepared from either the PAMAMG$_4$-NH$_2$ dendrimers alone or the conjugates at different concentrations. The pDNA concentration was kept constant in all situations. It can be observed that even at a concentration of 0.1 µM all of the dendrimers (pristine and functionalized dendrimers) completely condense the pDNA with no visible differences among them. For the pristine PAMAM dendrimers, this efficient compaction of the pDNA has been attributed to their positive charge at near-neutral pH[59–65]. In the case of the dendrimers functionalized with HBA and TFHBA, other types

of interactions may also occur with pDNA that result in its compaction. One possible type of interaction that may occur in the systems that possess TFHBA is halogen bonding[197–200].

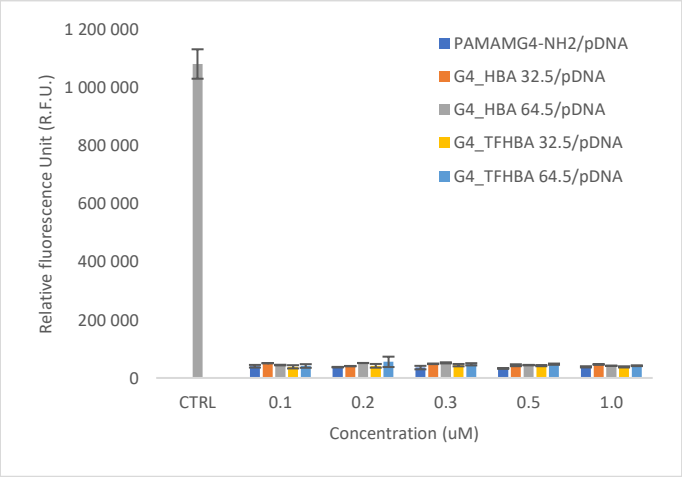

Figure 34: pDNA condensation assessment using the PicoGreen® assay (value ± standard deviation). Dendriplexes were prepared at different dendrimer concentrations.

3.3.2.1. ELS and DLS of the dendriplexes.

The pDNA compaction was also assessed by DLS and the results are shown in section 6.3 of the annex. The hydrodynamic diameter of the dendriplexes was shown to be much lower than that measured for pDNA and have similar values for all the dendrimers studied (around 400 nm). Nucleic acids possess a high negative charge due to the phosphate groups present along their chains and, since the cell membrane also has a net negative charge, repulsion may occur between both. As such, it is important not only to compact pDNA, but also to neutralize its negative charge in order to obtain a high transfection efficiency. Having this in mind, the ability of the pristine and functionalized dendrimers to neutralize the pDNA charge was evaluated by measuring the zeta potential of the dendriplexes.

In **Table 3** the zeta potential of the dendriplexes prepared using dendrimer concentrations of 0.1 and 0.5 µM are shown. The complete set of results assessed for the dendriplexes prepared using dendrimer concentrations ranging from 0.1 to 1 µM are presented in section 6.3 of the annex. The results show that all dendriplexes presented positive zeta potential values though not highly positive, which could compromise the cell viability. Positively charged particles are best to cross the cell membrane but, if too positive they might disrupt the cell membrane and lead to cell death[143,147,201]. Also, although not very markedly, the zeta potential increases with the concentration of the dendrimers used in the dendriplex formulation, which was expected since a higher number of protonated dendrimers will interact with the pDNA. Maintaining constant the concentration of

dendrimers used in the dendriplex preparations, the achieved zeta potential was higher in the case of the dendriplexes containing the pristine PAMAMG_4-NH_2 dendrimer as it has a higher number of protonated amine groups available to interact with pDNA. For the functionalized dendrimers, the number of available amines at the dendrimer surface is lower (decreasing with the degree of dendrimer functionalization) and that has a clear effect on the zeta potential of the correspondent dendriplexes. In fact, the zeta potential values are less positive for all except G4_TFHBA that with the increase in the functionalization degree the zeta potential increases.

Table 3: Zeta potential of the dendriplexes (value ± standard deviation).

Dendriplexes	**Zeta Potential (mV)**	
	0.1 µM	**0.5 µM**
PAMAMG_4-NH_2/pDNA	4.2 ± 0.2	4.5 ± 0.4
G4_HBA 32.5/pDNA	2.6 ± 0.2	3.9 ± 0.4
G4_HBA 64.5/pDNA	1.4 ± 0.2	3.0 ± 0.4
G4_TFHBA 32.5/pDNA	0.7 ± 0.6	3.9 ± 0.6
G4_TFHBA 64.5/pDNA	1.3 ± 0.4	3.7 ± 0.2

3.3.3. Cytotoxicity of the dendriplexes

Upon selection of the two dendrimer concentrations, 0.1 and 0.5 µM, the resazurin assay (**Figure 35**) was used to evaluate the cytotoxicity of the prepared dendriplexes. These two dendrimer concentrations were selected since they showed low cytotoxicity and proper pDNA condensation in the previous experiments.

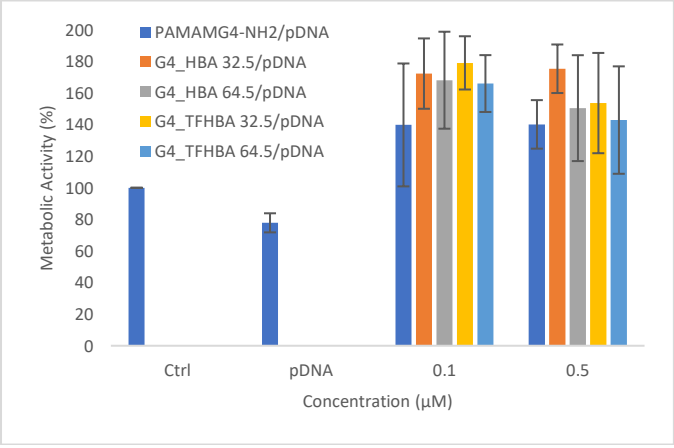

Figure 35: Metabolic activity of HEK293T cells assessed by the resazurin reduction assay after incubation of cells at 37^{o}C for 48h (value ± standard deviation). Dendriplexes were prepared at different dendrimer concentrations of 0.1 and 0.5 µM.

The analysis of **Figure 35** reveals that the dendriplexes do not present cytotoxicity. In fact, relative to the control, the metabolic activity of the cells even showed an increase when dendriplexes were present which should be related to an activation of the enzymes involved in the assay and not specifically with an increase in the number of viable cells. Additionally, no significant differences among the dendriplexes prepared from the pristine dendrimers or the functionalized dendrimers could be observed.

In order to validate the conclusions obtained through the resazurin reduction assay, the total protein content in culture was also determined. Indeed, this parameter can also be used as an indirect measure of cell viability, assuming that the number of viable cells will be proportional to the protein content. The BCA assay was used to assess the protein content in culture and the results are shown in **Figure 36**. Here, the same conclusions as in the resazurin reduction assay can be taken. That is, there was no significant difference in terms of cytotoxicity among the control and the samples containing the pristine and functionalized dendrimers. Since this assay is not enzyme activity-based, the values of total protein content achieved for the samples did not surpass those obtained for the control.

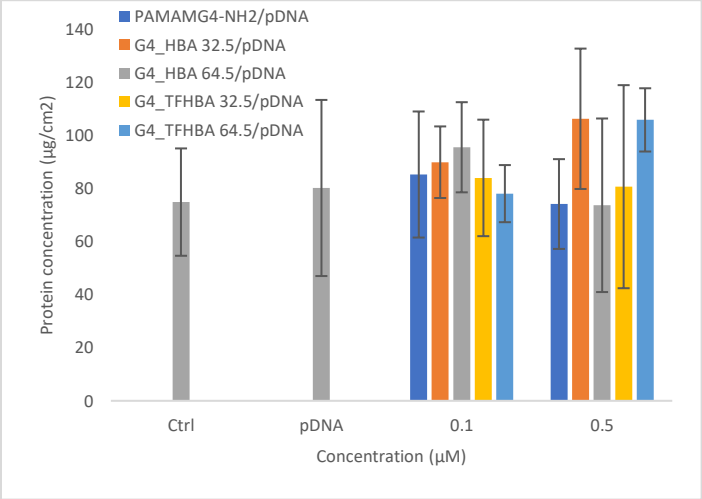

Figure 36: Total protein concentration in the culture assessed using the BCA assay after cell incubation at 37°C for 48h (value ± standard deviation). Dendriplexes were prepared at different dendrimer concentrations of 0.1 and 0.5 µM.

3.3.4. Transfection Studies

After observing that the dendriplexes were not cytotoxic, the dendriplexes prepared using dendrimer concentrations of 0.1 µM and 0.5 µM were used to transfect cells. A pDNA concentration of 0.1 µgµL^{-1} was kept constant in all experiments. Since pDNA encoding for the GFP and the luciferase reporter genes was used for transfection, the efficiency of the process was evaluated by fluorescence microscopy (for qualitative GFP detection) and by determining the activity of luciferase (to allow for the obtention of quantitative data).

3.3.4.1. GFP expression detection by fluorescence Microscopy

Figure 37 presents the images of HEK 293T cells after transfection using the pristine and the functionalized dendrimers as pDNA carriers. Both bright field and fluorescent images are presented. As controls, non-transfected cells (**Figure 34 A/B**) and cells transfected using only pDNA (**Figure 34 C/D)** were used. As it can be observed and as was expected, no GFP expression was detected in both controls. When the pristine dendrimer was used as a transfection agent, the number of transfected cells (green cells) was very low for both 0.1 and 0.5 µM dendrimer concentrations used. On the other hand, when the dendriplexes prepared with the functionalized dendrimers were applied, the number of transfected cells seems to increase, especially in the cases of G4_HBA 32.5/pDNA at 0.5 µM (**Figure 34 K/L**), G4_HBA 64.5/pDNA at 0.5 µM **(Figure 34 O/P**), and G4_TFHBA 64.5/pDNA at both concentrations **(Figure 34 U/V** and **W/X**). So, in general, the fluorescence microscopy results point out an enhancement in the levels of cell transfection and GFP protein expression when using dendriplexes prepared with a dendrimer concentration of 0.5 µM. Transfection seems to improve when the functionalized dendrimers are used as gene carriers. Interestingly, this last observation does not correlate with the values determined for the zeta potential of the dendriplexes that are less positive (although to a small extent) when functionalized dendrimers are being used as pDNA carriers. As a matter of fact, there should be other effects related to the presence of either HBA or TFHBA at the dendrimer surface that possibly contribute to their better interaction with pDNA and/or the cell surface and thus improve transfection efficiency[156–160]. As mentioned previously, one possible type of interaction that may occur in the systems that possess TFHBA that may be responsible for the improvement of transfection efficiency is halogen bonding[197–200].

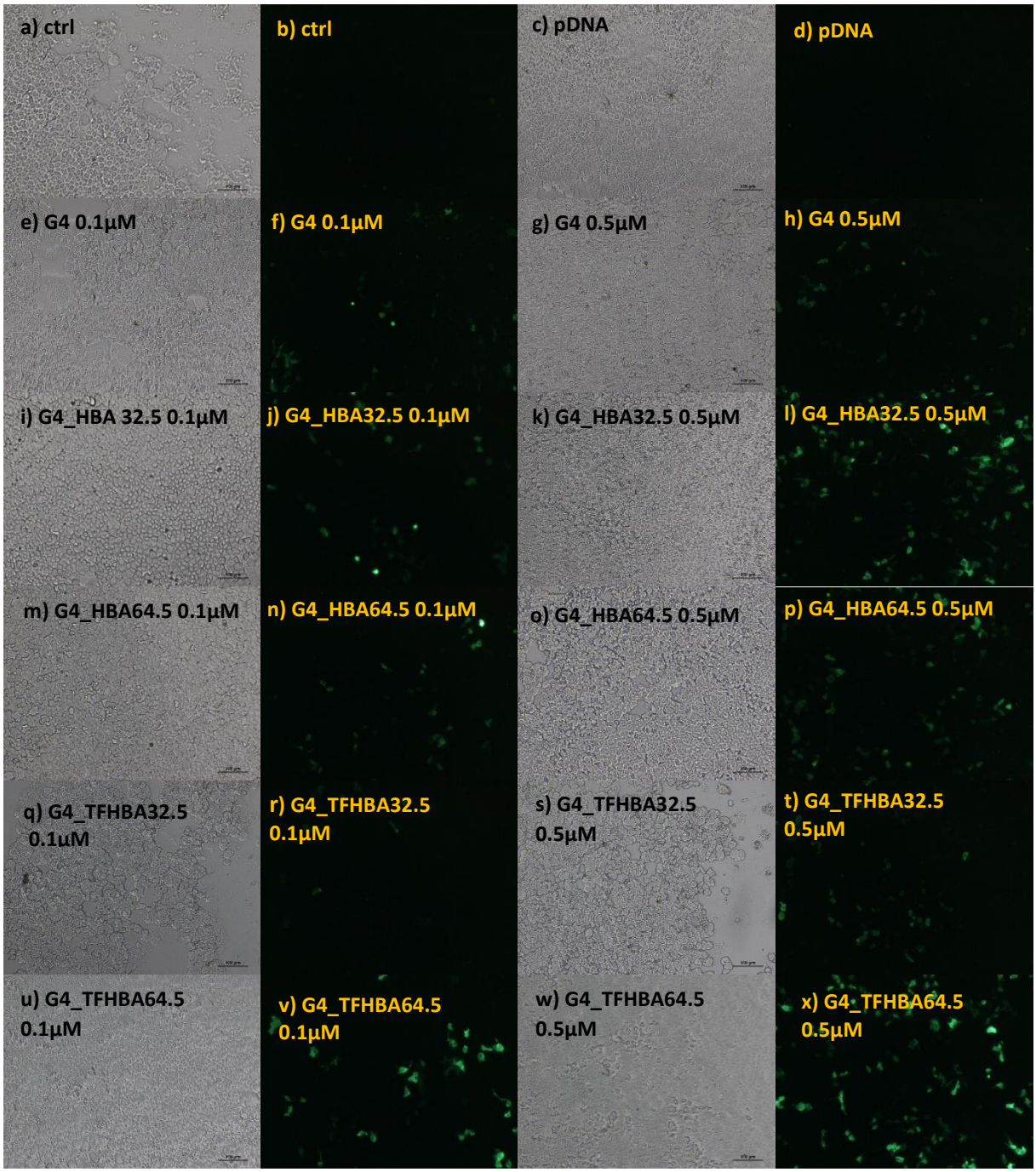

Figure 37: Fluorescence microscopy of the HEK293T cells transfected with pDNA encoding for GFP-Luc after 48h in culture. **a)** control BF; **b)** control GF; **c)** pDNA BF; **d)** pDNA GF **e)** PAMAMG_4-NH_2 at 0.1 µM BF; **f)** PAMAMG_4-NH_2 at 0.1 µM GF; **g)** PAMAMG_4-NH_2 at 0.5 µM BF; **h)** PAMAMG_4-NH_2 at 0.5 µM GF; **i)** G4_HBA 32.5 at 0.1 µM BF; **j)** G4_HBA 32.5 at 0.1 µM GF; **k)** G4_HBA 32.5 at 0.5 µM BF; **l)** G4_HBA 32.5 at 0.5 µM GF; **m)** G4_HBA 64.5 at 0.1 µM BF; **n)** G4_HBA 64.5 at 0.1 µM GF;**o)** G4_HBA 64.5 at 0.5 µM BF; **p)** G4_HBA 64.5 at 0.5 µM GF; **q)** G4_TFHBA 32.5 at 0.1 µM BF; **r)** G4_TFHBA 32.5 at 0.1 µM GF; **s)** G4_TFHBA 32.5 at 0.5 µM BF; **t)** G4_TFHBA 32.5 at 0.5 µM GF; **u)** G4_TFHBA 64.5 at 0.1 µM BF; **v)** G4_TFHBA 64.5 at 0.1 GF; **w)** G4_TFHBA 64.5 at 0.5 µM BF; **x)** G4_TFHBA 64.5 at 0.5 µM GF. Note: BF = Bright Field; GF = Green Field. Control contains only cells and complete medium.

3.3.4.2. Luciferase activity measurements

The results obtained for the activity of luciferase after cell transfection with pristine dendrimers and functionalized dendrimers are presented in **Figure 38.** In general, the obtained values follow the same tendency seen when analysing GFP expression by fluorescence microscopy. Confirming the previous results where the efficiency of the transfection increases with the concentration of the dendrimers used to prepare the dendriplexes (much higher enzyme activity values can be observed for 0.5 µM), it looks like the functionalized dendrimers have a better performance as transfection agents than the PAMAMG_4-NH_2 dendrimers without functionalization. Only for G4_TFHBA 64.5 is this not applicable which, anyway, is not very clear due to the high error associated with the determination of luciferase activity when the pristine dendrimer is used.

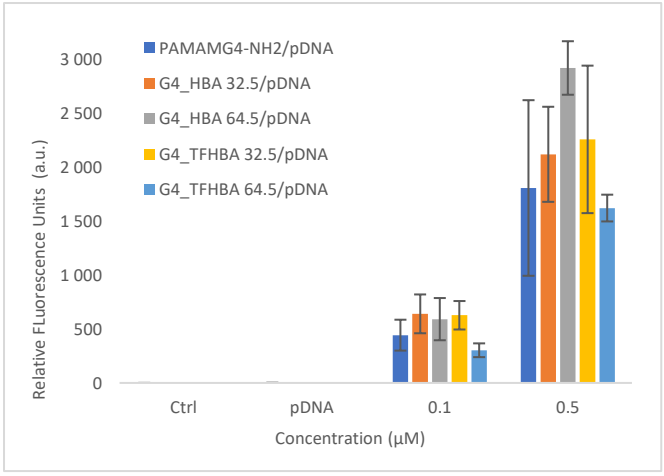

Figure 38: Normalized luciferase activity of the HEK 293T cells when analysing the transfection efficiency of the complexes at concentrations of 0.1 and 0.5 µM after 48h of incubation at 37°C.

Contrary to what was expected, at this phase of the study, no significant differences were seen between the dendrimers functionalized with either HBA or TFHBA. That is, no effect of the presence of fluoride on the dendrimer surface was evident in terms of gene delivery behaviour. In future assays, one will use a higher pDNA concentration which will clarify possible existent differences in this respect. The improvement in transfection with fluorination was expected since, according to the literature, fluorination improves cellular uptake, serum stability, endosomal escape, dissociation of the intracellular DNA from the dendrimer, and reduce cytotoxicity[124,127–130].

Chapter IV: Conclusion and Outlooks.

4.1. Conclusions

The functionalization of PAMAMG$_4$-NH$_2$ with the selected compounds, HBA and TFHBA, was successful. With a compound/dendrimer ratio of 32.5, and according to the calculations taken from the ^{1}H NMR of HBA, the functionalization degree attained was 50%. When the ratio was of 64.5, the functionalization degree remained at 84%, which may be due to the crowding of the surface of the dendrimer and steric hindrance. The achieved conjugation of the compound to the dendrimer was further confirmed by the hypsochromic shift of HBA and the bathochromic shift of TFHBA, as well as the change in pH, the fluorescence shift of the PAMAMG4-NH$_2$ intrinsic fluorescence band, and the FTIR that suggest that the conjugation may involve the -COOH of the HBA/TFHBA and the NH$_2$ of PAMAMG$_4$-NH$_2$. The conjugates displayed stability in D$_2$O at 25^{o}C and 37^{o}C for more than one month, as demonstrated by the ^{1}H NMR and ^{19}F NMR data.

The biological studies performed revealed that the conjugates are not cytotoxic, that at a concentration of 0.1 µM and 0.5 µM the functionalization improves cell viability, and the increase of the compound/dendrimer ratio lowers the cytotoxicity, except in the case of G4_HBA64.5 that presents the higher toxicity. The PAMAMG4-NH$_2$ dendrimer with TFHBA proved to be the better conjugate in terms of cytocompatibility, being G4_TFHBA 64.5 the best one.

On the evaluation of the pDNA compaction capability, all dendriplexes showed good efficiency. For the cytotoxicity of the dendriplexes at the selected concentrations (0.1 µM and 0.5 µM), they did not present cytotoxicity but an increase in metabolic activity, which may indicate that there was an activation of the enzyme involved in the resazurin reduction assay. Comparing pristine PAMAMG$_4$-NH$_2$ with the functionalized PAMAMG$_4$-NH$_2$ dendrimer, no significant difference was seen either in the condensation of the pDNA nor in the cytocompatibility.

The transfection studies revealed that the conjugation of the PAMAMG$_4$-NH$_2$ dendrimer with either HBA or TFHBA enhances the transfection efficiency. This is more evident with the concentration of the conjugates at 0.5 µM. The conjugates are better performing than pristine PAMAMG$_4$-NH$_2$ in the transfection of the pDNA.

In summary, a material composed of a PAMAMG$_4$-NH$_2$ dendrimer functionalized with either HBA or TFHBA, that shows fluorescence, low cytotoxicity, and can transfect HEK293T cells was successfully synthesized.

4.2. Outlook and future work

The successful conjugation of the PAMAMG_4-NH_2 dendrimer with TFHBA provided a fluorescent system that transfects cells. However, much remains to be done to understand and assess all its potential as a gene carrier and/or probe for imaging. Having this in mind, the full knowledge of the functionalization degree of the dendrimer with the compound is crucial. For HBA, the ^{1}H NMR data provided the answer, but when going to TFHBA this information was not totally achieved. To assess this, the trinitrobenzenesulfonic acid (TNBSA) assay[202,203], amine titration[204], and mass spectrometry might afford the solution.

As seen in the literature, with a decreasing pH of 6 the fluorescence intensity of the PAMAM dendrimer increases with a maximum at pH 2.5[82–85]. It would be interesting to assess this property of the synthesized samples to see if the variation of pH influences the fluorescence of the conjugates.

The cytotoxicity and transfection efficiency studies should be repeated to eliminate or at least avoid any errors. Flow cytometry is also a technique to be used to evaluate if the transfected cells are dead or alive. Other cell lines[65,113] for these studies will also be relevant for comparison purposes to see if the material is toxic and if it can transfect them too, particularly not so easily transfectable cells.

The use of an higher and a lower PAMAM-NH_2 dendrimer generation (i.e. PAMAMG_3-NH_2 and PAMAMG_5-NH_2) for the synthesis of the conjugates would also be a good way to compare if the dendrimer generation influences the cytotoxicity of the conjugate and the transfection efficiency. And if this leads to a difference between the functionalization with either HBA or TFHBA.

Chapter V: References:

(1) D. A. Tomalia, H. Baker, J. Dewald, M. HAll, G. Kallos, S. Martin, J. Roeck, J. Ryder, and P. S. A New Class of Polymers: Starburst-Dendritic Macromolecules. *Polym. J.* **1985**, *17*, 117–132.

(2) Vögtle, F.; Richardt, G.; Werner, N. *Dendrimer Chemistry*; 2009. https://doi.org/10.1002/9783527626953.

(3) Abbasi, E.; Aval, S.; Akbarzadeh, A.; Milani, M.; Nasrabadi, H.; Joo, S.; Hanifehpour, Y.; Nejati-Koshki, K.; Pashaei-Asl, R. Dendrimers: Synthesis, Applications, and Properties. *Nanoscale Res. Lett.* **2014**, *9*, 247. https://doi.org/10.1186/1556-276X-9-247.

(4) Klajnert, B.; Bryszewska, M. Dendrimers: Properties and Applications. *Acta Biochim. Pol.* **2001**, *48*, 199–208. https://doi.org/10.18388/abp.2001_5127.

(5) Trinchi, A.; Muster, T. H. A Review of Surface Functionalized Amine Terminated Dendrimers for Application in Biological and Molecular Sensing. *Supramol. Chem.* **2007**, *19*, 431–445. https://doi.org/10.1080/10610270601120363.

(6) Kojima, C.; Kono, K.; Maruyama, K.; Takagishi, T. Synthesis of Polyamidoamine Dendrimers Having Poly(Ethylene Glycol) Grafts and Their Ability to Encapsulate Anticancer Drugs. *Bioconjug. Chem.* **2000**, *11*, 910–917. https://doi.org/10.1021/bc0000583.

(7) Caminade, A.-M.; Majoral, J.-P. Which Dendrimer to Attain the Desired Properties? Focus on Phosphorhydrazone Dendrimers. *Molecules* **2018**, *23*, 622. https://doi.org/10.3390/molecules23030622.

(8) Caminade, A.-M.; Ouali, A.; Laurent, R.; Turrin, C.-O.; Majoral, J.-P. The Dendritic Effect Illustrated with Phosphorus Dendrimers. *Chem. Soc. Rev.* **2015**, *44*, 3890–3899. https://doi.org/10.1039/C4CS00261J.

(9) Tomalia, D. A. Dendritic Effects: Dependency of Dendritic Nano-Periodic Property Patterns on Critical Nanoscale Design Parameters (CNDPs). *New J. Chem.* **2012**, *36*, 264–281. https://doi.org/10.1039/C1NJ20501C.

(10) Krawczyszyn, J.; Krawczyszyn, T. Photomorphogenesis in Dracaena Draco. *Trees* **2016**, *30*, 647–664. https://doi.org/10.1007/s00468-015-1307-z.

(11) Tomalia, D. A.; Fréchet, J. M. J. Discovery of Dendrimers and Dendritic Polymers: A Brief Historical Perspective. *J. Polym. Sci. Part A Polym. Chem.* **2002**, *40*, 2719–2728. https://doi.org/10.1002/pola.10301.

(12) Spruston, N. Pyramidal Neurons: Dendritic Structure and Synaptic Integration. *Nat. Rev. Neurosci.* **2008**, *9*, 206–221. https://doi.org/10.1038/nrn2286.

(13) Astruc, D.; Diallo, A.; Ornelas, C. Catalysis by Dendrimer-Stabilized and Dendrimer-Encapsulated

Late-Transition-Metal Nanoparticles. In *Nanomaterials in Catalysis*; Wiley-VCH Verlag GmbH & Co. KGaA: Weinheim, Germany, 2012; pp 97–122. https://doi.org/10.1002/9783527656875.ch3.

(14) Satija, J.; Sai, V. V. R.; Mukherji, S. Dendrimers in Biosensors: Concept and Applications. *J. Mater. Chem.* **2011**, *21*, 14367–14386. https://doi.org/10.1039/c1jm10527b.

(15) McMahon, M. T.; Bulte, J. W. M. Two Decades of Dendrimers as Versatile MRI Agents: A Tale with and without Metals. *Wiley Interdiscip. Rev. Nanomedicine Nanobiotechnology* **2018**, *10*, e1496. https://doi.org/10.1002/wnan.1496.

(16) Froehling, P. E. Dendrimers and Dyes — a Review. *Dye. Pigment.* **2001**, *48*, 187–195. https://doi.org/10.1016/S0143-7208(00)00099-1.

(17) M, D.; M, M.; S, A. A Novel Fluorescent Disperse Dye Based on N-Polyamidoamine Dendrimer-1,8 Naphthalimide: Synthesis, Characterization and Dyeing Properties on Polyester Fibres. *J. Text. Sci. Eng.* **2018**, *08*, 1000363. https://doi.org/10.4172/2165-8064.1000363.

(18) Roeven, E.; Scheres, L.; Smulders, M. M. J.; Zuilhof, H. Design, Synthesis, and Characterization of Fully Zwitterionic, Functionalized Dendrimers. *ACS Omega* **2019**, *4*, 3000–3011. https://doi.org/10.1021/acsomega.8b03521.

(19) Mignani, S.; El Kazzouli, S.; Bousmina, M.; Majoral, J.-P. Expand Classical Drug Administration Ways by Emerging Routes Using Dendrimer Drug Delivery Systems: A Concise Overview. *Adv. Drug Deliv. Rev.* **2013**, *65*, 1316–1330. https://doi.org/10.1016/j.addr.2013.01.001.

(20) Mignani, S.; Rodrigues, J.; Roy, R.; Shi, X.; Ceña, V.; El Kazzouli, S.; Majoral, J.-P. Exploration of Biomedical Dendrimer Space Based on In-Vitro Physicochemical Parameters: Key Factor Analysis (Part 1). *Drug Discov. Today* **2019**, *24*, 1176–1183. https://doi.org/10.1016/j.drudis.2019.02.014.

(21) Augustus, E. N.; Allen, E. T.; Nimibofa, A.; Donbebe, W. A Review of Synthesis, Characterization and Applications of Functionalized Dendrimers. *Am. J. Polym. Sci.* **2017**, *7*, 8–14. https://doi.org/10.5923/j.ajps.20170701.02.

(22) Kesharwani, P.; Tekade, R. K.; Gajbhiye, V.; Jain, K.; Jain, N. K. Cancer Targeting Potential of Some Ligand-Anchored Poly(Propylene Imine) Dendrimers: A Comparison. *Nanomedicine Nanotechnology, Biol. Med.* **2011**, *7*, 295–304. https://doi.org/10.1016/j.nano.2010.10.010.

(23) Kaur, D.; Jain, K.; Mehra, N. K.; Kesharwani, P.; Jain, N. K. A Review on Comparative Study of PPI and PAMAM Dendrimers. *J. Nanoparticle Res.* **2016**, *18*, 146. https://doi.org/10.1007/s11051-016-3423-0.

(24) Wang, Y.; Salmon, L.; Ruiz, J.; Astruc, D. Metallodendrimers in Three Oxidation States with Electronically Interacting Metals and Stabilization of Size-Selected Gold Nanoparticles. *Nat. Commun.* **2014**, *5*, 3489. https://doi.org/10.1038/ncomms4489.

(25) Ashraful Alam, M. A Review on Dendrimers and Metallodendrimers, the Important Compounds as Catalyst in Material Chemistry. *Adv. Mater.* **2017**, *6*, 52. https://doi.org/10.11648/j.am.20170605.11.

(26) Qin, T.; Li, X.; Chen, J.; Zeng, Y.; Yu, T.; Yang, G.; Li, Y. Dendritic Ionic Liquids Based on Imidazolium-Modified Poly(Aryl Ether) Dendrimers. *Chem. - An Asian J.* **2014**, *9*, 3641–3649. https://doi.org/10.1002/asia.201402960.

(27) Shen, L.; Shi, M.; Li, F.; Zhang, D.; Li, X.; Shi, E.; Yi, T.; Du, Y.; Huang, C. Polyaryl Ether Dendrimer with a 4-Phenylacetyl-5-Pyrazolone-Based Terbium(III) Complex as Core: Synthesis and Photopysical Properties. *Inorg. Chem.* **2006**, *45*, 6188–6197. https://doi.org/10.1021/ic052148v.

(28) Saboktakin, M. R.; Maharramov, A.; Ramazanov, M. A. Synthesis and Characterization of Aromatic Polyether Dendrimer/Mesalamine (5-ASA) Nanocomposite as Drug Carrier System. *J. Am. Sci.* **2007**, *3*, 45. https://doi.org/10.7537/marsjas030407.08.

(29) Twibanire, J. D. amou. K.; Grindley, T. B. Polyester Dendrimers. *Polymers (Basel).* **2012**, *4*, 794–879. https://doi.org/10.3390/polym4010794.

(30) Al-Jamal, K. T.; Al-Jamal, W. T.; Akerman, S.; Podesta, J. E.; Yilmazer, A.; Turton, J. A.; Bianco, A.; Vargesson, N.; Kanthou, C.; Florence, A. T.; et al. Systemic Antiangiogenic Activity of Cationic Poly-L-Lysine Dendrimer Delays Tumor Growth. *Proc. Natl. Acad. Sci.* **2010**, *107*, 3966–3971. https://doi.org/10.1073/pnas.0908401107.

(31) Boyd, B. J.; Kaminskas, L. M.; Karellas, P.; Krippner, G.; Lessene, R.; Porter, C. J. H. Cationic Poly-l-Lysine Dendrimers: Pharmacokinetics, Biodistribution, and Evidence for Metabolism and Bioresorption after Intravenous Administration to Rats. *Mol. Pharm.* **2006**, *3*, 614–627. https://doi.org/10.1021/mp060032e.

(32) Vasil'ev, V. G.; Kramarenko, E. Y.; Tatarinova, E. A.; Milenin, S. A.; Kalinina, A. A.; Papkov, V. S.; Muzafarov, A. M. An Unprecedented Jump in the Viscosity of High-Generation Carbosilane Dendrimer Melts. *Polymer (Guildf).* **2018**, *146*, 1–5. https://doi.org/10.1016/j.polymer.2018.05.016.

(33) Zhang, X. Low Generation Triazine-Based Dendrimers-Synthesis, Characterization and in Vitro Biological Activity, 2015, https://digituma.uma.pt/bitstream/10400.13/1179/1/MestradoXupeng Zhang.pdf.

(34) Gautam, S. P.; Sharma, A. K. G. A.; Gautam, T. Synthesis and Analytical Characterization of Ester and Amine Terminated PAMAM Dendrimers. *Glob. J. Med. Res. Pharma* **2013**, *13*, 7–15.

(35) Fox, L. J.; Richardson, R. M.; Briscoe, W. H. PAMAM Dendrimer - Cell Membrane Interactions. *Adv. Colloid Interface Sci.* **2018**, *257*, 1–18. https://doi.org/10.1016/j.cis.2018.06.005.

(36) Márquez-Miranda, V.; Peñaloza, J. P.; Araya-Durán, I.; Reyes, R.; Vidaurre, S.; Romero, V.;

Fuentes, J.; Céric, F.; Velásquez, L.; González-Nilo, F. D.; et al. Effect of Terminal Groups of Dendrimers in the Complexation with Antisense Oligonucleotides and Cell Uptake. *Nanoscale Res. Lett.* **2016**, *11*, 66. https://doi.org/10.1186/s11671-016-1260-9.

(37) Thatikonda, S.; Kumar Yellanki, S.; Charan, S. D.; Balaji, A. Dendrimers -a New Class of Polymers. *Int. J. Pharm. Sci. Res. IJPSR* **2013**, *4*, 2174–2183. https://doi.org/10.13040/IJPSR.0975-8232.4(6).2174-83.

(38) Maciel, D.; Guerrero-Beltrán, C.; Ceña-Diez, R.; Tomás, H.; Muñoz-Fernández, M. Á.; Rodrigues, J. New Anionic Poly(Alkylideneamine) Dendrimers as Microbicide Agents against HIV-1 Infection. *Nanoscale* **2019**, *11*, 9679–9690. https://doi.org/10.1039/c9nr00303g.

(39) Islam, M. S. A Facile Synthesis of Palladium Containing Metallodindrimer Base on Diazine and Its Application as a Catalyst. *Int. J. Adv. Res.* **2019**, *7*, 1256–1265. https://doi.org/10.21474/IJAR01/8758.

(40) Hawker, C.; Fréchet, J. M. J. A New Convergent Approach to Monodisperse Dendritic Macromolecules. *J. Chem. Soc., Chem. Commun.* **1990**, 1010–1013. https://doi.org/10.1039/C39900001010.

(41) Leon, J. W.; Fréchet, J. M. J. Analysis of Aromatic Polyether Dendrimers and Dendrimer-Linear Block Copolymers by Matrix-Assisted Laser Desorption Ionization Mass Spectrometry. *Polym. Bull.* **1995**, *35*, 449–455. https://doi.org/10.1007/BF00297611.

(42) Saboktakin, M. R.; Maharramov, A.; Ramazanov, M. A. Synthesis and Characterization of Aromatic Polyether Dendrimer/ Poly(2-Hydroxyethyl Methacrylate) Copolymer as Nano Drug Carriers. *Life Sci. J.* **2008**, *5*, 1097–8135. https://doi.org/10.7537/marslsj050308.06.

(43) Dhanikula, R. S.; Hildgen, P. Synthesis and Evaluation of Novel Dendrimers with a Hydrophilic Interior as Nanocarriers for Drug Delivery. *Bioconjug. Chem.* **2006**, *17*, 29–41. https://doi.org/10.1021/bc050184c.

(44) Al-Hamra, M.; Ghaddar, T. H. Facile Synthesis of Poly-(l-Lysine) Dendrimers with a Pentaaminecobalt(III) Complex at the Core. *Tetrahedron Lett.* **2005**, *46*, 5711–5714. https://doi.org/10.1016/j.tetlet.2005.06.078.

(45) Boyd, B. J.; Kaminskas, L. M.; Karellas, P.; Krippner, G.; Lessene, R.; Porter, C. J. H. Cationic Poly-L-Lysine Dendrimers: Pharmacokinetics, Biodistribution, and Evidence for Metabolism and Bioresorption after Intravenous Administration to Rats. *Mol. Pharm.* **2006**, *3*, 614–627. https://doi.org/10.1021/mp060032e.

(46) Munoz-Fernandez, M. A.; Vacas-Córdoba, E.; Maly, M.; de la Mata, F. J.; Gómez, R.; Pion, M. Antiviral Mechanism of Polyanionic Carbosilane Dendrimers against HIV-1. *Int. J. Nanomedicine* **2016**, *11*, 1281. https://doi.org/10.2147/IJN.S96352.

(47) Galan, M.; Sanchez-Rodriguez, J.; Cangiotti, M.; Garcia-Gallego, S.; Jimenez, J. L.; Gomez, R.;

Ottaviani, M. F.; Munoz-Fernandez, M. A.; de la Mata, F. J. Antiviral Properties Against HIV of Water Soluble Copper Carbosilane Dendrimers and Their EPR Characterization. *Curr. Med. Chem.* **2012**, *19*, 4984–4994. https://doi.org/10.2174/092986731120902498 4.

(48) Chonco, L.; Pion, M.; Vacas, E.; Rasines, B.; Maly, M.; Serramía, M. J.; López-Fernández, L.; De la Mata, J.; Alvarez, S.; Gómez, R.; et al. Carbosilane Dendrimer Nanotechnology Outlines of the Broad HIV Blocker Profile. *J. Control. Release* **2012**, *161*, 949–958. https://doi.org/10.1016/j.jconrel.2012.04.050.

(49) Steffensen, M. B.; Hollink, E.; Kuschel, F.; Bauer, M.; Simanek, E. E. Dendrimers Based on [1,3,5]-Triazines. *J. Polym. Sci. Part A Polym. Chem.* **2006**, *44*, 3411–3433. https://doi.org/10.1002/pola.21333.

(50) Lates, V.; Gligor, D.; Darabantu, M.; Muresan, L. M. Electrochemical Behavior of a New S-Triazine-Based Dendrimer. *J. Appl. Electrochem.* **2007**, *37*, 631–636. https://doi.org/10.1007/s10800-007-9293-5.

(51) Lim, J.; Simanek, E. E. Triazine Dendrimers as Drug Delivery Systems: From Synthesis to Therapy. *Adv. Drug Deliv. Rev.* **2012**, *64*, 826–835. https://doi.org/10.1016/j.addr.2012.03.008.

(52) Golikand, A. N.; Didehban, K.; Irannejad, L. Synthesis and Characterization of Triazine-Based Dendrimers and Their Application in Metal Ion Adsorption. *J. Appl. Polym. Sci.* **2012**, *123*, 1245–1251. https://doi.org/10.1002/app.33893.

(53) Caminade, A.-M.; Majoral, J.-P. Nanomaterials Based on Phosphorus Dendrimers. *Acc. Chem. Res.* **2004**, *37*, 341–348. https://doi.org/10.1021/ar020077n.

(54) Caminade, A.-M.; Maraval, V.; Laurent, R.; Turrin, C.-O.; Sutra, P.; Leclaire, J.; Griffe, L.; Marchand, P.; Baudoin-Dehoux, C.; Rebout, C.; et al. Phosphorus Dendrimers: From Synthesis to Applications. *Comptes Rendus Chim.* **2003**, *6*, 791–801. https://doi.org/10.1016/j.crci.2003.04.009.

(55) Majoral, J.-P.; Caminade, A.-M.; Maraval, V. The Specific Contribution of Phosphorus in Dendrimer Chemistry. *Chem. Commun.* **2002**, *24*, 2929–2942. https://doi.org/10.1039/b207194k.

(56) Maiti, P. K.; Çağın, T.; Wang, G.; Goddard, W. A. Structure of PAMAM Dendrimers: Generations 1 through 11. *Macromolecules* **2004**, *37*, 6236–6254. https://doi.org/10.1021/ma035629b.

(57) Araújo, R.; Santos, S.; Igne Ferreira, E.; Giarolla, J. New Advances in General Biomedical Applications of PAMAM Dendrimers. *Molecules* **2018**, *23*, 2849. https://doi.org/10.3390/molecules23112849.

(58) Diaz, C.; Benitez, C.; Vidal, F.; Barraza, L. F.; Jiménez, V. A.; Guzman, L.; Fuentealba, J.; Yevenes, G. E.; Alderete, J. B. Cytotoxicity and in Vivo Plasma Kinetic Behavior of Surface-Functionalized PAMAM Dendrimers. *Nanomedicine Nanotechnology, Biol. Med.* **2018**, *14*, 2227–2234.

https://doi.org/10.1016/j.nano.2018.07.005.

(59) Janaszewska, A.; Mączyńska, K.; Matuszko, G.; Appelhans, D.; Voit, B.; Klajnert, B.; Bryszewska, M. Cytotoxicity of PAMAM, PPI and Maltose Modified PPIdendrimers in Chinese Hamster Ovary (CHO) and Human Ovarian Carcinoma (SKOV3) Cells. *New J. Chem.* **2012**, *36*, 428–437. https://doi.org/10.1039/C1NJ20489K.

(60) Duncan, R.; Izzo, L. Dendrimer Biocompatibility and Toxicity. *Adv. Drug Deliv. Rev.* **2005**, *57*, 2215–2237. https://doi.org/10.1016/j.addr.2005.09.019.

(61) Agashe, H. B.; Dutta, T.; Garg, M.; Jain, N. K. Investigations on the Toxicological Profile of Functionalized Fifth-Generation Poly(Propylene Imine) Dendrimer. *J. Pharm. Pharmacol.* **2006**, *58*, 1491–1498. https://doi.org/10.1211/jpp.58.11.0010.

(62) Lin, Q.; Jiang, G.; Tong, K. Dendrimers in Drug-Delivery Applications. *Des. Monomers Polym.* **2010**, *13*, 301–324. https://doi.org/10.1163/138577210X509552.

(63) Maiti, P. K. PAMAM Dendrimer: A pH-Controlled Nanosponge. *Can. J. Chem.* **2017**, *95*, 991–998. https://doi.org/10.1139/cjc-2017-0244.

(64) Čakara, D.; Borkovec, M. Microscopic Protonation Mechanism of Branched Polyamines: Poly (Amidoamine) versus Poly (Propyleneimine) Dendrimers. *Croat. Chem. Acta* **2007**, *80*, 421–428. https://doi.org/https://hrcak.srce.hr/18665.

(65) Wang, M.; Cheng, Y. The Effect of Fluorination on the Transfection Efficacy of Surface-Engineered Dendrimers. *Biomaterials* **2014**, *35*, 6603–6613. https://doi.org/10.1016/j.biomaterials.2014.04.065.

(66) Benini, P. G. Z.; McGarvey, B. R.; Franco, D. W. Functionalization of PAMAM Dendrimers with [RuIII(Edta)(H_2O)]−. *Nitric Oxide* **2008**, *19*, 245–251. https://doi.org/10.1016/j.niox.2008.04.027.

(67) Palmerston Mendes, L.; Pan, J.; Torchilin, V. Dendrimers as Nanocarriers for Nucleic Acid and Drug Delivery in Cancer Therapy. *Molecules* **2017**, *22*, 1401. https://doi.org/10.3390/molecules22091401.

(68) Qi, R.; Gao, Y.; Tang, Y.; He, R.-R.; Liu, T.-L.; He, Y.; Sun, S.; Li, B.-Y.; Li, Y.-B.; Liu, G. PEG-Conjugated PAMAM Dendrimers Mediate Efficient Intramuscular Gene Expression. *AAPS J.* **2009**, *11*, 395. https://doi.org/10.1208/s12248-009-9116-1.

(69) Lu, Y.; Han, S.; Zheng, H.; Ma, R.; Ping, Y.; Zou, J.; Tang, H.; Zhang, Y.; Xu, X.; Li, F. A Novel RGDyC/PEG Co-Modified PAMAM Dendrimer-Loaded Arsenic Trioxide of Glioma Targeting Delivery System. *Int. J. Nanomedicine* **2018**, *13*, 5937–5952. https://doi.org/10.2147/IJN.S175418.

(70) Bertero, A.; Boni, A.; Gemmi, M.; Gagliardi, M.; Bifone, A.; Bardi, G. Surface Functionalisation Regulates Polyamidoamine Dendrimer Toxicity on Blood–Brain Barrier Cells and the

Modulation of Key Inflammatory Receptors on Microglia. *Nanotoxicology* **2014**, *8*, 158–168. https://doi.org/10.3109/17435390.2013.765054.

(71) Jin, L.; Jiang, Y.; Zhang, M.; Li, H.; Xiao, L.; Li, M.; Ao, Y. Oriented Polyaniline Nanowire Arrays Grown on Dendrimer (PAMAM) Functionalized Multiwalled Carbon Nanotubes as Supercapacitor Electrode Materials. *Sci. Rep.* **2018**, *8*, 6268. https://doi.org/10.1038/s41598-018-24265-7.

(72) Harris, D. C. *Quantitative Chemical Analysis*, 7th ed.; W. H.Freeman and Company: New York, NY, 2007.

(73) Williams, F.; Berry, D. E.; Bernard, J. E. *Radiationless Processes*; DiBartolo, B., Ed.; Plenum Press, in cooperation with NATO Scientific Affairs Division: New York, NY, 1980.

(74) Bixon, M.; Jortner, J. Intramolecular Radiationless Transitions. *J. Chem. Phys.* **1968**, *48*, 715–726. https://doi.org/10.1063/1.1668703.

(75) Bueno, W. A. *Manual de Espectroscopia Vibracional*; Filho, M. M. de A., Ed.; Mc Graw-Hill: São Paulo, 1990.

(76) Suppan, P. *Chemistry and Light*; The Royal Society of Chemistry: Cambridge, 1994.

(77) Cheng, Y. *Dendrimer-Based Drug Delivery Systems: From Theory to Practice*; John Wiley & Sons, Ltd: Canada, 2012. https://doi.org/10.1007/978-3-211-89836-9_427.

(78) Marcu, L. Fluorescence Lifetime Techniques in Medical Applications. *Ann. Biomed. Eng.* **2012**, *40*, 304–331. https://doi.org/10.1007/s10439-011-0495-y.

(79) Elson, D.; Webb, S.; Siegel, J.; Suhling, K.; Davis, D.; Lever, J.; Phillips, D.; Wallace, A.; French, P. Biomedical Applications of Fluorescence Lifetime Imaging. *Opt. Photonics News* **2002**, *13*, 26. https://doi.org/10.1364/OPN.13.11.000026.

(80) Luo, W.; Jiang, R.; Liu, M.; Wan, Q.; Tian, J.; Wen, Y.; Cao, Q.; Hui, J.; Zhang, X.; Wei, Y. Synthesis of Fluorescent Dendrimers with Aggregation-Induced Emission Features through a One-Pot Multi-Component Reaction and Their Utilization for Biological Imaging. *J. Colloid Interface Sci.* **2018**, *509*, 327–333. https://doi.org/10.1016/j.jcis.2017.09.039.

(81) Trzepiński, P.; Klajnert-Maculewicz, B. Dendrimers for Fluorescence-Based Bioimaging. *J. Chem. Technol. Biotechnol.* **2017**, *92*, 1157–1166. https://doi.org/10.1002/jctb.5216.

(82) Grabchev, I.; Staneva, D.; Betcheva, R. Fluorescent Dendrimers As Sensors for Biologically Important Metal Cations. *Curr. Med. Chem.* **2012**, *19*, 4976–4983. https://doi.org/10.2174/092986731120902497 6.

(83) Wang, D.; Imae, T.; Miki, M. Fluorescence Emission from PAMAM and PPI Dendrimers. *J. Colloid Interface Sci.* **2007**, *306*, 222–227. https://doi.org/10.1016/j.jcis.2006.10.025.

(84) Wang, D.; Imae, T. Fluorescence Emission from Dendrimers and Its pH Dependence. *J. Am. Chem. Soc.* **2004**, *126*, 13204–13205. https://doi.org/10.1021/ja0454992.

(85) Caminade, A.-M.; Turrin, C.-O.; Laurent, R.; Ouali, A.; Delavaux-Nico, B. *Dendrimers: Towards Catalytic, Material, and Biomedical Uses*; John Wiley & Sons, Ltd: Toulouse, 2011.

(86) Ceroni, P.; Bergamini, G.; Marchioni, F.; Balzani, V. Luminescence as a Tool to Investigate Dendrimer Properties. *Prog. Polym. Sci.* **2005**, *30*, 453–473. https://doi.org/10.1016/j.progpolymsci.2005.01.003.

(87) Albertazzi, L.; Brondi, M.; Pavan, G. M.; Sato, S. S.; Signore, G.; Storti, B.; Ratto, G. M.; Beltram, F. Dendrimer-Based Fluorescent Indicators: In Vitro and In Vivo Applications. *PLoS One* **2011**, *6*, e28450. https://doi.org/10.1371/journal.pone.0028450.

(88) Paolucci, V.; Mejlsøe, S. L.; Ficker, M.; Vosch, T.; Christensen, J. B. Photophysical Properties of Fluorescent Core Dendrimers Controlled by Size. *J. Phys. Chem. B* **2016**, *120*, 9576–9580. https://doi.org/10.1021/acs.jpcb.6b05354.

(89) Cai, Y.; Ji, C.; Zhang, S.; Su, Z.; Yin, M. Synthesis of Water-Soluble Dye-Cored Poly(Amidoamine) Dendrimers for Long-Term Live Cell Imaging. *Sci. China Mater.* **2018**, *61*, 1475–1483. https://doi.org/10.1007/s40843-018-9246-6.

(90) Clulow, A. J.; Burn, P. L.; Meredith, P.; Shaw, P. E. Fluorescent Carbazole Dendrimers for the Detection of Nitroaliphatic Taggants and Accelerants. *J. Mater. Chem.* **2012**, *22*, 12507. https://doi.org/10.1039/c2jm32072j.

(91) Tomalia, D. A.; Klajnert-Maculewicz, B.; Johnson, K. A.-M.; Brinkman, H. F.; Janaszewska, A.; Hedstrand, D. M. Non-Traditional Intrinsic Luminescence: Inexplicable Blue Fluorescence Observed for Dendrimers, Macromolecules and Small Molecular Structures Lacking Traditional/Conventional Luminophores. *Prog. Polym. Sci.* **2019**, *90*, 35–117. https://doi.org/10.1016/j.progpolymsci.2018.09.004.

(92) Zhang Yuan, W.; Zhang, Y. Nonconventional Macromolecular Luminogens with Aggregation-Induced Emission Characteristics. *J. Polym. Sci. Part A Polym. Chem.* **2017**, *55*, 560–574. https://doi.org/10.1002/pola.28420.

(93) Caminade, A.-M.; Hameau, A.; Majoral, J.-P. Multicharged and/or Water-Soluble Fluorescent Dendrimers: Properties and Uses. *Chem. - A Eur. J.* **2009**, *15*, 9270–9285. https://doi.org/10.1002/chem.200901597.

(94) Konopka, M.; Janaszewska, A.; Klajnert-Maculewicz, B. Intrinsic Fluorescence of PAMAM Dendrimers-Quenching Studies. *Polymers (Basel).* **2018**, *10*. https://doi.org/10.3390/polym10050540.

(95) Ji, Y.; Qian, Y. A Study Using Quantum Chemical Theory Methods on the Intrinsic Fluorescence Emission and the Possible Emission Mechanisms of PAMAM. *RSC Adv.* **2014**, *4*, 58788–58794. https://doi.org/10.1039/C4RA09184A.

(96) Larson, C. L.; Tucker, S. A. Intrinsic Fluorescence of Carboxylate-Terminated Polyamido Amine

Dendrimers. *Appl. Spectrosc.* **2001**, *55*, 679–683. https://doi.org/10.1366/0003702011952596.

(97) Studzian, M.; Pułaski, Ł.; Tomalia, D. A.; Klajnert-Maculewicz, B. Non-Traditional Intrinsic Luminescence (NTIL): Dynamic Quenching Demonstrates the Presence of Two Distinct Fluorophore Types Associated with NTIL Behavior in Pyrrolidone-Terminated PAMAM Dendrimers. *J. Phys. Chem. C* **2019**, *123*, 18007–18016. https://doi.org/10.1021/acs.jpcc.9b02725.

(98) Lu, H.; Hu, Z.; Feng, S. Nonconventional Luminescence Enhanced by Silicone-Induced Aggregation. *Chem. - An Asian J.* **2017**, *12*, 1213–1217. https://doi.org/10.1002/asia.201700234.

(99) Qin, A.; Lam, J. W. Y.; Tang, B. Z. Luminogenic Polymers with Aggregation-Induced Emission Characteristics. *Prog. Polym. Sci.* **2012**, *37*, 182–209. https://doi.org/10.1016/j.progpolymsci.2011.08.002.

(100) Mei, J.; Hong, Y.; Lam, J. W. Y.; Qin, A.; Tang, Y.; Tang, B. Z. Aggregation-Induced Emission: The Whole Is More Brilliant than the Parts. *Adv. Mater.* **2014**, *26*, 5429–5479. https://doi.org/10.1002/adma.201401356.

(101) Chen, Y.; Lam, J. W. Y.; Kwok, R. T. K.; Liu, B.; Tang, B. Z. Aggregation-Induced Emission: Fundamental Understanding and Future Developments. *Mater. Horizons* **2019**, *6*, 428–433. https://doi.org/10.1039/C8MH01331D.

(102) Luo, J.; Xie, Z.; Lam, J. W. Y.; Cheng, L.; Tang, B. Z.; Chen, H.; Qiu, C.; Kwok, H. S.; Zhan, X.; Liu, Y.; et al. Aggregation-Induced Emission of 1-Methyl-1,2,3,4,5-Pentaphenylsilole. *Chem. Commun.* **2001**, *18*, 1740–1741. https://doi.org/10.1039/b105159h.

(103) Hong, Y.; Lam, J. W. Y.; Tang, B. Z. Aggregation-Induced Emission. *Chem. Soc. Rev.* **2011**, *40*, 5361. https://doi.org/10.1039/c1cs15113d.

(104) Liang, H.; Jia, D.; Liu, H.; Gu, Y.; Liu, C.; Zhao, F.; Chen, P.; Wang, D. Solvent Dependence of the Intrinsic Fluorescence from Amine-Containing Compounds. *Chem. Lett.* **2015**, *44*, 548–550. https://doi.org/10.1246/cl.141156.

(105) Chu, C.-C.; Imae, T. Fluorescence Investigations of Oxygen-Doped Simple Amine Compared with Fluorescent PAMAM Dendrimer. *Macromol. Rapid Commun.* **2009**, *30*, 89–93. https://doi.org/10.1002/marc.200800571.

(106) Lee, W. I.; Bae, Y.; Bard, A. J. Strong Blue Photoluminescence and ECL from OH-Terminated PAMAM Dendrimers in the Absence of Gold Nanoparticles. *J. Am. Chem. Soc.* **2004**, *126*, 8358–8359. https://doi.org/10.1021/ja0475914.

(107) Huang, J.-F.; Luo, H.; Liang, C.; Sun, I.-W.; Baker, G. A.; Dai, S. Hydrophobic Brønsted Acid−Base Ionic Liquids Based on PAMAM Dendrimers with High Proton Conductivity and Blue Photoluminescence. *J. Am. Chem. Soc.* **2005**, *127*, 12784–12785.

https://doi.org/10.1021/ja053965x.

(108) Fréchet, J. M. J. Dendrimers and Other Dendritic Macromolecules: From Building Blocks to Functional Assemblies in Nanoscience and Nanotechnology. *J. Polym. Sci. Part A Polym. Chem.* **2003**, *41*, 3713–3725. https://doi.org/10.1002/pola.10952.

(109) Ji, Y.; Yang, X.; Qian, Y. Poly-Amidoamine Structure Characterization: Amide Resonance Structure of Imidic Acid (HO–C⍰N) and Tertiary Ammonium. *RSC Adv.* **2014**, *4*, 49535–49540. https://doi.org/10.1039/C4RA09081K.

(110) Wang, D.; Imae, T.; Miki, M. Fluorescence Emission from PAMAM and PPI Dendrimers. *J. Colloid Interface Sci.* **2007**, *306*, 222–227. https://doi.org/10.1016/j.jcis.2006.10.025.

(111) Al-Jamal, K. T.; Ruenraroengsak, P.; Hartell, N.; Florence, A. T. An Intrinsically Fluorescent Dendrimer as a Nanoprobe of Cell Transport. *J. Drug Target.* **2006**, *14*, 405–412. https://doi.org/10.1080/10611860600834441.

(112) Lide, D. R. *CRC Handbook of Chemistry and Physics*, 90th ed.; Haynes, W. M., Ed.; CRC Press/Taylor and Francis: Florida, 2010.

(113) Wang, M.; Liu, H.; Li, L.; Cheng, Y. A Fluorinated Dendrimer Achieves Excellent Gene Transfection Efficacy at Extremely Low Nitrogen to Phosphorus Ratios. *Nat. Commun.* **2014**, *5*, 3053. https://doi.org/10.1038/ncomms4053.

(114) Muller, K.; Faeh, C.; Diederich, F. Fluorine in Pharmaceuticals: Looking Beyond Intuition. *Science (80-.).* **2007**, *317*, 1881–1886. https://doi.org/10.1126/science.1131943.

(115) Li, S.; Smith, K. D.; Davis, J. H.; Gordon, P. B.; Breaker, R. R.; Strobel, S. A. Eukaryotic Resistance to Fluoride Toxicity Mediated by a Widespread Family of Fluoride Export Proteins. *Proc. Natl. Acad. Sci.* **2013**, *110*, 19018–19023. https://doi.org/10.1073/pnas.1310439110.

(116) Vithanage, M.; Bhattacharya, P. Fluoride in Drinking Water: Health Effects and Remediation. In *CO2 Sequestration, Biofuels and Depollution*; Lichtfouse, E., Schwarzbauer, J., Robert, D., Eds.; Environmental Chemistry for a Sustainable World; Springer International Publishing: Cham, 2015; Vol. 5, pp 105–151. https://doi.org/10.1007/978-3-319-11906-9_4.

(117) Jagtap, S.; Yenkie, M. K.; Labhsetwar, N.; Rayalu, S. Fluoride in Drinking Water and Defluoridation of Water. *Chem. Rev.* **2012**, *112*, 2454–2466. https://doi.org/10.1021/cr2002855.

(118) Kanduti, D.; Sterbenk, P.; Artnik, A. Fluoride: A Review of Use and Effects on Health. *Mater. Socio Medica* **2016**, *28*, 133. https://doi.org/10.5455/msm.2016.28.133-137.

(119) Ullah, R.; Zafar, M. S.; Shahani, N. Potential Fluoride Toxicity from Oral Medicaments: A Review. *Iran. J. Basic Med. Sci.* **2017**, *20*, 841–848. https://doi.org/10.22038/ijbms.2017.9104.

(120) Gillis, E. P.; Eastman, K. J.; Hill, M. D.; Donnelly, D. J.; Meanwell, N. A. Applications of Fluorine in Medicinal Chemistry. *J. Med. Chem.* **2015**, *58*, 8315–8359.

https://doi.org/10.1021/acs.jmedchem.5b00258.

(121) Harsanyi, A.; Sandford, G. Organofluorine Chemistry: Applications, Sources and Sustainability. *Green Chem.* **2015**, *17*, 2081–2086. https://doi.org/10.1039/C4GC02166E.

(122) Purser, S.; Moore, P. R.; Swallow, S.; Gouverneur, V. Fluorine in Medicinal Chemistry. *Chem. Soc. Rev.* **2008**, *37*, 320–330. https://doi.org/10.1039/B610213C.

(123) Dalvit, C.; Invernizzi, C.; Vulpetti, A. Fluorine as a Hydrogen-Bond Acceptor: Experimental Evidence and Computational Calculations. *Chem. - A Eur. J.* **2014**, *20*, 11058–11068. https://doi.org/10.1002/chem.201402858.

(124) Yang, J.; Zhang, Q.; Chang, H.; Cheng, Y. Surface-Engineered Dendrimers in Gene Delivery. *Chem. Rev.* **2015**, *115*, 5274–5300. https://doi.org/10.1021/cr500542t.

(125) Percec, V.; Imam, M. R.; Peterca, M.; Leowanawat, P. Self-Organizable Vesicular Columns Assembled from Polymers Dendronized with Semifluorinated Janus Dendrimers Act As Reverse Thermal Actuators. *J. Am. Chem. Soc.* **2012**, *134*, 4408–4420. https://doi.org/10.1021/ja2118267.

(126) Ni, C.; Hu, J. The Unique Fluorine Effects in Organic Reactions: Recent Facts and Insights into Fluoroalkylations. *Chemical Society Reviews*. 2016, pp 5441–5454. https://doi.org/10.1039/c6cs00351f.

(127) Xiao, Y.-P.; Zhang, J.; Liu, Y.-H.; Zhang, J.-H.; Yu, Q.-Y.; Huang, Z.; Yu, X.-Q. Low Molecular Weight PEI-Based Fluorinated Polymers for Efficient Gene Delivery. *Eur. J. Med. Chem.* **2019**, *162*, 602–611. https://doi.org/10.1016/j.ejmech.2018.11.041.

(128) Ghaffari, M.; Dehghan, G.; Abedi-Gaballu, F.; Kashanian, S.; Baradaran, B.; Ezzati Nazhad Dolatabadi, J.; Losic, D. Surface Functionalized Dendrimers as Controlled-Release Delivery Nanosystems for Tumor Targeting. *Eur. J. Pharm. Sci.* **2018**, *122*, 311–330. https://doi.org/10.1016/j.ejps.2018.07.020.

(129) Wang, M.; Cheng, Y. Structure-Activity Relationships of Fluorinated Dendrimers in DNA and SiRNA Delivery. *Acta Biomater.* **2016**, *46*, 204–210. https://doi.org/10.1016/j.actbio.2016.09.023.

(130) Chen, G.; Wang, K.; Hu, Q.; Ding, L.; Yu, F.; Zhou, Z.; Zhou, Y.; Li, J.; Sun, M.; Oupický, D. Combining Fluorination and Bioreducibility for Improved siRNA Polyplex Delivery. *ACS Appl. Mater. Interfaces* **2017**, *9*, 4457–4466. https://doi.org/10.1021/acsami.6b14184.

(131) Kretzmann, J. A.; Ho, D.; Evans, C. W.; Plani-Lam, J. H. C.; Garcia-Bloj, B.; Mohamed, A. E.; O'Mara, M. L.; Ford, E.; Tan, D. E. K.; Lister, R.; et al. Synthetically Controlling Dendrimer Flexibility Improves Delivery of Large Plasmid DNA. *Chem. Sci.* **2017**, *8*, 2923–2930. https://doi.org/10.1039/c7sc00097a.

(132) Menaa, F.; Menaa, B.; Sharts, O. N. Importance of Fluorine and Fluorocarbons in Medicinal

Chemistry and Oncology. *J. Mol. Pharm. Pharm Org. Process Res.* **2013**, *1*, 1–6. https://doi.org/10.4172/jmpopr.1000104.

(133) Swallow, S. Fluorine in Medicinal Chemistry. *Prog. Med. Chem.* **2015**, *54*, 65–133. https://doi.org/10.1016/bs.pmch.2014.11.001.

(134) Jiang, Z.-X.; Yu, Y. B. Fluorous Mixture Synthesis of Asymmetric Dendrimers. *J. Org. Chem.* **2010**, *75*, 2044–2049. https://doi.org/10.1021/jo100102a.

(135) Murphy, C. D. Drug Metabolism in Microorganisms. *Biotechnol. Lett.* **2015**, *37*, 19–28. https://doi.org/10.1007/s10529-014-1653-8.

(136) Kim, T. K.; Eberwine, J. H. Mammalian Cell Transfection: The Present and the Future. *Anal. Bioanal. Chem.* **2010**, *397*, 3173–3178. https://doi.org/10.1007/s00216-010-3821-6.

(137) Ramamoorth, M.; Narvekar, A. Non Viral Vectors in Gene Therapy- An Overview. *J. Clin. DIAGNOSTIC Res.* **2015**, *9*, GE01–GE06. https://doi.org/10.7860/JCDR/2015/10443.5394.

(138) Zhi, D.; Zhang, S.; Wang, B.; Zhao, Y.; Yang, B.; Yu, S. Transfection Efficiency of Cationic Lipids with Different Hydrophobic Domains in Gene Delivery. *Bioconjug. Chem.* **2010**, *21*, 563–577. https://doi.org/10.1021/bc900393r.

(139) Chow, Y. T.; Chen, S.; Wang, R.; Liu, C.; Kong, C.-W.; Li, R. A.; Cheng, S. H.; Sun, D. Single Cell Transfection through Precise Microinjection with Quantitatively Controlled Injection Volumes. *Sci. Rep.* **2016**, *6*, 24127. https://doi.org/10.1038/srep24127.

(140) Chang, L.; Bertani, P.; Gallego-Perez, D.; Yang, Z.; Chen, F.; Chiang, C.; Malkoc, V.; Kuang, T.; Gao, K.; Lee, L. J.; et al. 3D Nanochannel Electroporation for High-Throughput Cell Transfection with High Uniformity and Dosage Control. *Nanoscale* **2016**, *8*, 243–252. https://doi.org/10.1039/C5NR03187G.

(141) Mehier-Humbert, S.; Guy, R. H. Physical Methods for Gene Transfer: Improving the Kinetics of Gene Delivery into Cells. *Adv. Drug Deliv. Rev.* **2005**, *57*, 733–753. https://doi.org/10.1016/j.addr.2004.12.007.

(142) Choi, J. S.; Nam, K.; Park, J.; Kim, J.-B.; Lee, J.-K.; Park, J. Enhanced Transfection Efficiency of PAMAM Dendrimer by Surface Modification with L-Arginine. *J. Control. Release* **2004**, *99*, 445–456. https://doi.org/10.1016/j.jconrel.2004.07.027.

(143) Khan, W.; Hosseinkhani, H.; Ickowicz, D.; Hong, P.-D.; Yu, D.-S.; Domb, A. J. Polysaccharide Gene Transfection Agents. *Acta Biomater.* **2012**, *8*, 4224–4232. https://doi.org/10.1016/j.actbio.2012.09.022.

(144) Wu, P.; Chen, H.; Jin, R.; Weng, T.; Ho, J. K.; You, C.; Zhang, L.; Wang, X.; Han, C. Non-Viral Gene Delivery Systems for Tissue Repair and Regeneration. *J. Transl. Med.* **2018**, *16*, 29. https://doi.org/10.1186/s12967-018-1402-1.

(145) Feng, L.; Zhang, S.; Liu, Z. Graphene Based Gene Transfection. *Nanoscale* **2011**, *3*, 1252.

https://doi.org/10.1039/c0nr00680g.

(146) Yao, J.; Fan, Y.; Du, R.; Zhou, J.; Lu, Y.; Wang, W.; Ren, J.; Sun, X. Amphoteric Hyaluronic Acid Derivative for Targeting Gene Delivery. *Biomaterials* **2010**, *31*, 9357–9365. https://doi.org/10.1016/j.biomaterials.2010.08.043.

(147) WANG, H.; SHI, H.-B.; YIN, S.-K. Polyamidoamine Dendrimers as Gene Delivery Carriers in the Inner Ear: How to Improve Transfection Efficiency. *Exp. Ther. Med.* **2011**, *2*, 777–781. https://doi.org/10.3892/etm.2011.296.

(148) Tomalia, D. A.; Christensen, J. B.; Boas, U. *Dendrimers, Dendrons, and Dendritic Polymers: Discovery, Applications, and Future*; Cambridge University Press: Cambridge, 2012.

(149) Haensler, J.; Szoka, F. C. Polyamidoamine Cascade Polymers Mediate Efficient Transfection of Cells in Culture. *Bioconjug. Chem.* **1993**, *4*, 372–379. https://doi.org/10.1021/bc00023a012.

(150) Sonawane, N. D.; Szoka, F. C.; Verkman, A. S. Chloride Accumulation and Swelling in Endosomes Enhances DNA Transfer by Polyamine-DNA Polyplexes. *J. Biol. Chem.* **2003**, *278*, 44826–44831. https://doi.org/10.1074/jbc.M308643200.

(151) Tang, Z. Research Progress on Synthesis and Characteristic about Dendrimers. *IOP Conf. Ser. Earth Environ. Sci.* **2017**, *100*, 012024. https://doi.org/10.1088/1755-1315/100/1/012024.

(152) Hawker, C. J.; Frechet, J. M. J. Preparation of Polymers with Controlled Molecular Architecture. A New Convergent Approach to Dendritic Macromolecules. *J. Am. Chem. Soc.* **1990**, *112*, 7638–7647. https://doi.org/10.1021/ja00177a027.

(153) Salvino, J. M.; Kumar, N. V.; Orton, E.; Airey, J.; Kiesow, T.; Crawford, K.; Mathew, R.; Krolikowski, P.; Drew, M.; Engers, D.; et al. Polymer-Supported Tetrafluorophenol: A New Activated Resin for Chemical Library Synthesis. *J. Comb. Chem.* **2000**, *2*, 691–697. https://doi.org/10.1021/cc0000491.

(154) Verdoes, M.; Oresic Bender, K.; Segal, E.; van der Linden, W. A.; Syed, S.; Withana, N. P.; Sanman, L. E.; Bogyo, M. Improved Quenched Fluorescent Probe for Imaging of Cysteine Cathepsin Activity. *J. Am. Chem. Soc.* **2013**, *135*, 14726–14730. https://doi.org/10.1021/ja4056068.

(155) Boehner, C. M.; Marsden, D. M.; Sore, H. F.; Norton, D.; Spring, D. R. High Throughput 'Catch-and-Release' Synthesis within Spatially Discrete Gel Arrays. *Tetrahedron Lett.* **2010**, *51*, 5930–5932. https://doi.org/10.1016/j.tetlet.2010.09.024.

(156) Swami, R.; Singh, I.; Kulhari, H.; Jeengar, M. K.; Khan, W.; Sistla, R. *p*-Hydroxy Benzoic Acid-Conjugated Dendrimer Nanotherapeutics as Potential Carriers for Targeted Drug Delivery to Brain: An in Vitro and in Vivo Evaluation. *J. Nanoparticle Res.* **2015**, *17*, 265. https://doi.org/10.1007/s11051-015-3063-9.

(157) Mishra, A.; Singh, S.; Shukla, S. Physiological and Functional Basis of Dopamine Receptors and

Their Role in Neurogenesis: Possible Implication for Parkinson's Disease. *J. Exp. Neurosci.* **2018**, *12*, 117906951877982. https://doi.org/10.1177/1179069518779829.

(158) Ayano, G. Dopamine: Receptors, Functions, Synthesis, Pathways, Locations and Mental Disorders: Review of Literatures. *J. Ment. Disord. Treat.* **2016**, *2*, 2–5. https://doi.org/10.4172/2471-271X.1000120.

(159) Yang, K.; Wang, C.; Sun, T. The Roles of Intracellular Chaperone Proteins, Sigma Receptors, in Parkinson's Disease (PD) and Major Depressive Disorder (MDD). *Front. Pharmacol.* **2019**, *10*. https://doi.org/10.3389/fphar.2019.00528.

(160) Rousseaux, C. G.; Greene, S. F. Sigma Receptors [σ Rs]: Biology in Normal and Diseased States. *J. Recept. Signal Transduct.* **2015**, *36*, 1–62. https://doi.org/10.3109/10799893.2015.1015737.

(161) Manuja, R.; Sachdeva, S.; Jain, A.; Chaudhary, J. A Comprehensive Review on Biological Activities of *p*-Hydroxy Benzoic Acid and Its Derivatives. *Int. J. Pharm. Sci. Rev. Res.* **2013**, *22*, 109–115.

(162) Cueva, C.; Moreno-Arribas, M. V.; Martín-Álvarez, P. J.; Bills, G.; Vicente, M. F.; Basilio, A.; Rivas, C. L.; Requena, T.; Rodríguez, J. M.; Bartolomé, B. Antimicrobial Activity of Phenolic Acids against Commensal, Probiotic and Pathogenic Bacteria. *Res. Microbiol.* **2010**, *161*, 372–382. https://doi.org/10.1016/j.resmic.2010.04.006.

(163) Merkl, R.; Hrádková, I.; Filip, V.; Šmidrkal, J. Antimicrobial and Antioxidant Properties of Phenolic Acids Alkyl Esters. *Czech J. Food Sci.* **2010**, *28*, 275–279. https://doi.org/10.17221/132/2010-CJFS.

(164) Miyazawa, T. Nuclear Magnetic Resonance in Biochemistry. *YAKUGAKU ZASSHI* **1985**, *105*, 1009–1018. https://doi.org/10.1248/yakushi1947.105.11_1009.

(165) Günther, H. *NMR Spectroscopy: Basic Principle, Concept, and Applications in Chemistry*, 2nd editio.; John Wiley & Sons, Ltd, 1996.

(166) Hore, P. J. *Nuclear Magnetic Ressonance*; Oxford University Press Inc.: Oxford, 1995.

(167) Movasaghi, Z.; Rehman, S.; ur Rehman, D. I. Fourier Transform Infrared (FTIR) Spectroscopy of Biological Tissues. *Appl. Spectrosc. Rev.* **2008**, *43*, 134–179. https://doi.org/10.1080/05704920701829043.

(168) Worsfold, P. J.; Zagatto, E. A. G. Spectrophotometry: Overview. In *Reference Module in Chemistry, Molecular Sciences and Chemical Engineering*; Elsevier, 2017; Vol. 9, pp 1–5. https://doi.org/10.1016/B978-0-12-409547-2.14265-9.

(169) Kuś, S.; Marczenko, Z.; Obarski, N. Derivative UV-VIS Spectrophotometry in Analytical Chemistry. *Chem. Analityczna* **1996**, *41*, 899–929.

(170) Melville, B.; Lucieer, A.; Aryal, J. *Assessing the Impact of Spectral Resolution on Classification of Lowland Native Grassland Communities Based on Field Spectroscopy in Tasmania, Australia*; 2018; Vol. 10. https://doi.org/10.3390/rs10020308.

(171) Matsuoka, M.; Saito, M.; Anpo, M. Photoluminescence Spectroscopy. In *Characterization of Solid Materials and Heterogeneous Catalysts*; Wiley-VCH Verlag GmbH & Co. KGaA: Weinheim, Germany, 2012; Vol. 1, pp 149–184. https://doi.org/10.1002/9783527645329.ch4.

(172) Sakho, E. H. M.; Allahyari, E.; Oluwafemi, O. S.; Thomas, S.; Kalarikkal, N. Dynamic Light Scattering (DLS). In *Thermal and Rheological Measurement Techniques for Nanomaterials Characterization*; Elsevier, 2017; Vol. 3, pp 37–49. https://doi.org/10.1016/B978-0-323-46139-9.00002-5.

(173) Bhattacharjee, S. DLS and Zeta Potential - What They Are and What They Are Not? *J. Control. Release* **2016**, *235*, 337–351. https://doi.org/10.1016/j.jconrel.2016.06.017.

(174) Kaszuba, M.; Corbett, J.; Watson, F. M.; Jones, A. High-Concentration Zeta Potential Measurements Using Light-Scattering Techniques. *Philos. Trans. R. Soc. A Math. Phys. Eng. Sci.* **2010**, *368*, 4439–4451. https://doi.org/10.1098/rsta.2010.0175.

(175) Riss, T. L.; Moravec, R. A.; Niles, A. L.; Duellman, S.; Benink, H. A.; Worzella, T. J.; Minor, L. *Cell Viability Assays*; 2004.

(176) Uzarski, J. S.; DiVito, M. D.; Wertheim, J. A.; Miller, W. M. Essential Design Considerations for the Resazurin Reduction Assay to Noninvasively Quantify Cell Expansion within Perfused Extracellular Matrix Scaffolds. *Biomaterials* **2017**, *129*, 163–175. https://doi.org/10.1016/j.biomaterials.2017.02.015.

(177) Zalata, A. A.; Tijn, N. L.; Christophe, A.; Comhair, F. H. The Correlates and Alleged Biochemical Background of the Resazurin Reduction Test in Semen. *Int. J. Androl.* **2002**, *21*, 289–294. https://doi.org/10.1046/j.1365-2605.1998.00126.x.

(178) Ahn, S. PicoGreen Quantitation of DNA: Effective Evaluation of Samples Pre- or Post-PCR. *Nucleic Acids Res.* **1996**, *24*, 2623–2625. https://doi.org/10.1093/nar/24.13.2623.

(179) Dragan, A. I.; Casas-Finet, J. R.; Bishop, E. S.; Strouse, R. J.; Schenerman, M. A.; Geddes, C. D. Characterization of PicoGreen Interaction with DsDNA and the Origin of Its Fluorescence Enhancement upon Binding. *Biophys. J.* **2010**, *99*, 3010–3019. https://doi.org/10.1016/j.bpj.2010.09.012.

(180) Leclerc, G. M.; Boockfor, F. R.; Faught, W. J.; Frawley, L. S. Development of a Destabilized Firefly Luciferase Enzyme for Measurement of Gene Expression. *Biotechniques* **2000**, *29*, 590–601. https://doi.org/10.2144/00293rr02.

(181) Greer, L. F.; Szalay, A. A. Imaging of Light Emission from the Expression of Luciferases in Living Cells and Organisms: A Review. *Luminescence* **2002**, *17*, 43–74. https://doi.org/10.1002/bio.676.

(182) Walker, J. M. The Bicinchoninic Acid (BCA) Assay for Protein Quantitation. In *Protein Protocols Handbook, The*; Humana Press: New Jersey, 1994; Vol. 32, pp 11–14.

https://doi.org/10.1385/1-59259-169-8:11.

(183) Menges, F. Spectragryph - Optical Spectroscopy Software, version 1.2.9, 2018, https://www.effemm2.de/spectragryph/.

(184) Sousa-Herves, A.; Novoa-Carballal, R.; Riguera, R.; Fernandez-Megia, E. GATG Dendrimers and PEGylated Block Copolymers: From Synthesis to Bioapplications. *AAPS J.* **2014**, *16*, 948–961. https://doi.org/10.1208/s12248-014-9642-3.

(185) Shadrack, D. M.; Mubofu, E. B.; Nyandoro, S. S. Synthesis of Polyamidoamine Dendrimer for Encapsulating Tetramethylscutellarein for Potential Bioactivity Enhancement. *Int. J. Mol. Sci.* **2015**, *16*, 26363–26377. https://doi.org/10.3390/ijms161125956.

(186) Gomez, M. V.; Guerra, J.; Velders, A. H.; Crooks, R. M. NMR Characterization of Fourth-Generation PAMAM Dendrimers in the Presence and Absence of Palladium Dendrimer-Encapsulated Nanoparticles. *J. Am. Chem. Soc.* **2009**, *131*, 341–350. https://doi.org/10.1021/ja807488d.

(187) Roveda, A. C.; Papa, T. B. R.; Castellano, E. E.; Franco, D. W. PAMAM Dendrimers Functionalized with Ruthenium Nitrosyl as Nitric Oxide Carriers. *Inorganica Chim. Acta* **2014**, *409*, 147–155. https://doi.org/10.1016/j.ica.2013.07.009.

(188) Zhang, Y.; Qu, R.; Xu, T.; Zhang, Y.; Sun, C.; Ji, C.; Wang, Y. Fabrication of Triethylenetetramine Terminal Hyperbranched Dendrimer-Like Polymer Modified Silica Gel and Its Prominent Recovery Toward Au (III). *Front. Chem.* **2019**, *7*, 577. https://doi.org/10.3389/fchem.2019.00577.

(189) Van Der Bolt, F. J. T.; Van Den Heuvel, R. H. H.; Vervoort, J.; Van Berkel, W. J. H. 19F NMR Study on the Regiospecificity of Hydroxylation of Tetrafluoro-4-Hydroxybenzoate by Wild-Type and Y385F p-Hydroxybenzoate Hydroxylase: Evidence for a Consecutive Oxygenolytic Dehalogenation Mechanism †. *Biochemistry* **1997**, *36*, 14192–14201. https://doi.org/https://pubs.acs.org/sharingguidelines.

(190) Li, Y.; He, H.; Lu, W.; Jia, X. A Poly(Amidoamine) Dendrimer-Based Drug Carrier for Delivering DOX to Gliomas Cells. *RSC Adv.* **2017**, *7*, 15475–15481. https://doi.org/10.1039/C7RA00713B.

(191) Charles, S.; Vasanthan, N.; Kwon, D.; Sekosan, G.; Ghosh, S. Surface Modification of Poly(Amidoamine) (PAMAM) Dendrimer as Antimicrobial Agents. *Tetrahedron Lett.* **2012**, *53*, 6670–6675. https://doi.org/10.1016/j.tetlet.2012.09.098.

(192) Buncel, E.; Rajagopal, S. Solvatochromism and Solvent Polarity Scales. *Acc. Chem. Res.* **1990**, *23*, 226–231. https://doi.org/10.1021/ar00175a004.

(193) Kamlet, M. J.; Taft, R. W. The Solvatochromic Comparison Method. I. The .Beta.-Scale of Solvent Hydrogen-Bond Acceptor (HBA) Basicities. *J. Am. Chem. Soc.* **1976**, *98*, 377–383. https://doi.org/10.1021/ja00418a009.

(194) Paul, A.; Sarpal, R. S.; Dogra, S. K. Effects of Solvent and Acid Concentration on the Absorption and Fluorescence Spectra of α,α-Diaminonaphthalenes. *J. Chem. Soc., Faraday Trans.* **1990**, *86*, 2095–2101. https://doi.org/10.1039/FT9908602095.

(195) Lobyshev, V. I.; Shikhlinskaya, R. E.; Ryzhikov, B. D. Experimental Evidence for Intrinsic Luminescence of Water. *J. Mol. Liq.* **1999**, *82*, 73–81. https://doi.org/10.1016/S0167-7322(99)00043-4.

(196) Dolenko, S. A.; Dolenko, T. A.; Fadeev, V. V.; Gerdova, I. V.; Kompitsas, M. Time-Resolved Fluorimetry of Two-Fluorophore Organic Systems Using Artificial Neural Networks. *Opt. Commun.* **2002**, *213*, 309–324. https://doi.org/10.1016/S0030-4018(02)02078-3.

(197) Scholfield, M. R.; Vander Zanden, C. M.; Carter, M.; Ho, P. S. Halogen Bonding (X-Bonding): A Biological Perspective. *Protein Sci.* **2013**, *22*, 139–152. https://doi.org/10.1002/pro.2201.

(198) Parker, A. J.; Stewart, J.; Donald, K. J.; Parish, C. A. Halogen Bonding in DNA Base Pairs. *J. Am. Chem. Soc.* **2012**, *134*, 5165–5172. https://doi.org/10.1021/ja2105027.

(199) Cavallo, G.; Metrangolo, P.; Milani, R.; Pilati, T.; Priimagi, A.; Resnati, G.; Terraneo, G. The Halogen Bond. *Chem. Rev.* **2016**, *116*, 2478–2601. https://doi.org/10.1021/acs.chemrev.5b00484.

(200) Priimagi, A.; Cavallo, G.; Metrangolo, P.; Resnati, G. The Halogen Bond in the Design of Functional Supramolecular Materials: Recent Advances. *Acc. Chem. Res.* **2013**, *46*, 2686–2695. https://doi.org/10.1021/ar400103r.

(201) Sinha, S.; Jing, H.; Das, S. Positive Zeta Potential of a Negatively Charged Semi-Permeable Plasma Membrane. *Appl. Phys. Lett.* **2017**, *111*, 063702. https://doi.org/10.1063/1.4989653.

(202) Li, M.; Yu, Y.; Hu, Y.; Li, X.; Liu, Y.; Sheng, W.; Yang, J. Spermine-Modified Antheraea Pernyi Silk Fibroin as a Gene Delivery Carrier. *Int. J. Nanomedicine* **2016**, *11*, 1013. https://doi.org/10.2147/IJN.S82023.

(203) Cayot, P.; Tainturier, G. The Quantification of Protein Amino Groups by the Trinitrobenzenesulfonic Acid Method: A Reexamination. *Anal. Biochem.* **1997**, *249*, 184–200. https://doi.org/10.1006/abio.1997.2161.

(204) Moaseri, E.; Baniadam, M.; Maghrebi, M.; Karimi, M. A Simple Recoverable Titration Method for Quantitative Characterization of Amine-Functionalized Carbon Nanotubes. *Chem. Phys. Lett.* **2013**, *555*, 164–167. https://doi.org/10.1016/j.cplett.2012.10.064.

Annexes.

6.1. NMR.

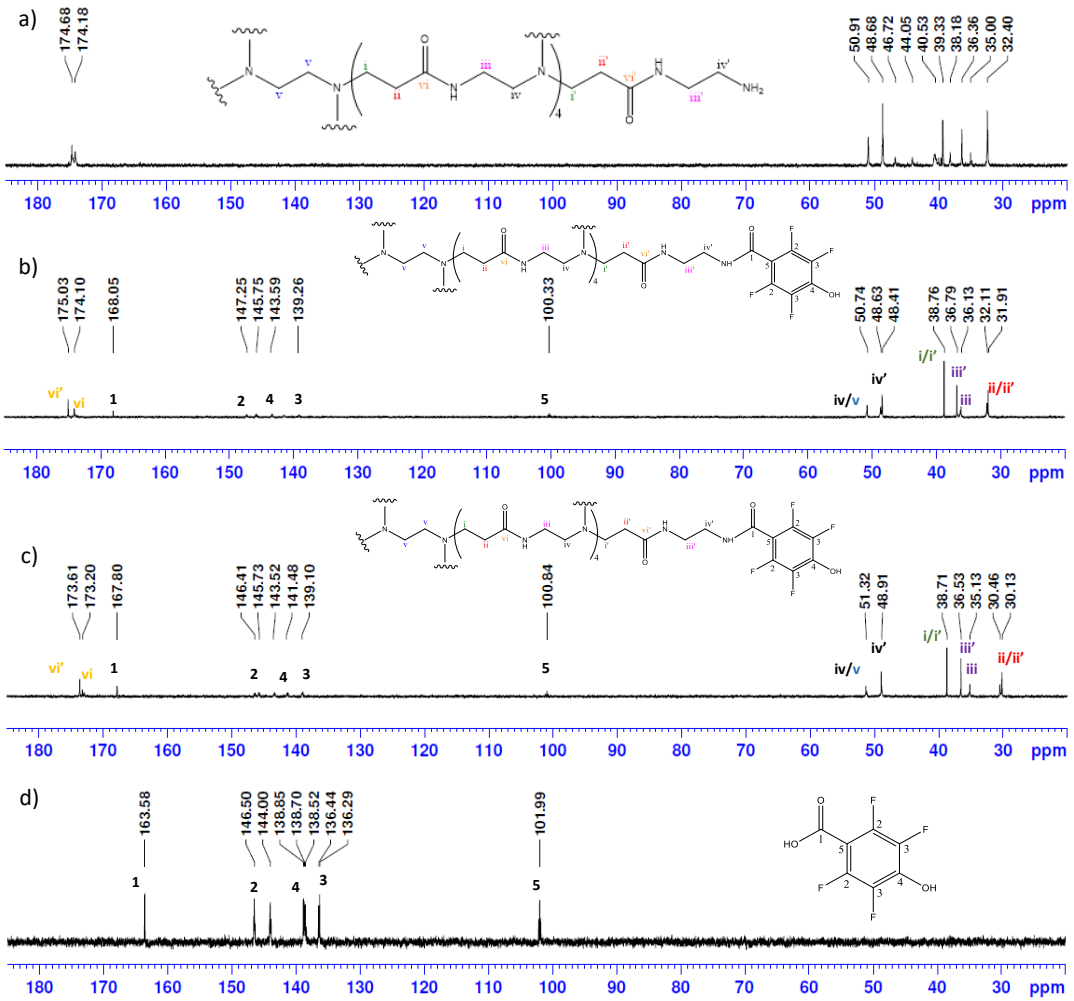

Figure A 1: ^{13}C NMR of a) $PAMAMG_4$-NH_2; b) G4_TFHBA 32.5; c) G4_TFHBA 64.5; and d) TFHBA

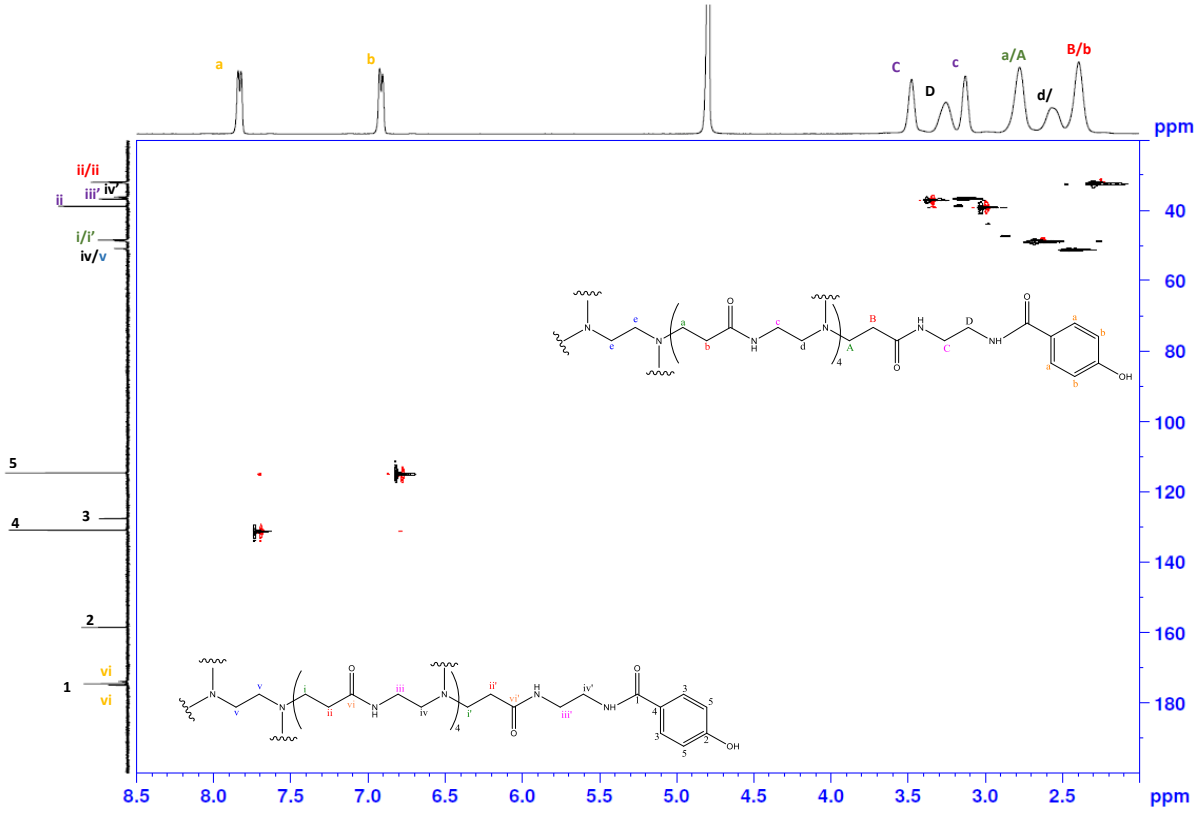

Figure A 2: HSQC of G4_HBA 64.5.

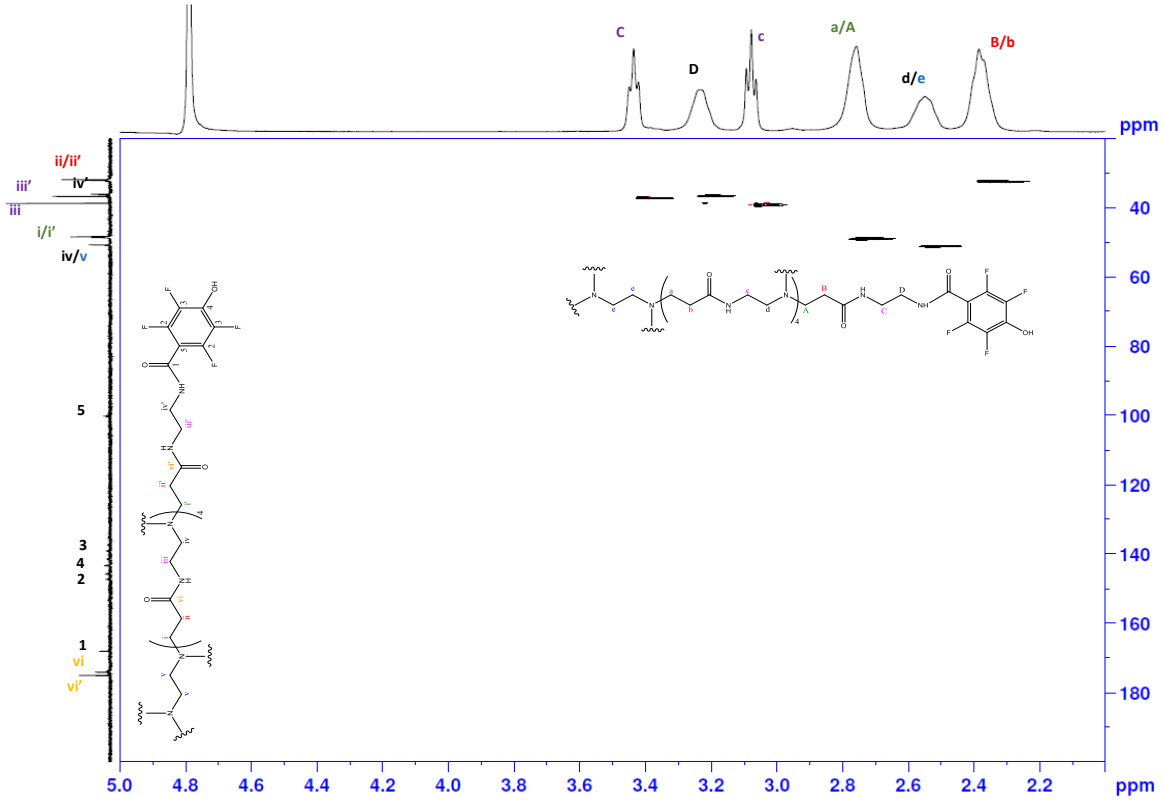

Figure A 3: HSQC of G4_TFHBA 32.5.

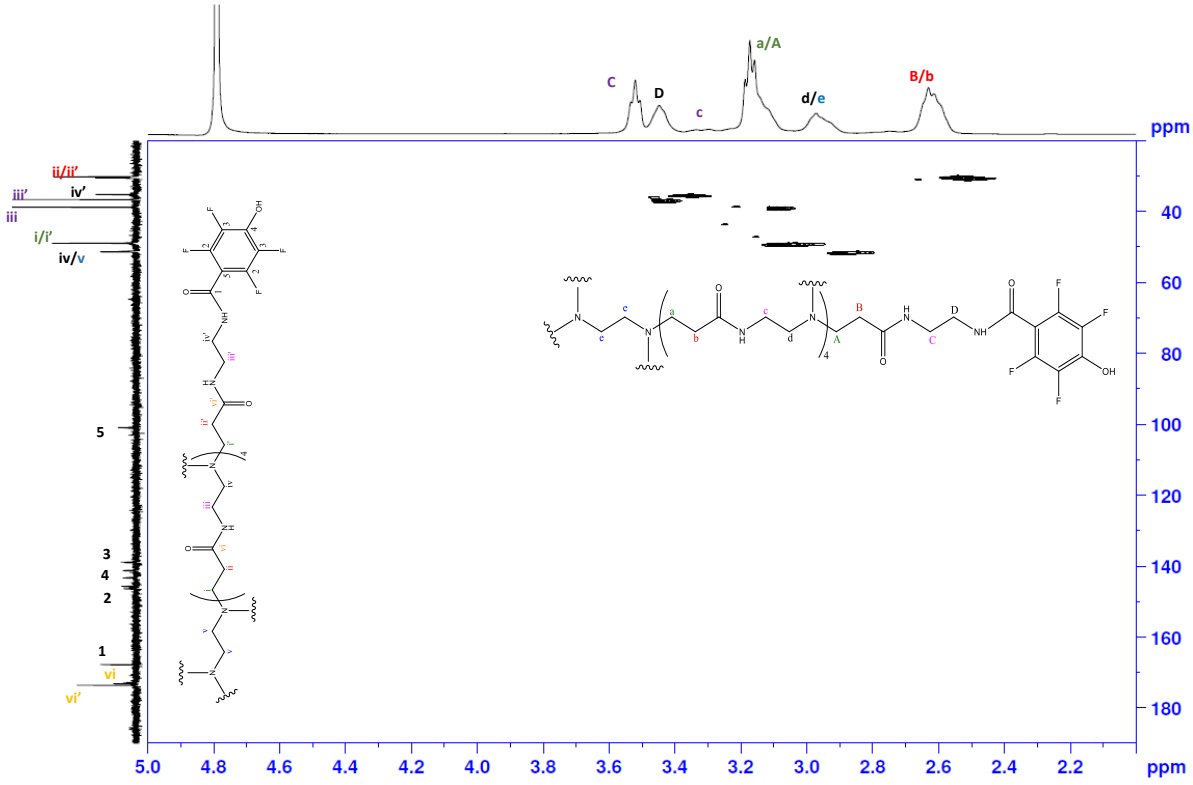

Figure A 4: HSQC of G4_TFHBA 64.5.

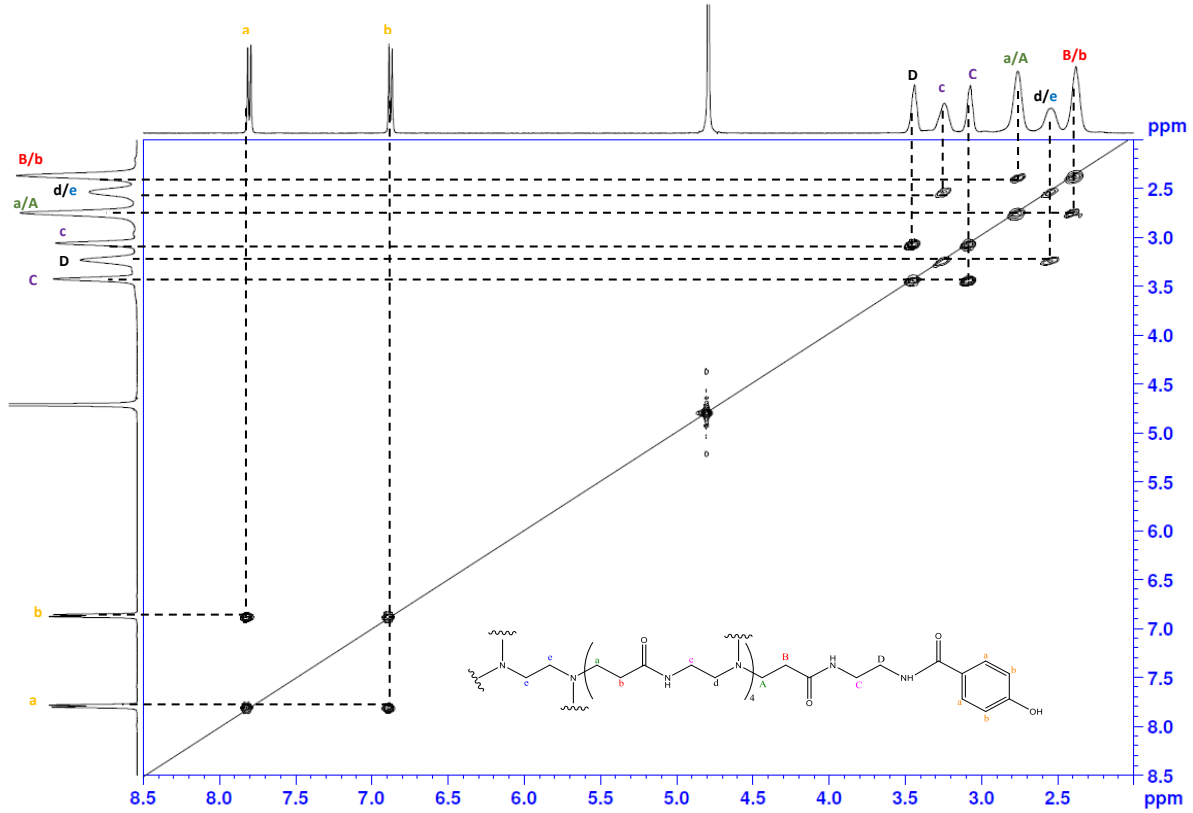

Figure A 5: COSY of G4_HBA 64.5.

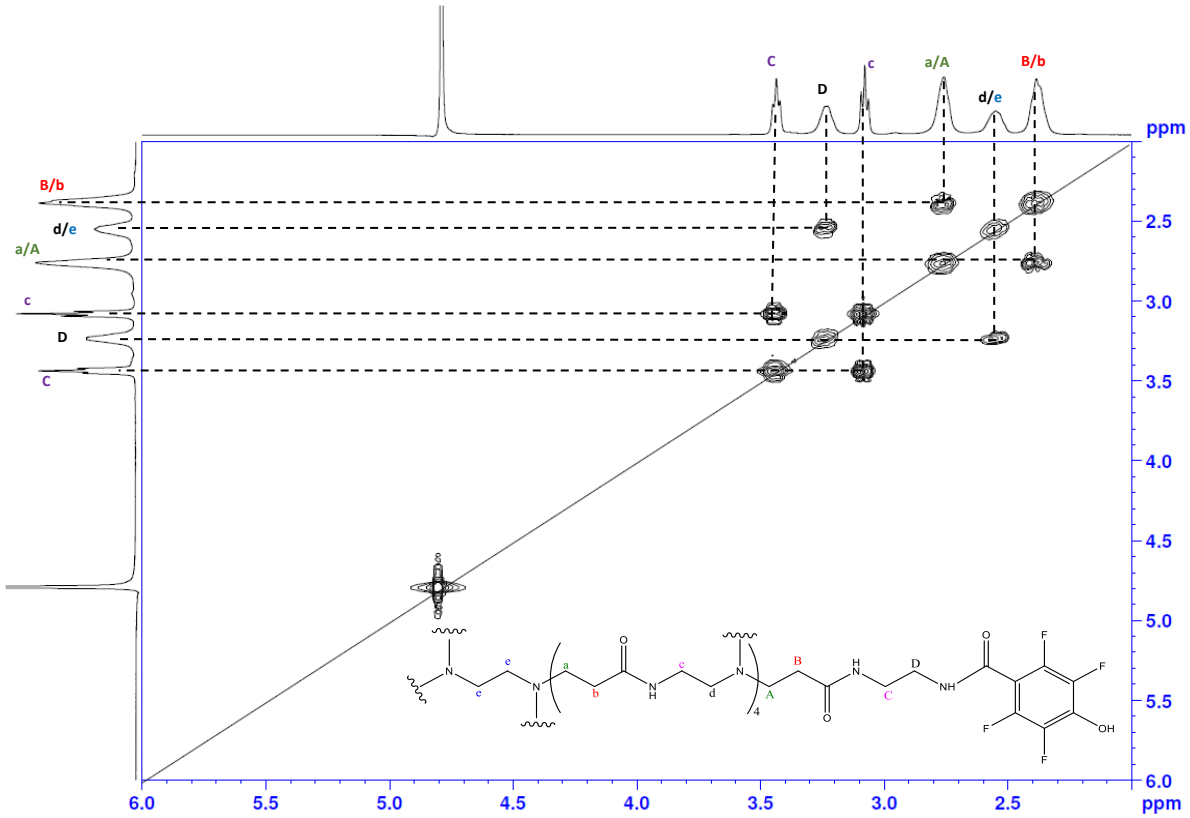

Figure A 6: COSY of G4_TFHBA 32.5.

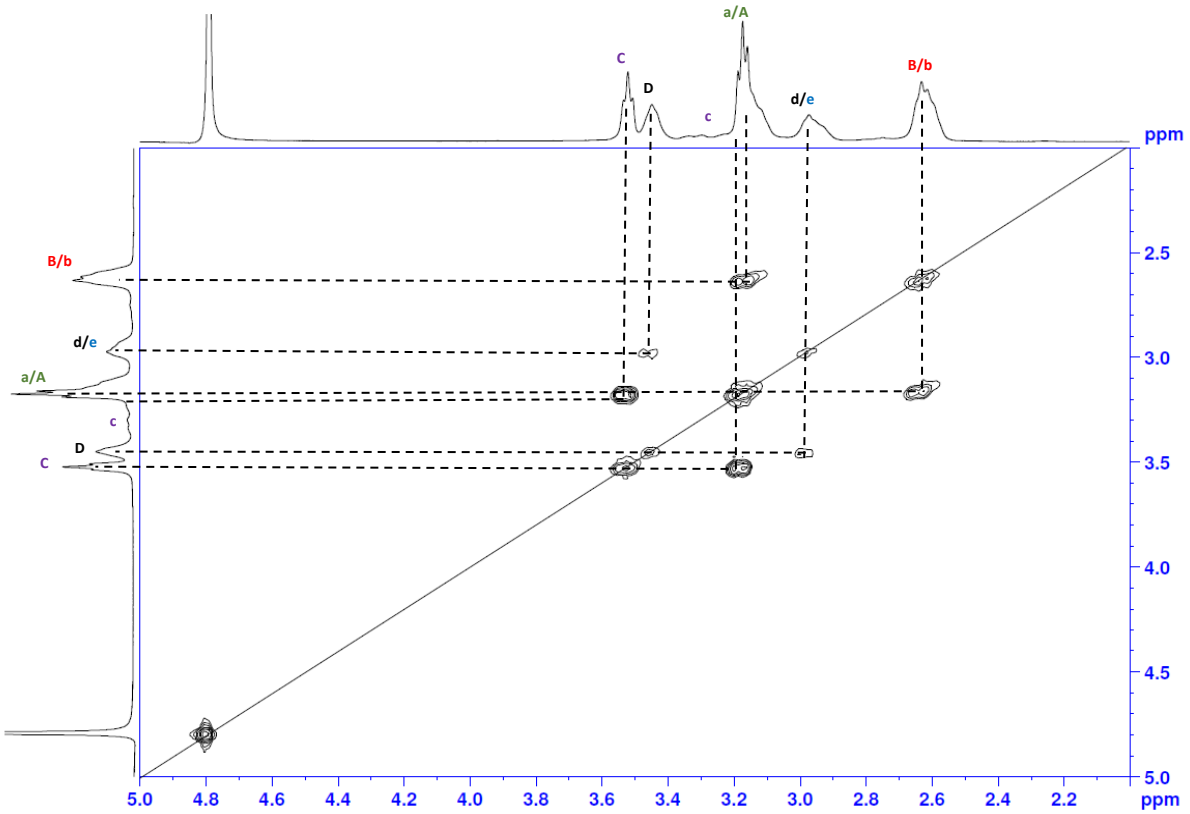

Figure A 7: COSY of G4_TFHBA 64.5.

6.2. DLS and ELS of the conjugates

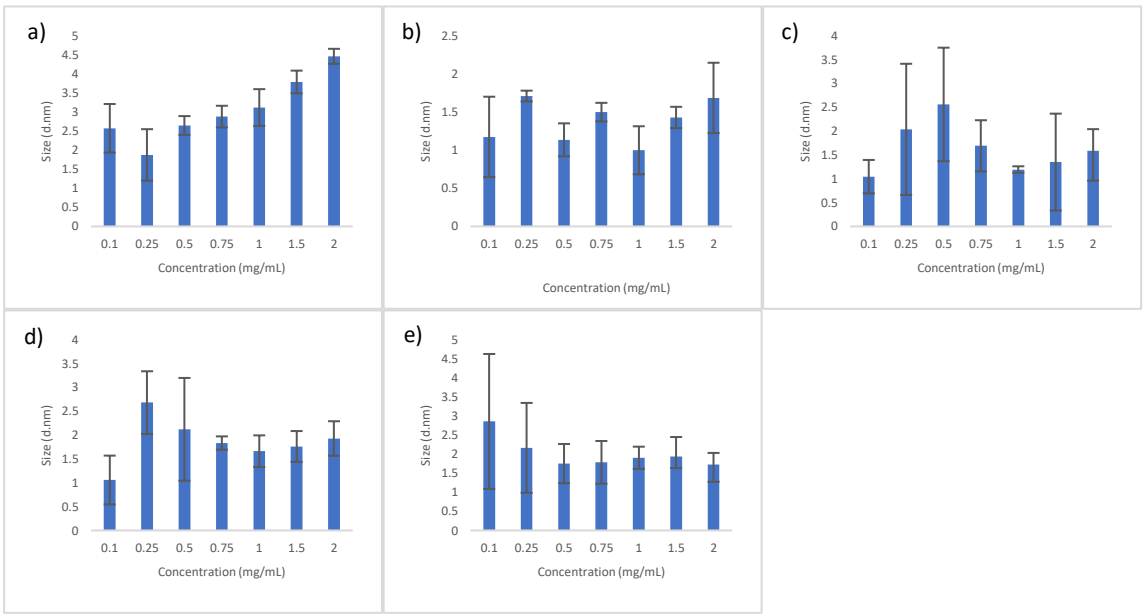

Figure A 8: DLS measurement of the conjugates with the different concentrations. a) PAMAMG$_4$-NH$_2$; b) G4_HBA 32.5; c) G4_HBA 64.5; d) G4_TFHBA 32.5; e) G4_TFHBA 64.5.

Table A 1: Charge assessment of the conjugates at a concentration of 1 mgmL^{-1} by ELS (value ± standard deviation).

Conjugates	Zeta Potential (mV)
PAMAMG$_4$-NH$_2$	5.79 ± 1.1
G4_HBA 64.5	23.5 ± 4.1
G4_HBA 32.5	16.6 ± 6.9
G4_TFHBA 64.5	12.3 ± 4.2
G4_TFHBA 32.5	7.32 ± 0.4
TFHBA	7.12 ± 1.2
HBA	2.07 ± 1.3

6.3. DLS and ELS of the dendriplexes

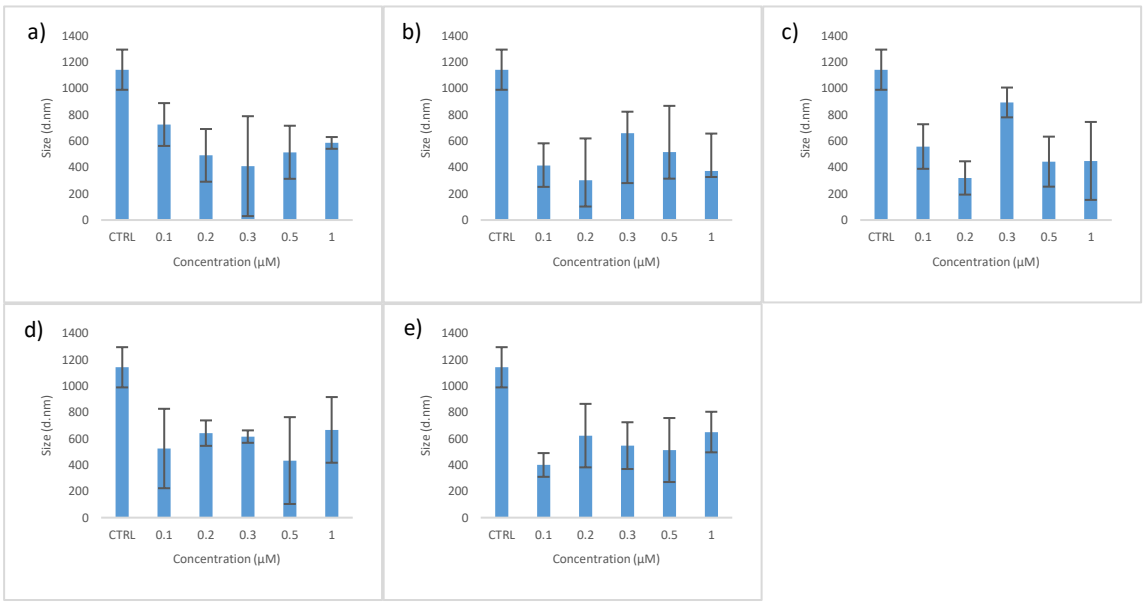

Figure A 9: Hydrodynamic diameter of the dendriplexes measured by DLS. Dendriplexes were prepared at different dendrimer's concentrations. a) PAMAMG_4-NH_2; b) G4_HBA 32.5; c) G4_HBA 64.5; d) G4_TFHBA 32.5; e) G4_TFHBA 64.5. Note: The CTRL represents the hydrodynamic diameter of pDNA alone.

Table A 2: Charge assessment of the dendriplexes at the different concentration by ELS (value ± standard deviation).

	Concentration (uM)															Ctrl (pDNA and buffer)		
Dendriplexes	0.1			0.2			0.3			0.5			1.0					
PAMAMG_4-NH_2/pDNA	1.4	±	0.2	4.0	±	0.6	4.0	±	0.5	4.5	±	0.3	6.0	±	0.1	-18.9	±	2.2
G4_HBA 32.5/pDNA	2.6	±	0.2	3.4	±	0.6	0.5	±	0.2	3.9	±	0.4	5.7	±	0.5			
G4_HBA 64.5/pDNA	1.4	±	0.2	3.8	±	0.3	0.4	±	0.4	3.0	±	0.4	5.0	±	0.2			
G4_TFHBA 32.5/pDNA	0.7	±	0.6	-0.2	±	0.2	0.3	±	0.3	3.9	±	0.6	5.2	±	0.1			
G4_TFHBA 64.5/pDNA	1.3	±	0.4	2.4	±	0.1	0.1	±	0.1	3.7	±	0.2	5.3	±	0.5			

6.1. Stability studies.

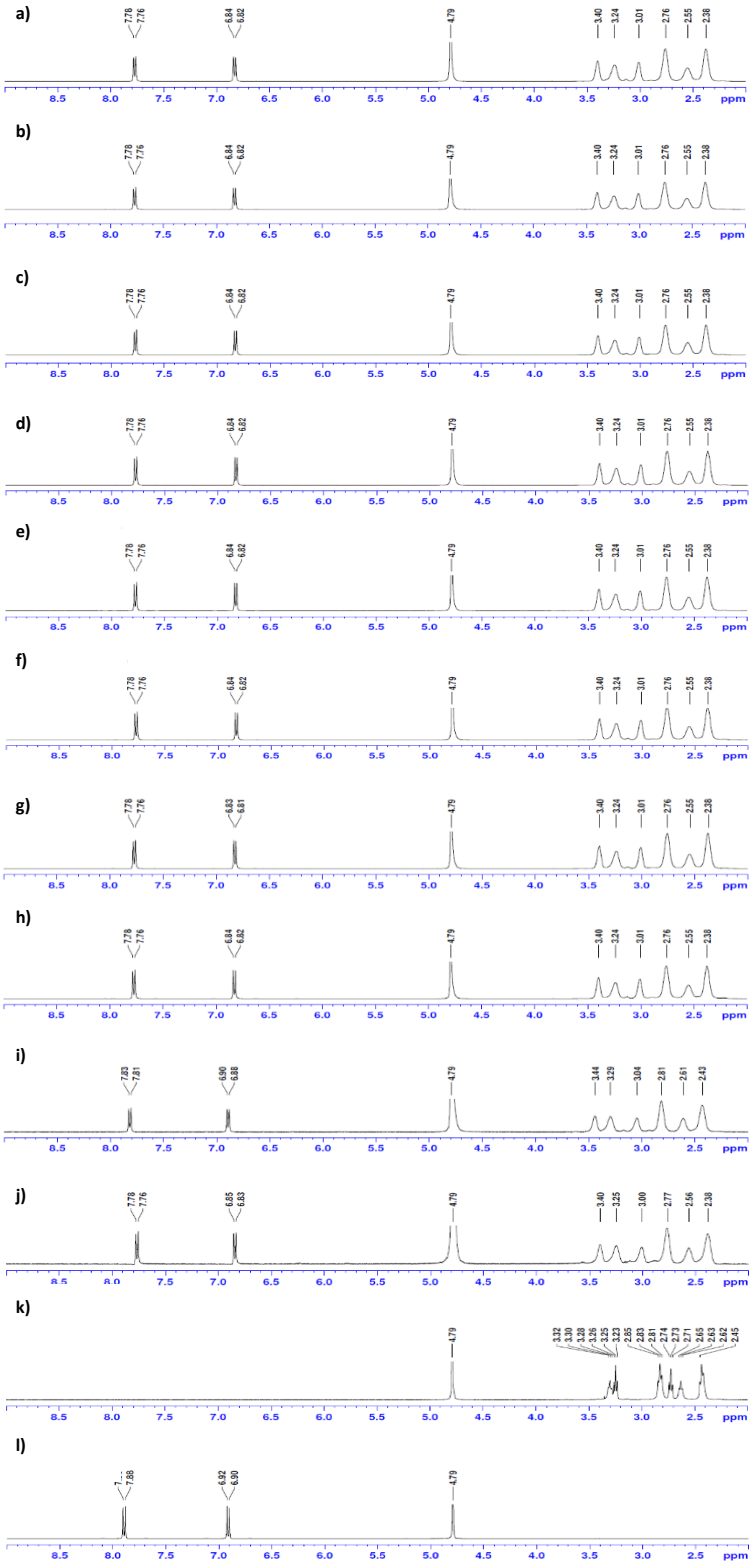

Figure A 10: Stability studies. ^{1}H NMR of G4_HBA 32.5 at 25^{o}C in D_2O. . a) t = 0; b) t = 30 min; c) t = 1h; d) t = 2h; e) t = 5h; f) t = 7h; g) t = 24h; h) t = 48h; i) t = 1 month; j) t = 2 months; k) PAMAMG$_4$-NH$_2$; and l) HBA.

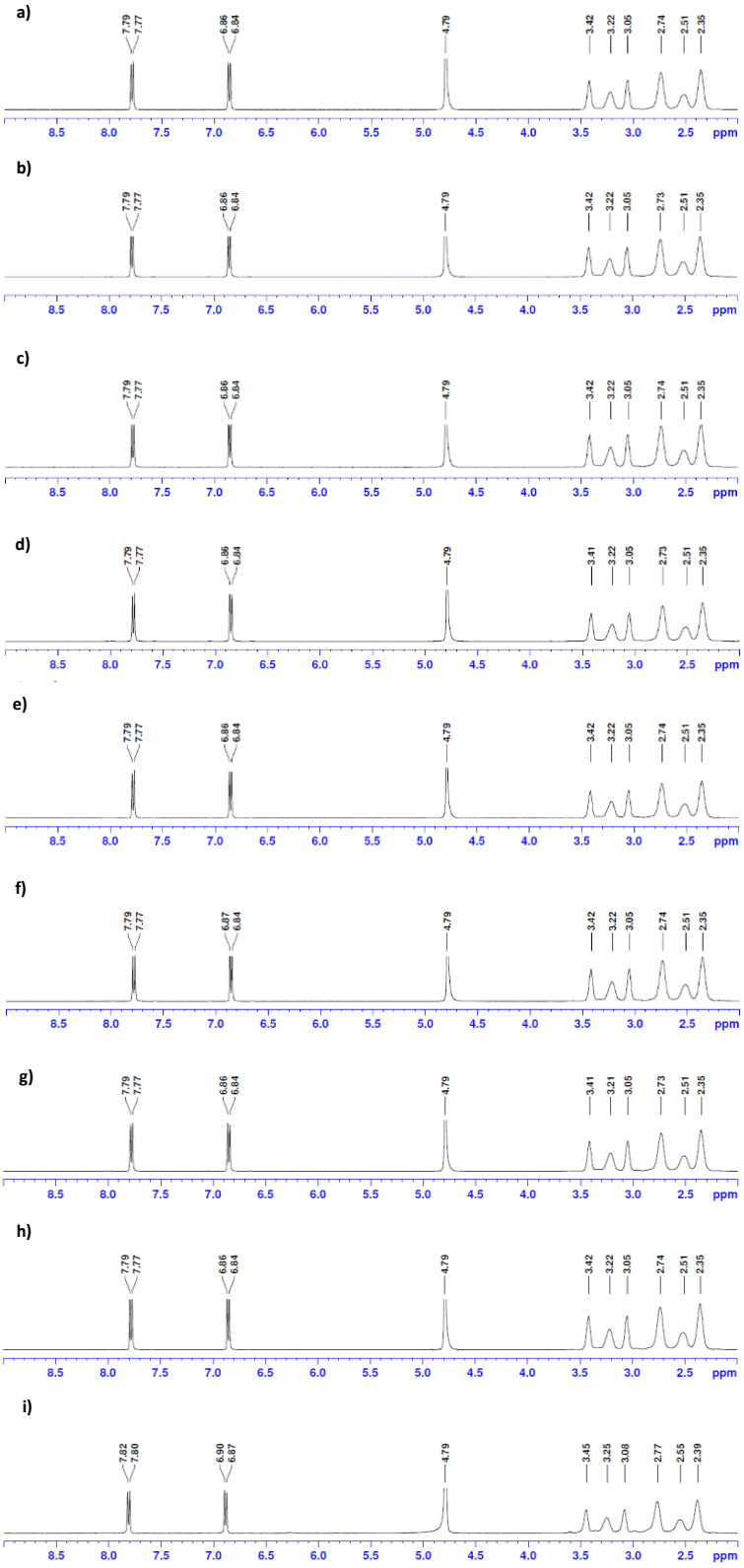

Figure A 11: Stability studies. ^{1}H NMR of G4_HBA 64.5 at 25^{o}C in D_2O. a) t = 0; b) t = 30 min; c) t = 1h; d) 2h; e) 5h; f) 7h; g) 24h; h) 48h; and i) 1 month**.**

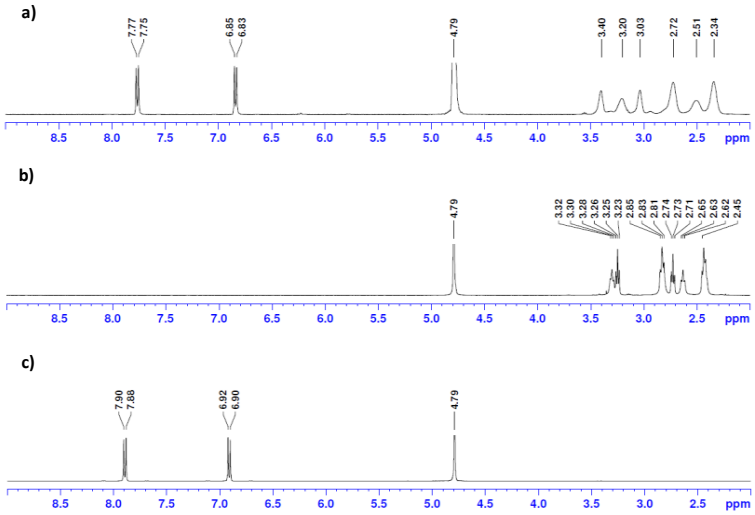

Figure A 12: Stability studies. ^{1}H NMR of G4_HBA 64.5 at 25^{o}C in D_2O. a) t = 2 months; b) t = PAMAMG$_4$-NH$_2$; and c) HBA.

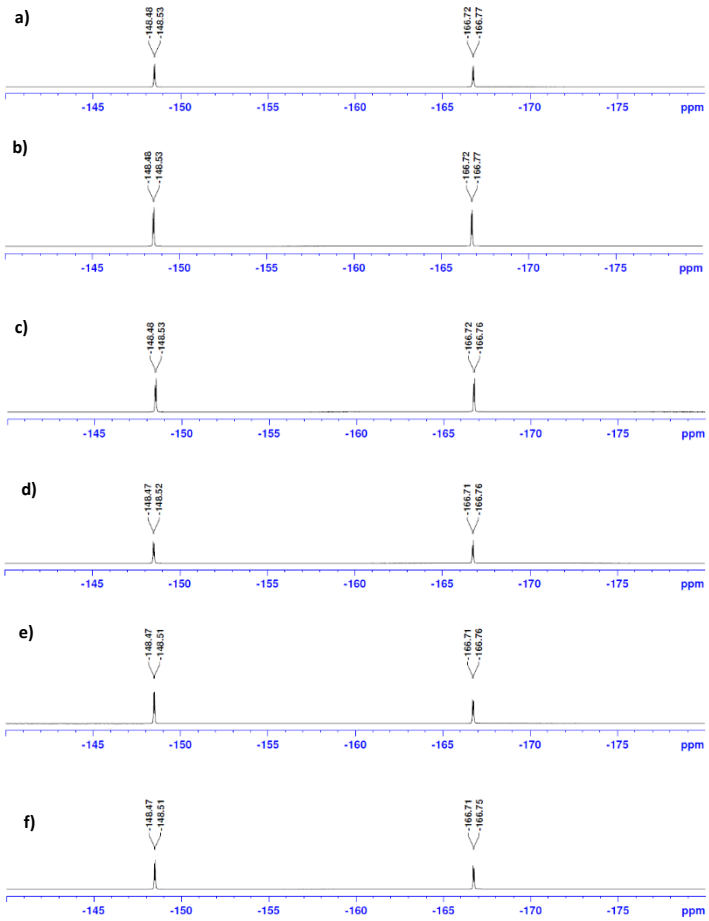

Figure A 13: Stability studies. ^{19}F NMR of G4_TFHBA 32.5 at 25^{o}C in D_2O. a) t = 0h; b) t = 30 min; c) t = 1h; d) t = 2h; e) t = 5h; and f) t = 7h.

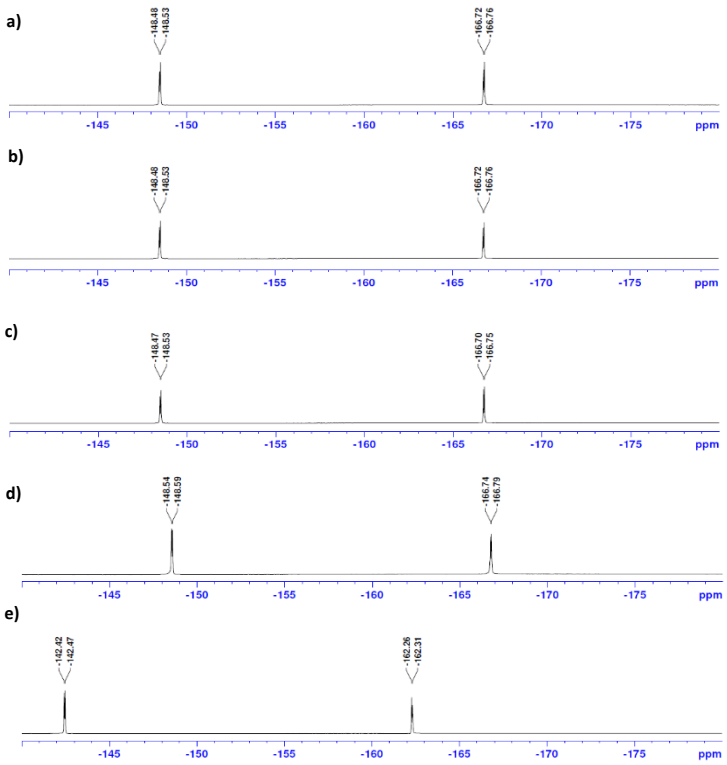

Figure A 14: Stability studies. ^{19}F NMR of G4_TFHBA 32.5 at 25°C in D_2O. a) t = 24h; b) t = 48h; c) t = 1 month; d) t= 2 months; and e) TFHBA**.**

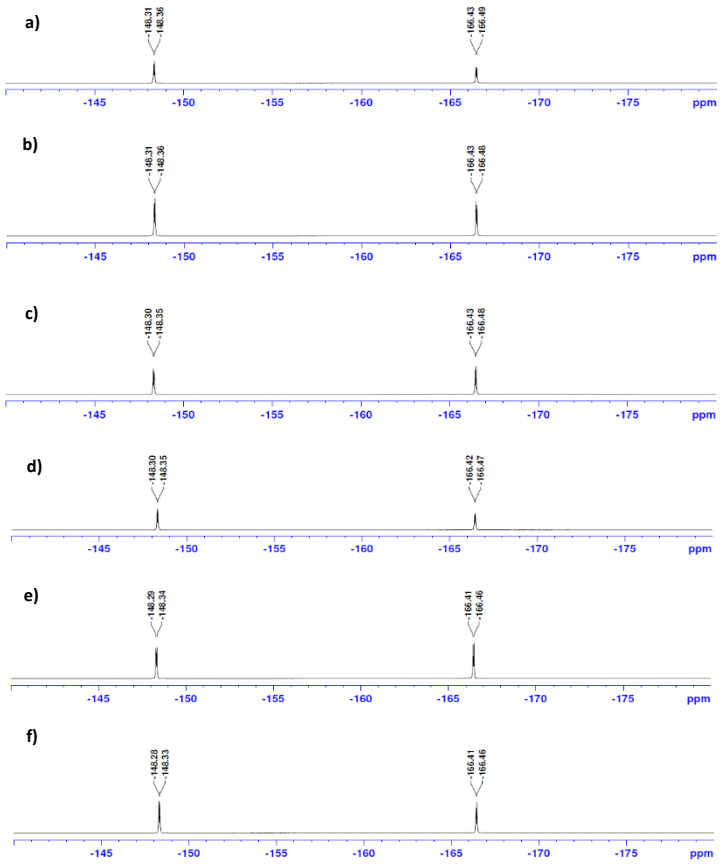

Figure A 15: Stability studies. ^{19}F NMR of G4_TFHBA 64.5 at 25°C in D_2O. a) t = 0h; b) t = 30 min; c) t = 1h; d) t = 2h; e) t = 5h; and f) t = 7h.

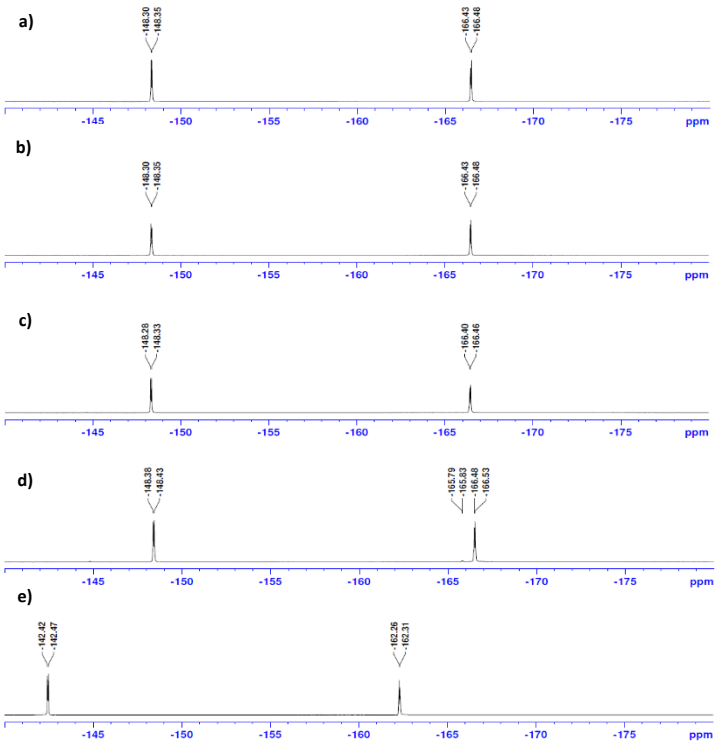

Figure A 16: Stability studies. ^{19}F NMR of G4_TFHBA 64.5 at 25^{o}C in D_2O. a) t = 24h; b) t = 48h; c) t = 1 month; d) t= 2 months; e) TFHBA.

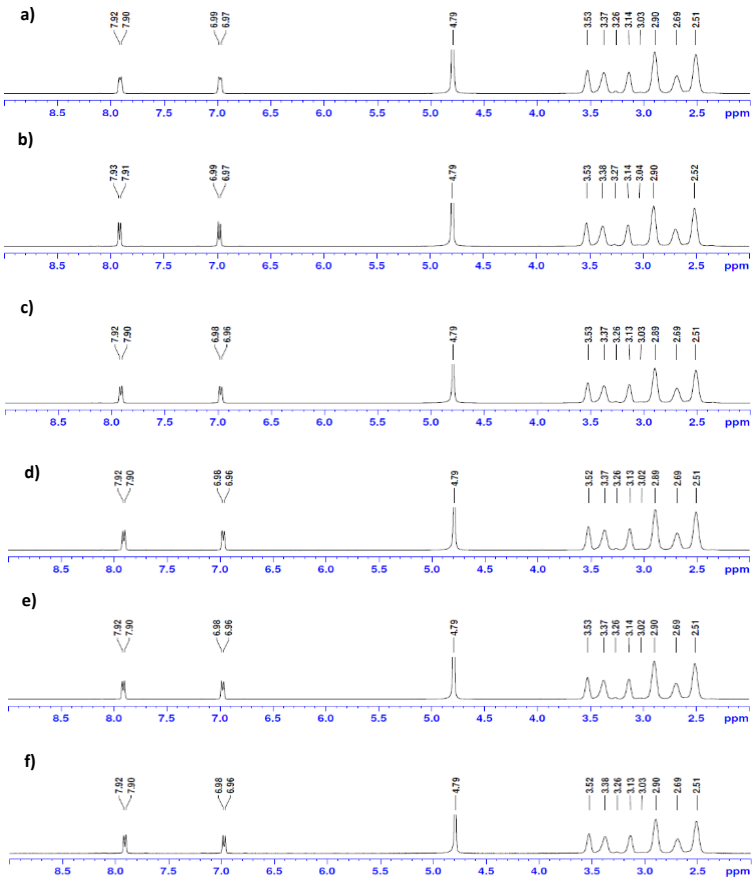

Figure A 17: Stability studies. ^{1}H NMR of G4_HBA 32.5 at 37^{o}C in D_2O. a) t = 0h; b) t = 30 min; c) t = 1h; d) t = 2h; e) t = 5h; and f) t = 7h;

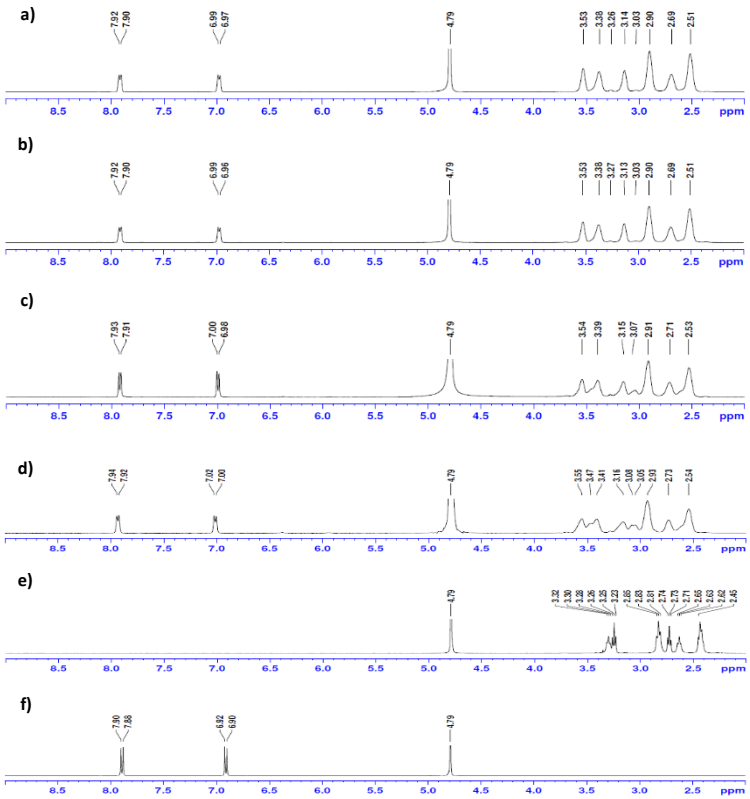

Figure A 18: Stability studies. ^{1}H NMR of G4_HBA 32.5 at 37°C in D_2O. a) t = 24h; b) t = 48h; c) t = 1 month; d) t= 2 months; e) $PAMAMG_4$-NH_2; and f) HBA.

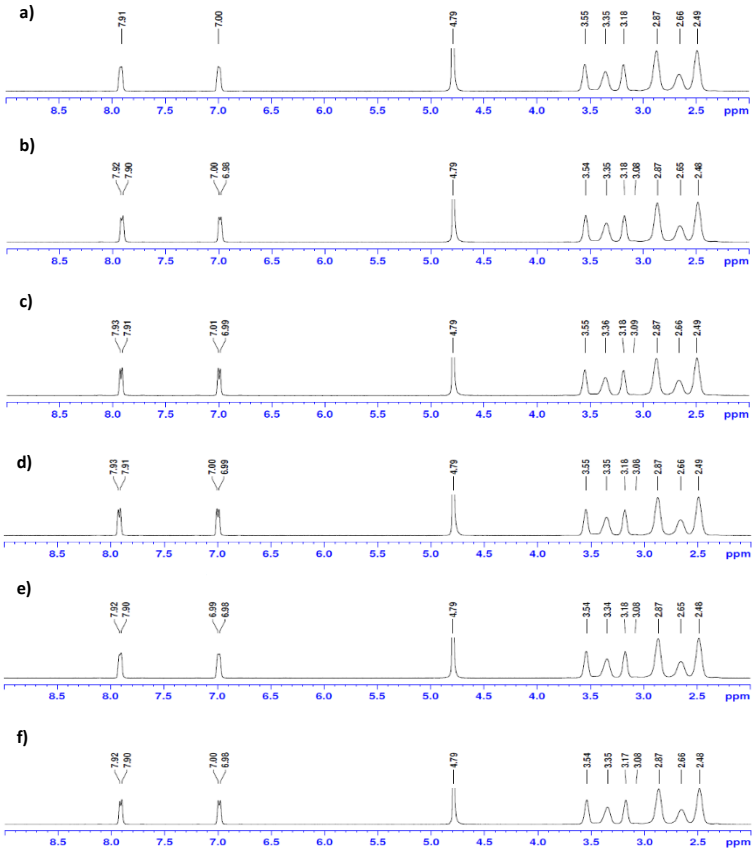

Figure A 19: Stability studies. ^{1}H NMR of G4_HBA 64.5 at 37°C in D_2O. a) t = 0h; b) t = 30 min; c) t = 1h; d) t = 2h; e) t = 5h; and f) t = 7h

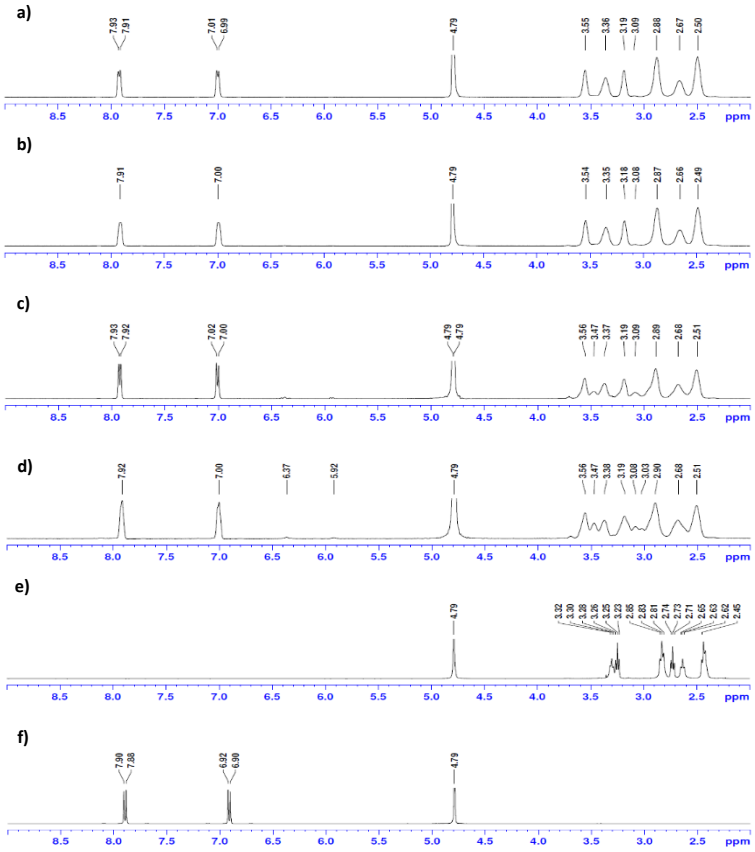

Figure A 20: Stability studies. ^{1}H NMR of G4_HBA 64.5 at 37°C in D_2O. a) t = 24h; b) t = 48h; c) t = 1 month; d) t= 2 months; e) PAMAMG_4-NH_2; and f) HBA.

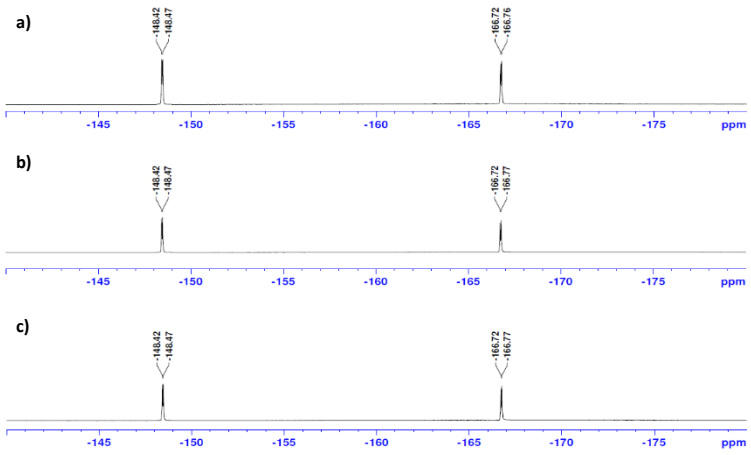

Figure A 21: Stability studies. ^{19}F NMR of G4_TFHBA 32.5 at 37°C in D_2O. a) t = 0h; b) t = 30 min; and c) t = 1h.

Figure A 22: Stability studies. ^{19}F NMR of G4_TFHBA 32.5 at 37°C in D_2O. a) t = 2h; b) t = 5h; c) t = 7h; d) t = 24h; e) t = 48h; f) t = 1 month; g) t= 2 months; and h) TFHBA.

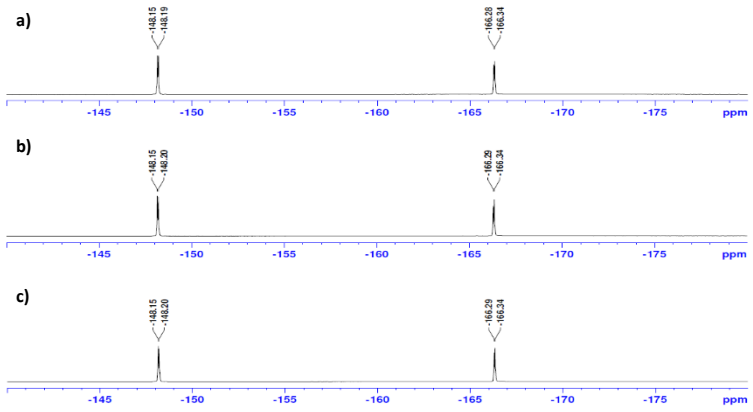

Figure A 23: Stability studies. ^{19}F NMR of G4_TFHBA 64.5 at 37°C in D_2O. a) t = 0h; b) t = 30 min; and c) t = 1h.

Figure A 24: Stability studies. ^{19}F NMR of G4_TFHBA 64.5 at 37^{o}C in D_2O. a) t = 2h; b) t = 5h; c) t = 7h; d) t = 24h; e) t = 48h; f) t = 1 month; g) t= 2 months; and h) TFHBA.

6.2. Luciferase assay supplier's information

SIGMA-ALDRICH®

sigma-aldrich.com

3050 Spruce Street, St. Louis, MO 63103 USA
Tel: (800) 521-8956 (314) 771-5765 Fax: (800) 325-5052 (314) 771-5757
email: techservice@sial.com sigma-aldrich.com

Product Information

Bicinchoninic Acid Protein Assay Kit

Catalog Numbers **BCA1 AND B9643**

TECHNICAL BULLETIN

Synonym: BCA

Product Description

Protein determination is one of the most common operations performed in biochemical research. The principle of the bicinchoninic acid (BCA) assay is similar to the Lowry procedure,[1] in that both rely on the formation of a Cu^{2+}-protein complex under alkaline conditions, followed by reduction of the Cu^{2+} to Cu^{1+}. The amount of reduction is proportional to the protein present. It has been shown that cysteine, cystine, tryptophan, tyrosine, and the peptide bond[2] are able to reduce Cu^{2+} to Cu^{1+}. BCA forms a purple-blue complex with Cu^{1+} in alkaline environments, thus providing a basis to monitor the reduction of alkaline Cu^{2+} by proteins.[3]

The BCA assay is more sensitive and applicable than either biuret or Lowry procedures. In addition, it has less variability than the Bradford assay. The BCA assay has many advantages over other protein determination techniques:

- It is easy to use.
- The color complex is stable.
- There is less susceptibility to detergents.
- It is applicable over a broad range of protein concentrations.

In addition to protein determination in solution, the BCA protein assay has other applications, including determination of protein covalently bound to agarose supports and protein adsorbed to multiwell plates.

There are two distinct ways to perform a protein assay. A protein assay can be set up to measure the concentration of the unknown protein sample (mg/ml), or it can be set up to determine the total amount of protein in the unknown protein sample (mg). The BCA assay has a linear concentration range between 200–1,000 µg of protein per milliliter. In the standard assay, only 0.1 ml protein sample is used, so the assay has a total linear protein range of 20–100 µg.

Reagents

Bicinchoninic Acid Solution, Catalog Number B9643
Reagent A is a 1,000 ml solution containing bicinchoninic acid, sodium carbonate, sodium tartrate, and sodium bicarbonate in 0.1 N NaOH (final pH 11.25).

Copper(II) Sulfate Pentahydrate 4% Solution, Catalog Number C2284
Reagent B is a 25 ml solution containing 4% (w/v) copper(II) sulfate pentahydrate.

Protein Standard (Bovine Serum Albumin - BSA) Solution, Catalog Number P0914
This product is supplied in 5 flame-sealed glass ampules, each containing 1.0 ml of a solution consisting of 1.0 mg/ml bovine serum albumin in 0.15 M NaCl with 0.05% sodium azide as a preservative.

Materials required depending on assay format used but not provided

- Spectrophotometer capable of accurately measuring absorbance in the 560 nm region.
- 96 well plates, Catalog Number M0156
- 96 well plate sealing film, Catalog Number Z369667
- Test tubes, 13 × 100 mm, Catalog Number CLS980013
- 1 ml Disposable Plastic Cuvettes, Catalog Number C5416

Precautions and Disclaimer

This product is for R&D use only, not for drug, household, or other uses. Please consult the Material Safety Data Sheet for information regarding hazards and safe handling practices.

Preparation Instructions

The BCA Working Reagent is prepared by mixing 50 parts of Reagent A with 1 part of Reagent B. Mix the BCA Working Reagent until it is light green in color.

Storage/Stability
Store Reagents A and B at room temperature. Reagent A, without Reagent B added, is stable for at least one year at room temperature in a closed container. The BCA Working Reagent (Reagent A mixed with Reagent B) is stable for one day.

Store the Protein Standard at 2–8 °C.

Procedure
In the standard assay, 20 parts of the BCA Working Reagent are then mixed with 1 part of a protein sample. For the 96 well plate assay, 8 parts of the BCA Working Reagent are mixed with 1 part of a protein sample. The sample is either a blank, a BSA protein standard, or an unknown sample. The blank consists of buffer with no protein. The BSA protein standard consists of a known concentration of bovine serum albumin, and the unknown sample is the solution to be assayed.

BCA assays are routinely performed at 37 °C. Color development begins immediately and can be accelerated by incubation at higher temperatures. Higher temperatures and/or longer incubation times can be used for increased sensitivity. Incubation at lower temperatures can slow down color development (see Procedures A and B). The absorbance at 562 nm is recorded and the protein concentration is determined by comparison to a standard curve.

A. Standard 2.1 ml Assay Protocol
(Linear concentration range is 200-1,000 µg/ml or 20-100 µg of total protein)
This is the standard assay that can be performed in a test tube. This procedure uses 0.1 ml of a protein sample and 2 ml of the prepared BCA Working Reagent. The instructions are a step-by-step procedure on how to perform the standard assay. If a nonstandard assay is used (96 well plate) adjust the volumes accordingly.
Note: It is necessary to create a standard curve during each assay, regardless of the format used.

1. Prepare the required amount of BCA Working Reagent needed for the assays (see Table 1). The final volume used in the assay depends upon the application and the equipment available. Table 1 can be used to determine the volume of BCA Working Reagent to prepare, depending on how many blanks, BSA protein standards, and unknown samples are to be assayed. Combine the volumes of Reagents A and B specified in the table. Mix until the BCA Working Reagent is a uniform, light green color.

Table 1.
Volume of BCA Working Reagent to prepare. This is dependent on how many blanks, BSA protein standards, and unknown samples are to be assayed.

Number of Assays		Amount of Each Reagent Used		
Number of 2.1 ml Standard Test tube assays	Number of wells in a 96 well plate assay	Reagent A (ml)	Reagent B (ml)	Total volume of BCA Working Reagent (ml)
4	40	8	0.16	8.16
8	80	16	0.32	16.32
9	96	19	0.38	19.38
12	127	25	0.5	25.5

2. Prepare standards of different concentrations. These BSA protein standards can range from 200–1,000 µg/ml (20–100 µg of total protein). This is accomplished by making serial dilutions starting from the 1 mg/ml standard, and then using 0.1 ml of each diluted standard in the assay. It is best to make the dilutions in the same buffer as the unknown sample (see Table 2). Deionized water may be used as a substitute for the buffer, but any interference due to the buffer will not be compensated for in the BSA protein standards.

Table 2
EXAMPLE of Standard Assay Set Up Table
For protein samples with unknown concentrations, it may be necessary to prepare a dilution scheme to ensure the concentration is within the linear range of 200–1,000 µg/ml. Two different unknown samples are represented in Table 2 by tubes 7 and 8. Tube 7 is an unknown sample with a 5-fold dilution, while tube 8 is a different unknown sample at a 10-fold dilution. Researchers must determine their own dilution schemes based on their estimation of the concentration of each unknown sample.

Tube No.	Sample (ml)	[BSA] Protein Standard (µg/ml)	BCA Working Reagent (ml)
1	0.1	0	2
2	0.1	200	2
3	0.1	400	2
4	0.1	600	2
5	0.1	800	2
6	0.1	1,000	2
7	0.1	(unknown 1)	2
8	0.1	(unknown 2)	2

3. Add 2 ml of the BCA Working Reagent to 0.1 ml of each BSA protein standard, blank, and unknown sample. Vortex gently for thorough mixing. The total liquid volume in the test tube is 2.1 ml.

4. The following incubation parameters may be used:
   60 °C for 15 minutes **Or**
   37 °C for 30 minutes **Or**
   25 °C (Room Temperature) from 2 hours to overnight

5. If required, allow the tubes to cool to room temperature.

6. Transfer the reaction solutions into a cuvette.

7. Measure the absorbance of the solution at 562 nm. Color development continues slowly after cooling to room temperature, but no significant error is seen if all the tubes are read within 10 minutes of each other. Create an assay table as needed and a standard curve based on either the BSA protein standard concentration or on the amount of protein present in the BSA protein standard (Examples are shown in the results).

8. Determine protein concentration by comparison of the absorbance of the unknown samples to the standard curve prepared using the BSA protein standards.

Results Based on the Standard Assay
Create a table with the absorbance results obtained during the assay. A separate standard curve should be generated for each assay performed. The amount of protein for tubes 1–6 was obtained from the known amount of BSA protein standard added.
Note: The data below should not be used as a replacement of a standard curve. The absorbance of the BSA protein standards (tubes 1–6) in each assay will differ from those presented here. The amount of protein recorded for tubes 7 and 8 was obtained from the standard curve.

Table 3.
EXAMPLE of Assay Data Table

Tube No.	A_{562}	Net A_{562}	Amount of protein (µg) in sample	[Protein] of protein sample (µg/ml)	Dilution Factor
1	0.045	0	0	0	-
2	0.207	0.162	20	200	-
3	0.364	0.319	40	400	-
4	0.510	0.465	60	600	-
5	0.661	0.616	80	800	-
6	0.823	0.778	100	1,000	-
7	0.587	0.542	70	700	5
8	0.743	0.698	90	900	10

After obtaining the results, create a standard curve to determine the protein concentration in the unknown sample. Plot the Net Absorbance at 562 nm versus the BSA protein standard concentrations (µg/ml, Tubes 1–6).

Graph 1.
Standard Curve produced from Assay Data

The standard curve indicates the unknown protein sample in test tube 7 (Net A_{562} = 0.542) contains 700 µg/ml of protein.

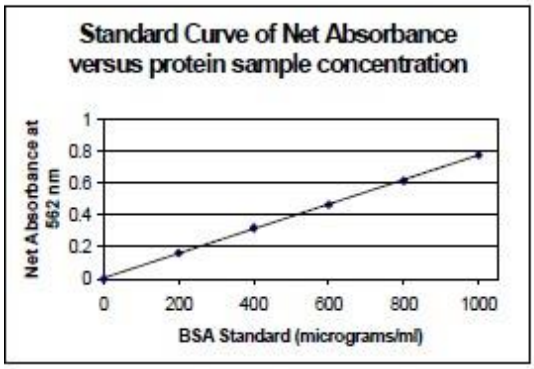

The actual concentration of protein present in the unknown sample is calculated as follows:

(µg/ml of unknown protein sample) times (Dilution Factor)

(700 µg/ml) × (5) = 3,500 µg/ml of protein

B. 96 Well Plate Assay
(Linear concentration range is 200-1,000 µg/ml or 5-25 µg of total protein)
The BCA assay can be adapted for use in 96 well plates. These plates can be used as long as five main points remain unchanged:

1. Read the absorbance at 562 nm. For a plate reader, which does not have the exact wavelength filter, a filter in the range of 540-590 nm can be substituted.

2. The ratio of BCA Working Reagent to protein sample will have to be modified from the Standard Assay.
   Examples:
   Standard Assay - (Test Tube): 0.10 ml protein sample to 2 ml BCA Working Reagent (1:20)

   96 well plate - 25 µl protein sample to 200 µl BCA Working Reagent (1:8). When using multiwell plates, make sure the unknown samples, blanks, or standards are present in the wells prior to adding the BCA Working Reagent to facilitate mixing.

3. Make sure the protein assay containers are sealed (cover the plates with film) and incubate the samples for:
   60 °C for 15 minutes **Or**
   37 °C for 30 minutes **Or**
   25 °C (Room Temperature) from 2 hours to overnight

4. Keep the protein sample concentration between 200–1,000 µg/ml (5–25 µg total protein).

5. A separate standard curve will have to be determined for each assay protocol. The pathlength in each assay is dependent on the assay container (cuvettes or multiwell plates) and/or the reaction volume. These and others changes like the BCA Working Reagent to protein sample ratio affect the Net Absorbance values.

C. TCA Concentration-BCA Assay Protocol
By using this procedure it is possible to remove some of the interfering substances that are described in the compatibility chart. It is also possible to increase the concentration of the unknown sample using this procedure.

1. Add the unknown samples and BSA protein standards to separate microcentrifuge tubes and adjust the final volumes to 1 ml with deionized water. Larger volumes can also be used by adjusting the following volumes accordingly.

2. Add 0.1 ml of a 0.15% (w/v) solution of sodium deoxycholate (Catalog Number D5670) prepared with deionized water.

3. Mix and let stand for 10 minutes at room temperature. It is also acceptable to let stand on ice for 10 minutes.

4. Add 0.1 ml of 6.1 N (~100% w/v) solution of trichloroacetic acid (TCA, Catalog Number T0699).

5. Cap and vortex each sample.

6. Incubate for 5 minutes at room temperature. It is also possible to let stand on ice for 5 minutes.

7. Centrifuge the samples for 15 minutes at room temperature in a microcentrifuge at full speed.

8. Carefully decant or pipette the supernatant of each sample. Do not disturb the pellet.

9. Solubilize each pellet by adding 0.04 ml of a 5% (w/v) solution of sodium dodecyl sulfate (SDS, Catalog Number L6026) prepared with a 0.1 N sodium hydroxide solution (Catalog Number 72076). Mix well until the pellet is completely dissolved.
10. Pipette 0.06 ml of deionized water into the tube to bring the sample volume to 0.10 ml, which can then be used in the standard 2.1 ml assay procedure. It is possible to add less water if a smaller volume assay is to be performed.
11. Vortex each sample and proceed onto the 2.1 ml standard assay protocol or a custom assay.

Compatibility Chart

The amount listed is the maximum amount of material allowed in the protein sample without causing a noticeable interference.

Incompatible Substances	Amount Compatible
Buffer Systems	
N-Acetylglucosamine (10 mM) in PBS, pH 7.2	10 mM
ACES, pH 7.8	25 mM
Bicine, pH 8.4	20 mM
Bis-Tris, pH 6.5	33 mM
CelLytic™ B Reagent	undiluted no interference
Calcium chloride in TBS, pH 7.2	10 mM
CHES, pH 9.0	100 mM
Cobalt chloride in TBS, pH 7.2	0.8 M
EPPS, pH 8.0	100 mM
Ferric chloride in TBS, pH 7.2	10 mM
HEPES	100 mM
MOPS, pH 7.2	100 mM
Nickel chloride in TBS	10 mM
PBS; Phosphate (0.1 M), NaCl (0.15 M), pH 7.2	undiluted no interference
PIPES, pH 6.8	100 mM
Sodium acetate, pH 4.8	200 mM
Sodium citrate, pH 4.8 or pH 6.4	200 mM
Tricine, pH 8.0	25 mM
Triethanolamine, pH 7.8	25 mM
Tris	250 mM
TBS; Tris (25 mM), NaCl (0.15 M), pH 7.6 (Catalog Number T5030)	undiluted no interference
Tris (25 mM), Glycine (1.92 M), SDS (0.1%), pH 8.3 (Catalog Number T4904)	undiluted no interference
Zinc chloride (10 mM) in TBS, pH 7.2	10 mM

Incompatible Substances (Continued)	Amount Compatible
Buffer Additives	
Ammonium sulfate	1.5 M
Aprotinin	10 mg/L
Cesium bicarbonate	100 mM
Glucose	10 mM
Glycerol	10%
Guanidine•HCl	4 M
Hydrochloric acid	100 mM
Imidazole	50 mM
Leupeptin	10 mg/L
PMSF	1 mM
Sodium azide	0.20%
Sodium bicarbonate	100 mM
Sodium chloride	1 M
Sodium hydroxide	100 mM
Sodium phosphate	25 mM
Sucrose	40%
TLCK	0.1 mg/L
TPCK	0.1 mg/L
Sodium orthovanadate in PBS, pH 7.2	1 mM
Thimerosal	0.01%
Urea	3 M
Chelating agents	
EDTA	10 mM
EGTA	not compatible
Sodium citrate	200 mM
Detergents	
Brij™ 35	5%
Brij 52	1%
CHAPS	5%
CHAPSO	5%
Deoxycholic acid	5%
Nonidet P-40 (IGEPAL® CA-630)	5%
Octyl β-glucoside	5%
Octyl β-thioglucopyranoside	5%
SDS	5%
Span® 20	1%
TRITON® X-100	5%
TRITON X-114	1%
TRITON X-305	1%
TRITON X-405	1%
TWEEN® 20	5%
TWEEN 60	5%
TWEEN 80	5%
Zwittergents®	1%

Incompatible Substances (Continued)	Amount Compatible
Reducing & Thiol Containing Agents	
Dithioerythritol (DTE)	1 mM
Dithiothreitol (DTT)	1 mM
2-Mercaptoethanol	1 mM
Tributyl Phosphine	0.01%
Solvents	
Acetone	10%
Acetonitrile	10%
DMF	10%
DMSO	10%
Ethanol	10%
Methanol	10%

Note: This is not a complete compatibility chart. There are many substances that can affect different proteins in different ways. One may assay the protein of interest in deionized water alone, then in the buffer with possible interfering substances. Comparison of the readings will indicate if an interference exists. Refer to References for additional information on interfering substances.[1-4]

Note: Reagents that chelate metal ions, change the pH of the assay, or reduce copper will interfere with the BCA assay. Examples are shown below:

1. Metal chelators such as EDTA (>10 mM) and EGTA (any level).
2. Thiol containing reagents such as cysteine (any level), DTT (>1 mM), dithioerythritol (>1 mM), and 2-mercaptoethanol (>0.01%).
3. High salt or buffers concentrations such as ammonium sulfate (>1.5 M), Tris (>0.25 M), and sodium phosphate (>0.1 M).

Troubleshooting Guide - Protein sample contains incompatible reagents or substances.

1. If the starting concentration of the protein is high, try diluting the sample so the substance no longer interferes.
2. Use the TCA Concentration-BCA procedure and discard the incompatible liquid after the pellet is spun down.
3. The interference caused by chelating reagents decreases when the relative amount of the copper(II) sulfate solution is increased in the prepared BCA Working Reagent. The standard preparation has 50 parts of bicinchoninic acid solution to 1 part copper(II) sulfate solution. The amount of copper(II) sulfate solution may be increased to 3 parts.

Technical Tips

1. Make sure the glassware being used has been cleaned well.
2. Consider a different protein assay procedure. If certain incompatible reagents cannot be removed from the assay, consider the use of the Bradford Reagent (Catalog Number B6916).
3. If the protein levels are too low, try using the QuantiPro BCA Kit (Catalog Number QPBCA).

References

1. Lowry, O.H. et al., J. Biol. Chem., **193**, 265-275 (1951).
2. Wiechelman, K. et al., Anal. Biochem., **175**, 231-237 (1988).
3. Smith, P.K. et al., Anal. Biochem., **150**, 76-85 (1985).
4. Brown, R.E. et al., Anal. Biochem., **180**, 136-139 (1989).

FF,JDS,MAM 02/11-1

6.3. BCA assay supplier's information

Luciferase Assay Systems

INSTRUCTIONS FOR USE OF PRODUCTS E1483, E1500, E1501, E1531, E4030, E4530 AND E4550.

Quick PROTOCOL

Standard 96 Well Plate Assay

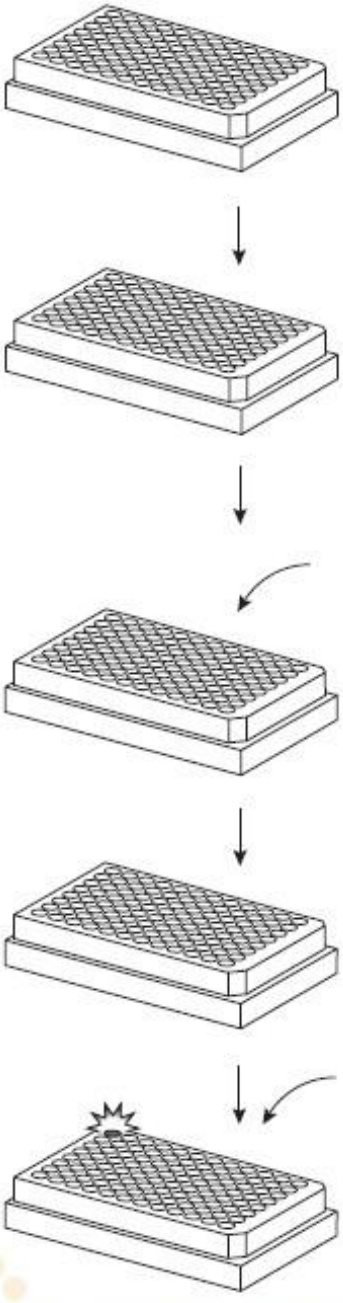

Standard Culture Dish Assay

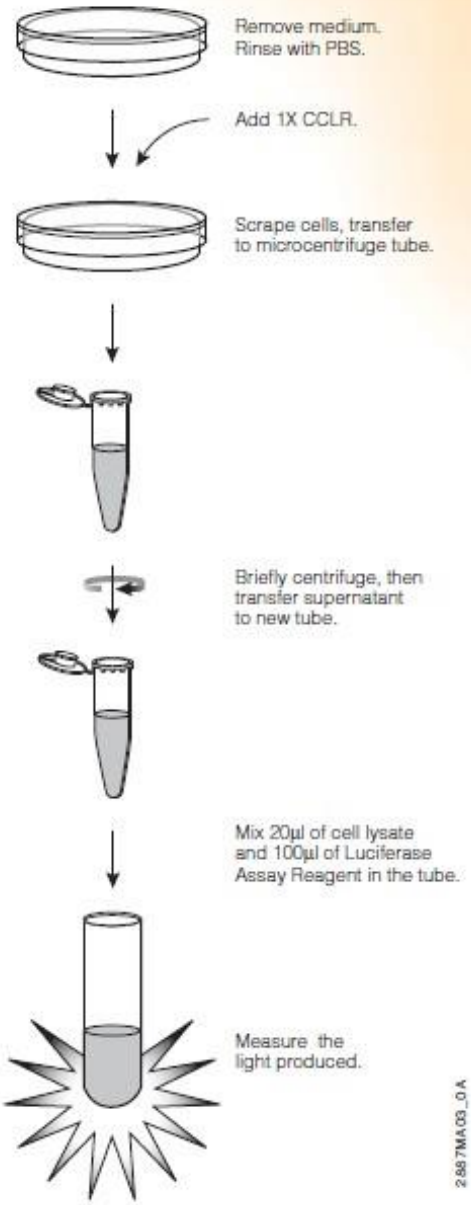

ORDERING/TECHNICAL INFORMATION:

www.promega.com • Phone 608-274-4330 or 800-356-9526 • Fax 608-277-2601

Printed in USA Revised 3/09.
Part #9FB026

UNIVERSIDADE da MADEIRA

CQM CENTRO DE QUÍMICA DA MADEIRA

FCT
Fundação para a Ciência e a Tecnologia
MINISTÉRIO DA CIÊNCIA, TECNOLOGIA E ENSINO SUPERIOR

Pest-OE/UID/QUI/00674/2019

arditi agência regional para o desenvolvimento da investigação tecnologia e inovação

Project M1420-01-0145-FEDER-000005

Molecular Materials®
RESEARCH GROUP
MADEIRA ISLAND - PORTUGAL

Co-financed by:

MADEIRA 14-20

REGIÃO AUTÓNOMA DA MADEIRA

PORTUGAL 2020

UNIÃO EUROPEIA
Fundo Europeu de Desenvolvimento Regional